INVESTIGATING A MECHANISM FOR P38-MAPK REGULATION OF NOTCH IN PROSTATE EPITHELIAL DIFFERENTIATION

By

Sander Barkley Frank

A DISSERTATION

Submitted to
Michigan State University
in partial fulfillment of the requirements
for the degree of

Genetics—Doctor of Philosophy

2016

PUBLIC ABSTRACT

INVESTIGATING A MECHANISM FOR P38-MAPK REGULATION OF NOTCH IN PROSTATE EPITHELIAL DIFFERENTIATION

By

Sander Barkley Frank

Prostate cancer is the second most common cancer in American men today. There are a handful of genes known to be commonly altered in prostate tumors, however the specific details about how these genes drive the formation and progression of cancer is not well understood. My work has sought to understand how some of these genes may be connected (p38-MAPK, Myc, and Notch) and what their function is in the normal prostate gland. The prostate contains two different types of cells that are believed to give rise to tumors: basal and luminal cells. Some basal cells can differentiate and become luminal cells. I believe that defects during this process stall the cell in a precarious state and allow tumor formation. Thus, understanding how genes function in healthy cells during differentiation is key to understanding prostate cancer initiation.

In order to test how genes are involved in differentiation, I utilized a variety of tools to manipulate expression of specific genes in human prostate cells in a culture dish. During my time I took one of these tools (a viral shRNA vector called Tet-pLKO) and modified it to make it easier to use for others. Additionally, I wrote a streamlined protocol explaining exactly how to use this tool in an easy and efficient manner.

In my primary thesis work, I used Tet-pLKO shRNA and chemical inhibitors to antagonize specific genes. I sought to investigate how a gene called p38-MAPK was involved in differentiation. I found that decreasing p38-MAPK with shRNA or chemical inhibitors prevented differentiation. Similarly, I also found that the cells needed Myc and Notch, two other gene pathways. I then proceeded to study how these pathways were connected and determined how p38-MAPK regulates Notch in prostate cells. Moreover, I found that one of the four Notch receptors, Notch3, was unique. I did some investigation to understand what was different about

Notch3. Recent work by others suggests Notch3 may play a unique role in differentiation in part by regulating genes differently than the other Notch members. My work supports this idea, as I have identified some specific genes that Notch3 regulates which are likely very important for differentiation.

All together, my research began by engineering a variety of molecular tools to ask very detailed questions about how specific genes function during differentiation. Using these tools I revealed multiple novel connections between three different pathways and identified a special role for Notch3 in prostate cells. With this work I have enhanced our understanding of the function of these genes in prostate differentiation. Future work will build on these findings and further increase our understanding of these pathways in the prostate, with the ultimate goal of bringing new insights into tumor biology.

ABSTRACT

INVESTIGATING A MECHANISM FOR P38-MAPK REGULATION OF NOTCH IN PROSTATE EPITHELIAL DIFFERENTIATION

By

Sander Barkley Frank

Many pathways misregulated in prostate cancer are also involved in epithelial differentiation. However, specific mechanisms for the cellular and molecular origins of prostate cancer remain elusive. Better understanding of these genes and their specific functions in differentiation may enlighten us as to how their misregulation could drive oncogenesis. My thesis work focused on understanding how p38-MAPK drives prostate epithelial differentiation. My primary hypothesis was that p38-MAPK regulation of Notch3, via Myc, is required for normal prostate epithelial differentiation.

Differentiation in the prostate is a homeostatic process between two cell types in an epithelial bilayer: basal and luminal cells. Each layer has its own progenitor population, but there are also bipotent cells capable of basal-to-luminal differentiation. I utilized primary prostate epithelial cells and induced differentiation *in vitro* to interrogate signaling pathways. I utilized shRNA, pharmacologic inhibition, and constitutive activation to study the effects of manipulating p38-MAPK, Myc, and Notch signaling during differentiation. I created various dox-inducible shRNA and cDNA overexpressing lentiviral constructs. In the process, I modified and improved a commonly used lentiviral dox-inducible shRNA vector, Tet-pLKO-Puro. In addition to modifying the vector, I also created a streamlined protocol for quick and efficient design and screening of cloned shRNAs.

Using my bevy of molecular tools, I investigated p38-MAPK during differentiation. Inhibition (SB202190, BIRB796) or shRNA knockdown of p38α or p38δ prevented formation of a luminal layer. Additionally, treatment with a γ-secretase inhibitor (RO4929097) or shRNA knockdown of Notch1 or Notch3 greatly impaired differentiation and caused premature luminal

cell death. Knowing that p38-MAPK and Notch were required for differentiation, I next investigated how the pathways may be connected.

Activation of p38-MAPK (via a constitutive MKK6 mutant) increased Notch3 mRNA expression. Upregulation of Notch3 was dependent in part on Myc, as siRNA or inhibition of Myc (10058-F4) diminished the effect by more than half. I further investigated transcriptional regulation of Notch3 by validating two enhancer elements using a combination of ChIP, RNA-seq, and Luciferase reporter assays. Additionally, I found that p38-MAPK also regulates Notch3 via increased mRNA stability. Lastly, I investigated upstream (ligand) and downstream (Hes/Hey) Notch signaling during differentiation. I observed differential Notch ligand regulation and divergent regulation of several target genes by Notch1 and Notch3.

My findings reveal a new mechanistic link between p38-MAPK and Notch signaling during epithelial differentiation. Moreover, this work demonstrates novel mechanisms of Notch3 regulation at both the transcriptional and post-transcriptional level by p38-MAPK and Myc. Additional experiments suggest Notch3 may play a unique role in driving differentiation by differentially regulating a subset of Notch target genes. Future work will build on these findings and further increase our understanding of these pathways in the prostate, with the ultimate goal of bringing new insights into tumor biology.

Dedicated to my mother, Terrie Barkley Frank,
whose memory inspires, encourages, and comforts me
through all my endeavors

ACKNOWLEDGEMENTS

I would like to state my sincere gratitude to all my colleagues, teachers, and mentors who have helped me achieve this goal and my friends and family who have supported me during these years. In particular I want to thank Cindy, my mentor, who has helped me at every step of the way to grow into a diligent, analytic, and ever-curious scientist. Specific technical acknowledgements include Penny Berger who helped greatly with ChIP and some immunofluorescence experiments and Kellie Spahr who helped with the TetR-NICD1 vs NICD3 qRT-PCR experiment. Also thanks to Mats Ljungman whose lab ran the BrU-seq sequencing and analysis.

TABLE OF CONTENTS

LIST OF TABLES

LIST OF FIGURES

KEY TO ABBREVIATIONS

ActD	Actinomycin D
AR	Androgen Receptor
CDH1	Cadherin1, E-Cadherin
CHX	Cyclohexamide
CSL	CBF1/SuH/Lag-1 (also known as *RBPJ,* the official human gene name)
Dox	Doxycycline, an analogue of tetracycline
eRNA	enhancer RNA
IP	Immunoprecipitation
KGF	Keratinocyte Growth Factor / FGF7
NICD	Notch Intra-Cellular Domain
PCa	Prostate Cancer
PEG	Polyethylene Glycol
PIN	Prostatic Intraepithelial Neoplasia
PrEC	Prostate Epithelial Cell
PSA	Prostate Specific Antigen
RE	Restriction Enzyme
RNAi	RNA interference
rtTA	Reverse Tetracycline Trans Activator
shRNA	short hairpin RNA
siRNA	small interfering RNA
T-ALL	T-Cell Acute Lymphoblastic Leukemia
TetR	Tet Repressor
TRAMP	Transgenic Adeonocarcinoma of the Mouse Prostate

CHAPTER 1 — BACKGROUND

A. General prostate cancer background

i. Statistics and treatment options

Prostate cancer (PCa) is the most common non-skin cancer and second leading cause of cancer deaths in American men[1]. Currently there are approximately 180,000 new cases in the USA each year and about 26,000 deaths due to the disease. Age is one of the greatest risk factors for PCa; incidence rate increases as men age and most patients receive a diagnosis over the age of 65. About 80% of men have locally confined prostate cancer at the time of diagnosis[2]. Treatment for locally confined PCa is highly effective (>99% 5-year survival) and typically involves radiation therapy or removal of the prostate gland. However, for those patients that show metastatic disease at diagnosis, 5-year survival rates drop to ~28%[3]. Metastatic PCa has a propensity for metastasizing to the bone, which is the primary source of morbidity and mortality in late stage disease.

The standard treatment for metastatic PCa is androgen deprivation therapy, which uses drugs to ablate Testosterone levels in the body, which prostate tumors require for survival. This therapy often shows great effectiveness initially in reducing tumor burden for up to a few years, but relapse is virtually inevitable at which point the tumor has gained resistance to current anti-androgen therapies. In recent years new drugs that target androgen synthesis enzymes (e.g. Abiraterone) or the Androgen Receptor (AR) protein (e.g. Enzalutamide) have extended lifespan by a few months but still lead to resistance[4,5]. Further advances in immune-based therapies have also begun to show promise, though trials are ongoing and still seeking to improve the percent of patients that respond[6].

Due to the difficulty in treating metastatic PCa, a large effort has focused on screening to detect tumors as early as possible. Increased awareness and screening methods, including yearly physical examinations and Prostate Specific Antigen (PSA) testing have aided detection

of early stage tumors[7]. A positive screening result is followed by needle biopsy and tumor grade assignment using the Gleason score system. Though the Gleason score is a moderate predictor of tumor aggressiveness, even small, low grade tumors can potentially turn aggressive and metastasize[8]. With the push to focus on catching tumors as early as possible, the risk of overtreatment has more recently become a complex cause for concern.

Part of the explanation for why so many PCa tumors are caught early is that prostate tumors are often very slow-growing. The vast majority of men who live past 70 will have some form of prostate cancer, and most men will die of other causes without PCa ever becoming a life-threatening issue[9]. Moreover, for men diagnosed with locally-confined prostate cancer, those who opt for immediate prostatectomy only show slight benefit in survival (10% vs 14% chance of death due to PCa within 5-years) compared to those who forgo surgery, i.e. watchful waiting[7]. Thus, immediate aggressive treatment is most beneficial for younger patients or those with clearly identified high grade tumors. However, older patients with moderate grade tumors are much harder to predict.

When considering cancer therapies, it is crucial to consider not only absolute survival but also quality of life. PCa treatment is not without considerable personal as well as financial cost. The direct costs alone of surgery can range up to ~$45,000[10]. Additionally, treatment (radiation or surgery) carries serious, common side effects including incontinence, impotence, and psychological stress[11]. Other less common but serious risks of surgery include infection and even death[11]. For the majority of PCa patients, who are over 65 years old and show low or mid grade tumors, the decision to undergo surgery or watchful waiting is a very difficult one with potentially dire consequences.

ii. Challenges for the field

There are many areas of focus in the prostate cancer field, however most try to address three primary goals: 1) To better understand the risk factors for developing the disease; 2) To

help improve prognostic ability for patients with localized disease; and 3) To more effectively treat metastatic disease.

Risk factors for PCa have been identified but the mechanistic explanations for them have not been well understood. The primary risk factor is age, with most cases diagnosed above the age of 60[7]. However, other risk factors include having a first degree relative with the disease, being of African American descent, obesity, and a Western diet[12]. Additionally, genetic association studies have identified very few high-risk loci and a couple dozen lower-risk loci. However it is still not clear exactly how most of these risk loci affect gene expression and impact PCa[2,13].

For the second goal, efforts have been made to better classify prostate tumors in a way to predict indolent vs aggressive disease. Beyond Gleason score, there are few commonly accepted subtypes of PCa. One example of a clear subtype are neuroendocrine prostate tumors, which have a somewhat nebulous phenotypic characterization but clearly represent a more rare form of prostate tumors associated with highly castration-resistant disease[14,15]. It is not entirely clear if these neuroendocrine tumors represent a different cell of origin or trans-differentiation which may be an adaptation to anti-androgen therapies[16]. Other attempts to classify prostate tumors based on specific molecular signatures have shown some promise but have not resolved into clear-cut subtypes. Examples of such signatures include *TMPRSS2-ERG* fusions and hyper-methylation phenotypes, which will be discussed further in the next section[17].

As for the third goal of targeting metastatic disease, one fact that is clear about prostate tumors is their addiction to androgen signaling. For this reason, many strategies (including hormone ablation therapy) seek to target the AR pathway. The reason that hormone ablation eventually fails is due to a wide array of resistance mechanism tumors use for maintaining AR signaling. A few of such mechanisms include genomic amplification of *AR*, mutations causing ligand promiscuity, autonomous androgen synthesis, and *AR* splice variants that create constitutively active protein[18]. As previously mentioned there have been some advances in

using small molecules to target AR[4,5]. However, even these newest treatments are still ultimately met with tumor resistance.

Beyond *AR*, other targeted pathways include the PI3K pathway, which is commonly upregulated in prostate tumors due to PTEN loss. Though initial trials were ineffective, work from our lab has suggested that PI3K inhibition may still be viable in conjunction with other therapies to combat parallel survival pathways in tumors[19,20]. Another potential target is the DNA repair pathway, in particular PolyA-Ribose Polymerase (*PARP*). A subset of prostate tumors with *BRCA* mutations has proven to be especially sensitive to PARP inhibition[21].

Another overall goal of current research is to better understand the molecular origins of PCa. This achievement may allow new classifications for tumors and also identify new proteins for targeted therapies. Such knowledge will not only aid the selection of proper therapies for those with advanced disease, but it will also spare a large number of men from unnecessary surgery and diminished quality of life. With a better understanding of the genes commonly misregulated in PCa, and the signaling consequences thereof, researchers and physicians will be much better suited to treat this pervasive disease.

iii. Common genetic aberrations in PCa

While there are still no widely accepted subcategories of PCa, there are some established genetic alterations associated with the disease. Fundamentally, prostate tumors rely on *AR* signaling. However, as previously mentioned, targeting AR has proven very difficult. Beyond the *AR* alterations in advanced tumors, three of the most common genetic alterations in PCa are: overexpression of *MYC*, loss of the tumor suppressor *PTEN*, and fusion of *ETS* genes with upstream *AR* regulated promoter sequences (e.g. *TMPRSS2-ERG*)[22,23].

The *MYC* gene is commonly amplified in PCa (**Table 1**) and protein levels correlate with poor prognosis[24]. *MYC* is a well-studied oncogene that drives the expression of thousands of targets, including genes required for cell growth and cell cycle progression. *Myc* overexpression

in the mouse prostate is sufficient to drive adenocarcinoma but not metastasis[25]. The importance of *MYC* in PCa is well established, though not entirely understood, and will be discussed in further detail in a later section.

% 8q Gain[a]	**Tumor Type**	**Method**	**Citation**
38	Primary + LN met	SNP, qPCR	Liu, 2008[26]
27	Primary + LN met	CGH	Lapointe, 2007[27]
72	CRPC	CGH	Nupponen, 1998[28]
% 8q24 Gain[a]	**Tumor Type**	**Method**	**Citation**
9	Primary (LG)	FISH	Gurel, 2008[29]
28	Primary (HG)	FISH	Gurel, 2008
% *MYC* Gain[a]	**Tumor Type**	**Method**	**Citation**
77	CRPC	FISH	Nupponen, 1998[28]
21	Primary	DNA Array	Edwards, 2003[30]
63	CRPC	DNA Array	Edwards, 2003
Myc IHC Score	**Tumor Type**	**Method**	**Citation**
2.6	Normal	IHC	Gurel, 2008[29]
8.6	LG-PIN	IHC	Gurel, 2008
25.8	HG-PIN	IHC	Gurel, 2008
27.1	Primary	IHC	Gurel, 2008
14.9	Met	IHC	Gurel, 2008

Table 1: *MYC* overexpression in PCa. Summary of publications measuring *MYC* in prostate tumors. [a]percentage of tumors displaying the change. Abbreviations: LN, lymph node; CRPC, castration-resistant PCa; LG, low grade; HG, high grade; Met, metastasis

Another prevalent aberration in PCa is loss of the tumor suppressor PTEN (**Table 2**), a negative regulator of the PI3K pathway. At least one copy of the *PTEN* locus is lost in up to 70% of prostate tumors and complete loss of PTEN protein is seen in ~60% of late stage tumors[31-36]. Loss of one copy of *Pten* greatly increases PCa progression in the TRAMP mouse model and Pten dosage has a marked impact on tumor latency and progression[37,38]. Moreover, complete loss of *Pten* in the mouse prostate is sufficient to drive adenocarcinoma[39,40].

Activation of the ETS pathway is also a common occurrence in PCa (**Table 3**), most frequently through the fusion of the oncogene *ERG* downstream of the androgen-regulated promoter of *TMPRSS2*[41,42]. Specific genetic rearrangements that drive tumor progression are relatively rare in solid cancers, but the *TMPRSS2-ERG* fusion is a notable exception and is observed in about 50% of prostate tumors[27,36,43-46]. The identification of additional fusions of AR-driven promoters to other ETS members (as well as other targets) strongly suggests this type of rearrangement is a major driver of PCa[47-52]. This has important implications about the role of *AR* in prostate cancer development and may explain the dependency on *AR* for tumorigenesis. In the normal secretory epithelium, *AR* is primarily required for maintaining secretory functions and is not intrinsically required for survival or proliferation of the secretory epithelium[53,54]. In fact, *AR* is inhibitory to cell proliferation in normal cells[55,56]. But an opposite response is triggered in tumor cells, where both proliferation and survival depends on *AR*. The trigger is unknown, but prostate-specific oncogenes driven by *AR* are likely to be part of the answer.

% *PTEN* Del[a] (1x)	Tumor Type	Method	Citation
39	PIN	FISH	Yoshimoto, 2007[57]
20	Primary	FISH, CGH	Verhagen, 2006[35]
30	Primary	Sequencing	Barbieri, 2012[33]
31	Primary	FISH	Yoshimoto, 2013[36]
36	Primary	FISH	Lotan, 2011[34]
65	Primary	Sequencing, PCR	Gray, 1998[31]
% *PTEN* Del[a] (2x)	**Tumor Type**	**Method**	**Citation**
5	Primary	FISH	Yoshimoto, 2007[57]
6	Primary	FISH	Yoshimoto, 2013[36]
22	Primary + CRPC	FISH, PCR	Verhagen, 2006[35]
20	Met	FISH	Yoshimoto, 2006[58]
% Mutation[a]	**Tumor Type**	**Method**	**Citation**
4	Primary	Sequencing	Barbieri, 2012[33]
8	Primary	Sequencing	Verhagen, 2006[35]
14	Primary	Sequencing	Gray, 1998[31]
% Protein Loss[a]	**Tumor Type**	**Method**	**Citatiaon**
12	PIN	IHC	Lotan, 2011[34]
40	Primary	IHC	Lotan, 2011
40	Primary	IHC	Verhagen, 2006[35]
60	Met	IHC	Lotan, 2011

Table 2: *PTEN* loss in PCa. Summary of publications measuring PTEN expression in prostate tumors. [a]percentage of tumors displaying the change. Abbreviations: Del, deletion on one (1x) or two (2x) chromosomes; CRPC, castration-resistant PCa; Met, metastasis

% with Fusion[a]	Tumor Type	Method	Citation
13	PIN	qPCR	Furusato, 2008[45]
20	PIN	FISH	Perner, 2007[46]
45	Primary	FISH	Yoshimoto, 2013[36]
50	Primary	FISH	Perner, 2007
67	Primary	qPCR	Furusato, 2008
30	Met	FISH	Perner, 2007

Table 3: *TMPRSS2-ERG*-fusions in PCa. Summary of publications measuring *ERG* fusions in prostate tumors. [a]percentage of tumors displaying the change. Abbreviations: Met, metastasis

Thus, the contribution of *AR*-driven ETS activation and the mechanisms that drive tumor initiation and tumor progression are in need of much further investigation. The ETS family of transcription factors can potentially regulate a wide range of cellular processes, including development, differentiation, invasion, and proliferation[59]. Sun et al. reported that the *TMPRSS2-ERG* fusion activates *MYC* and prevents terminal prostate epithelial differentiation in the VCaP prostate cancer line[49]. Additionally, Yu et al. reported that ERG and AR binding sites have considerable overlap and ERG functions in part by disrupting AR binding to its target genes in VCaP cells[48]. Moreover, Yu et al. found that *ERG* activates *EZH2*, which is part of the polycomb repression complex and in turn down regulates an *AR*-driven differentiation program. The authors propose that *TMPRSS2-ERG* is likely to be an early mutational event that drives selection of cells with hyper activated or mutated *AR* to overcome the antagonistic effects of *ERG* activation on *AR*[48]. Conversely, Chen et al. used transgenic mice and reported that *Erg* activation aids *AR* signaling by increasing AR binding to target genes, though only in the context of *Pten* loss[60]. The Chen et al. group suggest that an explanation for the difference in their findings from those of Yu et al. is that the latter did their studies in VCaP cells, which retain *PTEN* expression. If the Chen et al. finding is to be believed, then *ETS* activation may be a later event that must follow *PTEN* loss. There are multiple mouse models of *Erg* overexpression, but only some of them produce PIN and none develop adenocarcinoma[47,61-63]. In the most aggressive model, overexpression of the N-terminal truncated *Erg* fusion product in luminal cells (via a modified *Probasin* promoter) produces PIN in about 40% of mice but still fails to drive adenocarcinoma[47]. The combination of *Erg* overexpression with single copy loss of *Pten* drives progression to adenocarcinoma but does not result in metastasis[61,62]. These findings from mouse models further support the idea that *ETS* activation is a later event in PCa progression and must follow *PTEN* loss. More research on *ETS* and its specific function in PCa tumorigenesis and/or progression are required to fully understand the significance of this common mutation.

In 2015, the publication of the The Cancer Genome Atlas study for PCa helped identify some other common alterations in PCa[17]. The study involved a thorough molecular analysis of 333 primary prostate tumors. In addition to the big three (*AR*, *MYC*, *PTEN*) the report included a few additional recurrent mutations, including *IDH1*, *SPOP*, and *FOXA1*. *IDH1* mutations cause a DNA hyper-methylated phenotype, while mutations in *SPOP* led to increased *AR* signaling. Interestingly, *SPOP* mutations were mutually exclusive with *ETS* fusion mutations. However, the specific function of *SPOP* is not clear, other than its function in an E3 ligase complex that somehow regulates *AR* activity. Despite this effort to identify new mutations and classify tumors based on key alterations, none of the molecular subtypes showed a clear association with tumor grade or aggressiveness.

As will be discussed in this chapter, genes that are frequently altered in prostate cancer (*MYC*, *PTEN*, *ERG*) can be tied to normal prostate differentiation. Likewise, key epithelial differentiation pathways (p38-MAPK, NOTCH) are also misregulated in human and mouse models of PCa. Thus I propose the overarching hypothesis of my thesis: <u>prostate tumors arise from a defect in epithelial differentiation of a transiently-differentiating prostate epithelial cell.</u> In the remainder of this chapter I will discuss what is known about MYC, p38-MAPK, and NOTCH with respect to their roles in both cancer and differentiation.

iv. Prostate structure and differentiation

To understand prostate oncogenesis you must have a grasp of the cellular organization of the organ. Prostate adenocarcinoma arises from the epithelia of the gland. Prostate epithelium is organized in a bi-layer of basal and luminal cells, along with a few rare embedded neuroendocrine cells (**Fig. 1**). The epithelium is surrounded by a laminin (LM5, LM10) and collagen (COL IV, COLVII) matrix and fibromuscular stromal cells which transmit signals to regulate the epithelium[64]. The prostate epithelium contains layer-specific markers, with the basal

layer characterized by p63, basal keratins (K5, K14), and integrins (α6β4, α3β1) among others. The luminal layer contains markers such as NKX3.1, luminal keratins (K8, K18), and AR.

Prostate tumors are characterized by a loss of basal cells and reduced matrix diversity (i.e. loss of LM5 and COLIV) (**Fig. 1**). Moreover, tumor cells generally express a luminal phenotype driven by *AR*. However, tumors also express basal integrins, especially α6β1 which is an abnormal pairing that drives PCa growth and survival[20,65]. Similarly, tumor cells often co-express basal and luminal keratins, such as K5 and K8[66-68]. Other basal markers reportedly expressed in tumor cells include BCL2, EGFR, and MET[69-74]. The co-expression of a subset of luminal and basal markers supports the hypothesis that prostate tumors arise from the disruption of normal differentiation pathways which normally restrict basal and luminal marker expression to their respective cell types. However, the cell of origin, i.e. the cell that is the oncogenic target that gives rise to the tumor, has not been clearly resolved in PCa.

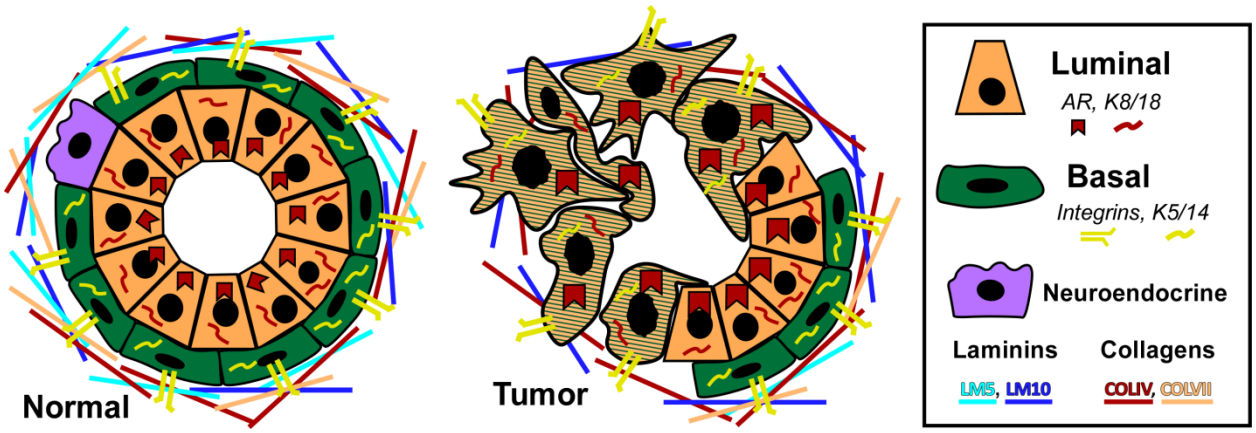

Figure 1: Prostate epithelial structure. The normal prostate epithelium is composed of a bi-layer of basal and luminal cells and a few rare neuroendocrine cells. The epithelium is separated from the underlying stroma by a basement membrane containing laminins (LM5, LM10) and collagens (COL IV, COLVII). Basal cells express integrins that specifically interact with the basement membrane, namely α6β4, α3β1, and α2β1 as well as basal keratins K5 and K14. Luminal cells do not express integrins, but express AR and keratins K8 and K18. A prominent characteristic of prostate tumors is the loss of basal cells and LM5/COLIV. Correspondingly, the integrins that interact with these matrices, α3β1 and α6β4, are lost via downregulation of the α3 and β4 subunits. Thus, integrin α6β1 remains which prefers the LM10 matrix. Similarly, tumor cells often co-express basal and luminal keratins, such as K5 and K8.

The struggle to define a clear cell of origin is complicated by the fact that the mechanism of prostate epithelial differentiation is not well understood. In the adult prostate, luminal cells are regularly shed and replaced by cells from the basal layer through differentiation[75]. A simplistic view of this observation is that a basal progenitor or stem cell gives rise to the both basal and luminal populations through a transient-differentiation or amplification process[66,76-78]. However, findings from mouse models paint a more complicated picture of basal, luminal, and bipotent progenitors. Ousset et al. utilized cell lineage tracing to clearly demonstrate the existence of layer-specific epithelial progenitor cells in the developing mouse prostate[79]. Wang et al. demonstrated that a luminal progenitor, marked by expression of Nkx3.1, resists luminal regression induced by castration and repopulates the majority of the mouse prostate during regeneration with androgen[80]. On the other hand, using tissue recombination and renal capsule implants, Leong et al. showed that a single prostate stem cell is able to produce both epithelial layers[81]. The Witte group also identified basal stem-like cells in the mouse prostate that produce both basal and luminal cells[82-85]. Other researchers identified a small population of bipotent progenitor cells that give rise to both basal and luminal cells[79,80]. These rare bipotent cells are marked by their co-expression of basal and luminal keratins (K5/K8) and are also found in the developing human prostate[79,86]. Thus, the mouse studies support the idea there are at least three different prostate epithelial progenitor populations, but which ones initiate prostate cancer still remains unresolved.

Several studies demonstrate either basal or luminal progenitors can be the initiating cancer cell. The Witte group demonstrated that oncogenic disruption in the basal cell population drives tumor formation in mice[87-89]. On the other hand, two groups reported that both basal and luminal epithelial cells can give rise to tumors upon knockout of *PTEN* [68,90]. Thus, mouse studies suggest distinct stem cell populations may be responsible for tumor initiation and seemingly disfavor the transient amplification theory. However, introduction of genetic mutations early in development and puberty in mice does not reflect the normal situation in humans were

oncogenesis occurs in a fully developed gland. Moreover, the signals and cell types that regulate gland maintenance vs. development may be different. Transgenic mouse models rely on Cre recombination via commonly used 'layer-specific' promoters, such as *K5* or *Nkx3.1*. Thus, these studies still leave open the possibility that it is not a pure basal or luminal cell that becomes oncogenic, but rather a bipotent or transient-differentiating cell expressing multiple layer markers. Moreover, the progenitor cell of origin and the progenitor cell of propagation for PCa may not be the same, though understanding the molecular origins of each will be paramount for understanding tumor initiation and progression.

While studies in the mouse are highly informative, translation of these findings to understanding the human organ is complicated due to a lack of models for studying human oncogenesis. The mouse model is useful for genetic manipulations, but it is not without limitations[91,92]. For example, mice are not prone to develop spontaneous prostate cancers like humans. Secondly, although the mouse and human prostate have similar cell types, the structure is different; the mouse prostate is lobular while the human is compact and consists of zones[93,94]. Additionally, there are far fewer basal cells in the mouse prostate and some luminal cells directly contact the basement membrane, unlike in humans where there is a continuous layer of basal cells. Based on these important differences, there is reason to consider that signaling mechanisms for differentiation in human and mouse epithelial cells may be different.

As an alternative to transgenic mouse models, some researchers are using human prostate cells and xenografts in mice to study prostate development and differentiation. The Cunha group found that human basal cells can be induced to form a basal and luminal bilayer when combined with rat urogenital sinus mesenchyme and implanted in the mouse renal capsule[95]. The Witte group developed a similar method to isolate and genetically modify epithelial progenitor cells from human prostates[96]. The isolated progenitor cells were infected with virus to allow manipulation of desired oncogenes/tumor suppressors, and then the cells were implanted into mice along with stroma. Using this approach, they found that the induction

of AKT and ERG in human basal progenitors is sufficient to induce PIN, a PCa precursor lesion, when xenografted into mice[87]. Other groups are inducing the differentiation of primary basal cells *in vitro*, including our group which has developed a reliable *in vitro* differentiation model that recapitulates many aspects seen *in vivo*[71,97-99]. These reports demonstrate that human basal cells can be induced to differentiate into luminal cells *in vitro,* thus providing a model to study epithelial differentiation in a controlled setting using human cells. The ability to manipulate cells i*n vitro* during differentiation and then implant them into mice provides a useful approach to study how manipulation of trans-differentiating human prostate epithelial cells can become tumorigenic.

Based on the building knowledge of normal prostate differentiation, as well as findings from other epithelial tissues, it is becoming apparent that many of the pathways involved in normal epithelial differentiation are misregulated in PCa. In the remainder of the chapter I will describe in more depth how some of these key pathways are involved in both differentiation and cancer, with the goal of illuminating how prostate oncogenesis in humans may arise from a disruption of normal differentiation. Furthermore, aggressive tumors are pathologically characterized by a less differentiated phenotype, and the aggressiveness of the tumor may be tied to its cell of origin[68,90]. Better understanding of prostate differentiation pathways will help us understand how the normal cellular process goes awry in cancer. The ultimate goal of this work is to aid prognostic ability and predict which tumors will be most likely to rapidly progress and which will not. I envision a future where tumor grade will not be based solely on histological classification, but also on expression analysis of key differentiation pathways to better understand tumor origin.

B. MYC

i. Background

The general importance of *MYC* in PCa is well established, but it is less clear precisely how *MYC* drives tumor initiation and progression[24]. In addition to its oncogenic role, *MYC* is also crucial for promoting epithelial differentiation[100-102]. Knowledge about normal prostate differentiation is limited, and much of it is based on mouse studies. More detailed investigations into the role of *MYC* in prostate differentiation may help us understand how its misregulation leads to PCa.

There are three genes in the MYC family: *c-MYC*, *N-MYC*, and *L-MYC*. *c-MYC* (*MYC*) is the best studied and most relevant in PCa. *MYC* is a basic helix-loop-helix transcription factor that typically functions as a heterodimer with a cofactor from the MAX or MIZ families[103]. Transcriptional regulation by *MYC* is mediated through recruitment or activation of basal transcription machinery, promoting RNA Polymerase II elongation, or through recruitment of chromatin modifying enzymes[104,105]. The MYC/MAX heterodimer is usually a transcriptional activator complex that competes with MAD/MAX dimers for binding at E-box sites, the classic regulatory element recognized by MYC complexes. MYC also represses genes by binding with SP1 or MIZ1, which together repress transcription by blocking p300[106,107]. Alternately, MYC can repress targets post-transcriptionally via activation of miRNAs[108,109].

MYC is downstream of many pathways and is tightly regulated at the mRNA and protein levels[106,110]. *MYC* mRNA and protein have short half-lives, and higher activity is usually associated with lower stability[111]. *MYC* potentially regulates thousands of genes, with one estimate predicting as much as 15% of the genome[112,113]. While there are thousands of potential targets for *MYC*, its functional role in cellular processes is highly dependent on the level of expression, duration of activation, and expression of its cofactors.

ii. Role in PCa

The vast majority of prostate tumors overexpress *MYC* (**Table 1**), which correlates with poor prognosis[24,114,115]. While *MYC* mRNA is elevated in as many as 80% of prostate tumors, there is less certainty about MYC protein levels[24]. The de Marzo group published a study showing that MYC protein expression is very low in normal prostate epithelium but higher and more nuclear localized in PIN and prostate tumors[29]. The most common mechanism of *MYC* overexpression is through amplification of the gene locus, usually through gain of 8q. The narrower *MYC* region 8q24 is more selectively amplified in late metastatic tumors[23,26,27,116-118]. However, early prostate tumors also overexpress *MYC* but rarely have *MYC* amplifications, suggesting other mechanisms driving *MYC* overexpression which are less well understood[24]. *MYC* amplification is specifically observed in castration resistant tumors[28,30]. Bernard et al. demonstrated that *MYC* overexpression in the hormone-sensitive LNCaP line confers resistance to androgen deprivation or *AR* knockdown[119]. Conversely, *AR* knockdown decreases *MYC* expression, indicating *MYC* is downstream of *AR*. In another study, the ability of AR to upregulate *MYC* was ligand independent[120]. Alternatively, *MYC* reportedly upregulates *AR*, suggesting there may be feedback mechanisms between the two genes[121,122].

Another potential mechanism for *MYC* upregulation is via β-catenin, the downstream target of WNT signaling. Constitutive β-catenin is sufficient to upregulate *Myc* and induce prostate tumor formation in a mouse model[123]. Furthermore, the *APC* gene (an antagonist of β-catenin) is often silenced by hypermethylation in at least 50% of human prostate tumors[124,125]. However, the specific role of *APC* and β–catenin in human PCa is still unclear and it is unknown if the potential oncogenic activity is due to *MYC* upregulation. As will be discussed later, some groups report increased NOTCH signaling in prostate tumors, which may also drive transcription of *MYC* as is the case in T-cell acute lymphoblastic leukemia[126,127].

Myc overexpression in the mouse prostate with a weak promoter drives low grade PIN but not adenocarcinoma[128]. Using stronger variants of the *Probasin* promoter to regulate *Myc* overexpression in luminal cells, researchers were able to drive progression to adenocarcinoma though not metastasis[25]. In this model, when *Myc* is driven by the endogenous *Probasin* promoter (Lo-Myc) mice take much longer to develop tumors than those with a stronger promoter (Hi-Myc)[25]. Finally, mice with knockout of *Mxi1* (a Myc antagonist) show prostate dysplasia but do not develop adenocarcinoma[129]. All together, these models demonstrate that *Myc* can drive PCa in the mouse, and the level of Myc expression is related to the aggressiveness of carcinoma that develops.

MYC has many potential oncogenic and tumor-promoting targets. One group of genes known to be regulated by *MYC* is cell cycle regulators, such as E2F members, cyclins, and cyclin-dependent kinases[130]. Additionally, *MYC* can regulate cell growth by upregulating tRNAs and rRNAs[130]. Other important targets of *MYC* include stem cell genes, such as *TERT* and *EZH2*[24,48,130]. *MYC* is one of the four original genes whose overexpression was initially used to create pluripotent stem cells, along with *OCT4*, *SOX2*, and *KLF4*[131]. Although overexpression of *MYC* was later found not to be necessary for stem cell induction, MYC activity is required for embryonic stem cell self-renewal[132-135]. Another key point regarding *MYC* is that the level and timing of its expression is critical for deciding what function the protein will play, for example deciding whether *MYC* drives proliferation or stem cell maintenance[130]. However, which of these targets is critical for PCa development and progression is not clear. In summary, *MYC* amplification is common in late metastatic tumors and can act as a driver in mouse models but specific mechanisms of *MYC* regulation and downstream targets are poorly understood.

iii. Role in differentiation

Beyond its multifaceted role in cancer, *MYC* is also important for differentiation. A shift from MYC/MAX to MAD/MAX binding is associated with terminal differentiation[136,137]. Transient

expression of *MYC* aids induced pluripotent stem cell transformation while sustained expression stimulates down regulation of integrin α6 and drives differentiation of embryonic stem cells[138]. In keratinocyte differentiation, MYC protein is expressed in the basal layer and decreases during differentiation of the suprabasal layers[139,140]. On the other hand, knockdown of *MYC* prevents *in vitro* keratinocyte proliferation while transient overexpression induces premature terminal differentiation[141-143]. Overall a short, high spike in MYC appears to be required for proliferation, while a more moderate and extended increase in MYC is characteristic for differentiation[101]. Supporting this idea, our lab published a paper in 2014 showing that transient expression of *MYC* is required for normal prostate differentiation, in part due to its upregulation of *ING4*, a chromatin remodeler and tumor suppressor in PCa[102]. However, the myriad of other functions for *MYC* signaling during prostate differentiation are still to be elucidated.

One mechanism by which *MYC* triggers differentiation is through its control of a cell adhesion program. About 40% of the genes downregulated upon *MYC* activation in mouse skin are involved in cell adhesion and cytoskeleton, including integrins α6, β1, and β4[144]. Integrin expression is lost as cells from the basal layer rise into upper layers during keratinocyte differentiation[145]. This adhesion profile is largely regulated via *MIZ1*, given that a *MYC* mutant unable to bind MIZ1 loses the ability to suppress integrin α6 and β1 transcription[142].

Another mechanism by which *MYC* may regulate differentiation is via interactions with chromatin remodeling proteins[105,146,147]. Chromatin modifications are often associated with cell programming, such as patterns for stem or terminally differentiated cells[147,148]. Pellakuru et al. published a study looking at *MYC* and H3K27me3 in prostate differentiation and cancer[147]. H3K27me3 is a marker of polycomb activity, which induces heterochromatin and gene repression. The group reported that basal prostate cells have lower levels of H3K27me3 than luminal cells as determined by immunostaining with human tissue sections[147]. Furthermore, using a tissue micro array they also found that cases of human PIN show decreased H3K27me3 compared to normal luminal cells. Levels of H3K27me3 are also decreased in prostate tumors

from Hi-Myc mice. Additionally, they showed that *MYC* knockdown in the PC3 and LNCaP prostate cancer lines leads to an increase in H3K27me3[147]. The authors were unable to provide a mechanism for how *MYC* controls H3K27me3, but they previously reported that *MYC* upregulates *EZH2*, which is the catalytic member of the polycomb complex and is often overexpressed in PCa[147,149]. However, *EZH2* overexpression does not correlate with higher H3K27me3 levels in this study, which led the authors to propose that regulation of *EZH2* activation may be a separate event[147]. Seemingly answering the idea proposed by Pellakuru et al., a later study reported that EZH2, upon phosphorylation at Ser21, plays a non-polycomb role in castration resistant PCa acting as an AR coactivator[150].

vi. Conclusions

MYC amplifications are very common in advanced prostate tumors but *MYC* is also upregulated in early tumors through currently unknown mechanisms[24]. Normal upregulation of *MYC* is required for proliferation and differentiation, and it is the level and timing of *MYC* expression that largely determines which of those decisions the cell will make[101]. The upregulation of *MYC* seen in PCa may explain how tumors arise from a transient amplifying or differentiating prostate cell which requires a temporary upregulation of MYC expression [102]. However, additional oncogenic events are required to prevent terminal differentiation and death due to the oncogenic stress of sustained MYC activation[106]. As typically happens with other cancers, loss of p53 can relieve apoptotic stress; however, p53 loss is a fairly rare event in primary prostate tumors (~8%) and is usually only seen in a small subset of metastatic tumors[17,151]. Thus, other yet to be identified mechanisms must be involved in PCa development. Abnormal *MYC* expression and its role in regulating a cell adhesion program may also help explain why prostate tumors show a large general loss in integrin and matrix expression, except for the retention of the tumor-promoting integrin α6β1 pairing[20,142,144]. Additionally, prolonged *MYC* activation in a transient-differentiating cell may drive changes in chromatin structure, as

evidenced by the fact that basal and intermediate prostate cells show low levels of heterochromatin markings compared to tumors[147]. There is accumulating evidence to suggest that MYC contributes to an altered differentiation program in PCa, but more studies are required to work out particular mechanisms.

C. p38-MAPK

i. Background

The three classic branches of mitogen-activated protein kinase (MAPK) signaling are p38-MAPK (p38), ERK, and JNK. MAPK signaling involves kinase cascades that control a wide range of functions in the cell including proliferation, stress response, and differentiation[152]. The MAPK pathways can regulate gene expression through a variety of mechanisms at the RNA and protein levels. ERK signaling is most classically associated with growth factor signaling, while JNK and p38 are commonly associated with stress responses to insults such as inflammation and radiation[153]. p38 and JNK have specific direct upstream kinases: MKK3/6 activate p38 and MKK4/7 activate JNK (though MKK4 can potentially activate p38 in some cases)[152]. However, p38 and JNK share some common activating kinases further upstream, such as ASK1 and TAK1[153]. This upstream convergence makes identifying the contribution of each pathway difficult. In epithelial differentiation, upstream p38 activation is via activation of the receptor tyrosine kinase FGFR2, specifically the FGFR2b/FGFR2IIIb isoform, by KGF/FGF7 or FGF10 ligands[97,154,155]. MAPKs are also negatively regulated by a host of MAPK phosphatases which inactivate MAPK members[156]. While the MAPK pathways share some overlapping features, p38 has a distinctive role in epithelial differentiation[152].

There are four isoforms of p38: *MAPK14* (p38α), *MAPK11* (p38β), *MAPK12* (p38γ), and *MAPK13* (p38δ). They share ~60% homology and have some compensatory ability, though they also have differential target preferences[152]. p38α is ubiquitously expressed, while p38β is moderately expressed in many tissues and p38γ/δ are more tissue specific. The p38 kinases can signal through many different effectors, including other kinases, phosphatases, transcription factors, and mRNA binding proteins[152]. Due to this range of potential targets, p38 can regulate gene expression at the transcriptional, post-transcriptional, and post-translational levels.

ii. Role in PCa

There are a handful of studies that investigated p38 signaling in PCa (**Table 4**). Unfortunately, most studies only interrogate p38α (referred to generally as p38). In the TRAMP mouse model of prostate cancer, Uzgare et al. reported that p38 is highly activated in PIN lesions and more well-differentiated tumors but is absent in late stage and metastatic tumors[157]. However, most other studies report that p38 activation correlates with PCa progression and treatment with a p38 inhibitor in a rat prostate cancer model led to decreased angiogenesis and reduced tumor formation[158]. Utilizing 25 primary prostate tumors and a combination of immunoblotting, ELISA, and IHC, Royuela et al. reported that phospho-p38 (p-p38) is upregulated in prostate tumors[159]. Based on immunoblot analysis, tumors showed ~50% higher expression of p-p38 than normal prostate. Furthermore, about 17% of normal prostate epithelium stains positive for p-p38 while nearly 90% of the tumor samples were positive[159]. Additionally, a report by Lotan et al. demonstrated that MKK4 and MKK6 proteins are minimally expressed in normal prostate luminal cells, moderately expressed in basal cells, and highly upregulated in PIN lesions[160]. However, this study did not look specifically at the active (phosphorylated) MKK proteins and also found that total MKK4/6 levels are not statistically different in low vs. high grade tumors[160]. Ricote et al. looked at upstream (MKK6) and downstream (ATF2, ELK1) p38 targets in PCa progression[161]. They reported that MKK6 is not detected in normal prostate samples, but it appears upregulated in PCa. Also, they detect p-ATF2 and p-ELK1 protein in normal basal cells but expression of both is higher in PCa (~2.5 and ~3 fold, respectively). ATF2 and ELK1 are also potential JNK targets, but the authors did not detect any JNK in the PCa samples so they attributed all of the ATF and ELK activation to p38[161]. Together, these reports suggest upregulated p38 activity in PCa progression, at least in part due to upregulation of the upstream activating kinases, such as MKK6.

p-p38α Protein[a]	Tumor Type	Method	Citation
1.0	Normal	WB	Royuela, 2002[159]
1.2	BPH	WB	Royuela, 2002
1.5	Primary	WB	Royuela, 2002
1.0	Normal	IHC	Royuela, 2002
3.5	BPH	IHC	Royuela, 2002
5.0	Primary	IHC	Royuela, 2002
MKK4 Protein[b]	**Tumor Type**	**Method**	**Citation**
0.3	Normal	IHC	Lotan, 2007[160]
2.4	HG-PIN	IHC	Lotan, 2007
0.7	Normal	IHC	Lotan, 2007
1.9	Primary	IHC	Lotan, 2007
MKK6 Protein[c]	**Tumor Type**	**Method**	**Citation**
1.0	Normal	IHC	Lotan, 2007[160]
2.6	HG-PIN	IHC	Lotan, 2007
0.9	Normal	IHC	Lotan, 2007
2.0	Primary	IHC	Lotan, 2007
29.0	BPH	WB	Ricote, 2006[161]
70.0	Primary	WB	Ricote, 2006
p-ELK1 Protein[c]	**Tumor Type**	**Method**	**Citation**
13	Normal	WB	Ricote, 2006[161]
47	BPH	WB	Ricote, 2006
34	Primary	WB	Ricote, 2006
p-ATF2 Protein[c]	**Tumor Type**	**Method**	**Citation**
5	Normal	WB	Ricote, 2006[162]
14	BPH	WB	Ricote, 2006
22	Primary	WB	Ricote, 2006
% MKP1 Protein[d]	**Tumor Type**	**Method**	**Citation**
100	PIN	ISH	Loda, 1996[163]
94	Primary (LG)	ISH	Loda, 1996
28	Primary (HG)	ISH	Loda, 1996
0	Met	ISH	Loda, 1996
100	BPH	IHC	Rauhala, 2005[164]
12	Primary	IHC	Rauhala, 2005
3	CRPC	IHC	Rauhala, 2005

Table 4: p38 signaling pathway alterations in PCa. Summary of published reports. [a]relative to normal samples. [c]average intensity. [b]IHC score, +1, +2, +3. [d] % of tumors staining in med-high range. Abbreviations: CRPC, castration-resistant PCa; LG, low grade; HG, high grade; Met, metastasis

MKP-1 (*DUSP1*) is a nuclear MAPK phosphatase that antagonizes JNK and p38α/β activation[156]. Several reports indicate *MKP-1* is overexpressed in early prostate tumors but is downregulated in high grade and castration resistant tumors, as well as a portion of PIN lesions[163-167]. MKP-1 can be activated by p38 in a negative feedback mechanism, so it is possible that down regulation of *MKP-1* may be a necessary precursor to p38 upregulation in more advanced PCa tumors[168].

IL-6, a key regulator of inflammation, is also linked with PCa and p38 signaling[169-172]. Ueda et al. reported that IL-6 activates transcription of *AR* targets in a p38-dependant manner in LNCaP cells[169]. Ricote et al. reported that TNFα, a cytokine and known activator of MAPK stress response, induces apoptosis in LNCaP cells but not PC3. Moreover, TNFα activates p38 in LNCaP cells, and p38 inhibition increases apoptosis[162]. Building on that finding, Gan et al. reported that LNCaP cells can be sensitized to docetaxel by blocking p38, which prevents p53 activation and apoptosis[173]. Moreover, this was not observed with PC3 or DU145 cells, which do not have functional p53. These findings were supported by a second group which further investigated the role of p53 in docetaxel resistance in the same cell lines[174]. Thus, over-activation of p38 is likely to trigger an apoptotic response without additional pathway alterations to compensate, which may include p53 loss in a subset of late PCa tumors but also likely involves other unknown mechanisms.

Though the FGFR2b receptor is crucial for differentiation, there are reports suggesting that growth factors such as EGFR and IGF1R can also activate p38[175-177]. Prostate tumors often show downregulation of *FGFR2b* and *KGF* and upregulation of other FGFs and FGFRs which drive proliferation[178]. Overexpression of *Fgf10* in mouse prostate stromal cells causes adenocarcinoma when combined with normal mouse prostate epithelium and implanted in the mouse renal capsule[179]. Furthermore, the degree of tumor progression correlated with the amount of *Fgf10*-expressing stroma implanted, suggesting a dose-dependent function of *Fgf10*[179]. Additionally, the *Fgf10* driven tumors are more resistant to androgen deprivation. This

group also found that blocking Fgfr1 activation in the epithelium with a dominant-negative mutant rescued oncogenic transformation, while dominant negative *Fgfr2* only moderately reduced invasion[179]. Moreover, another study reported that Fgfr1 activation in prostate epithelium could drive PCa in the mouse[180]. Whether the ability of *Fgf10* or *Fgfr1* to drive tumorigenesis is dependent on p38 was not determined. Thus, it is likely that the oncogenic potential of *Fgf10* is not through Fgfr2b. Together, these findings support the idea that Fgfr2b, which is a potential tumor suppressor in the prostate, inhibits tumor formation by driving differentiation (via p38) instead of proliferation (via other MAPKs or PI3K)[181]. Moreover, alternate mechanisms of upstream p38 activation may contribute to PCa progression.

iii. Role in differentiation

p38 promotes differentiation in a range of tissues including intestine, lung, bone, and cornea[182-185]. Most research has focused on p38α and much less is known about the expression of specific p38 isoforms in the prostate. I detected mRNA for all four isoforms in human prostate epithelial cells, but protein only for p38α and p38δ; the latter of which is often associated with endocrine glands but is also expressed in other epithelium such as skin[186]. *p38α* null mice are embryonic lethal, while *p38γ* or *p38δ* knockout results in apparently normal mice[187,188]. Despite the lack of an obvious phenotype, Schindler et al. that found *p38δ*$^{-/-}$ mice have normal skin but are resistant to skin tumor formation[189]. While p38δ may have overlapping functions with p38α, there is evidence that it also has some unique functions that are not well defined[189,190].

How p38 regulates epithelial differentiation is not well understood. In muscle differentiation, p38α/β (and possibly p38γ) activate MYOD and MEF2 transcription factors and the SWI-SNF chromatin remodeling complex, both of which are required for muscle differentiation[191]. Other roles for p38 include inhibiting proliferation, which is a necessary prerequisite for differentiation[192-194]. More specifically, p38 activity represses ERK and JNK phosphorylation, which is reported to be a cellular switch from proliferation to

differentiation[190,193,195]. While p38 is essential in a range of differentiation models, investigation of its role in prostate differentiation is lacking, as is an understanding of the contribution of specific isoforms. However, p38 and its role in other differentiation models may serve as a good starting point for further investigation within the prostate.

Unlike other growth factors, KGF is an epithelial-specific differentiation factor that is typically secreted by surrounding stroma[196-198]. KGF and FGF10 bind the same receptor, FGFR2b, and share many overlapping functions including upstream activation of p38 signaling[97,154,155]. KGF or FGF10 is sufficient to drive prostate differentiation *in vitro*[71,97]. In mouse knockout models, *Fgf10* and *Fgfr2* are both required for proper development of the prostate[199,200]. Additionally, *Fgf10* overexpression can drive tumor formation as previously discussed, suggesting that the dosage of Fgf10 is very important for proper prostate homeostasis[179]. Thus, FGFR2b signaling through p38 is likely a critical step for prostate differentiation and aberrant expression of FGF ligands and receptors promotes PCa.

iv. Conclusions

p38 activation correlates with PCa progression in many reports[159] (**Table 4**). Activation of p38 in PCa may be due to a combination of upregulated upstream kinases (MKK3/6) and downregulated MAPK phosphatases[160,165-167]. MKP-1 (*DUSP1*), which targets p38α/β, is often downregulated in late stage PCa tumors, which suggests p38δ may act as an early oncogenic activator while p38α is a later event. However, p38δ appears to play a tumor suppressive role in mouse skin and it would be useful to investigate p38δ in prostate tumors to see if its loss correlates with p38α overexpression[189]. Alternatively, the role of p38 in PCa may be dictated by its activating receptor as more aggressive prostate tumors shift from expression of FGFR2b to FGFR2c, which would prevent differentiation and induce proliferative signals[181]. Over-activated p38 may drive basal cells to differentiate prematurely, which may partially explain the lack of basal cells in PCa tumors and the mixture of basal and luminal markers in cancer cells.

D. NOTCH

i. Background

NOTCH is well known for its role in cell fate decisions, such as stem cell renewal, development, and differentiation[201]. There are four NOTCH transmembrane receptors in rodents and mammals, NOTCH1-4, that are activated by transmembrane ligands on adjacent cells[202]. In mammals, there are five classic ligands from two families: Jagged (*JAG1/2*) and Delta-like (*DLL1/3/4*). Recent work demonstrates that NOTCH signaling can also be activated by a variety of non-canonical proteins, such as DLK1/2, LRP1, and TPS2[203]. Initially, the NOTCH receptor protein undergoes a cleavage event upon emergence from the endoplasmic reticulum and is then transported to the cell membrane. Upon ligand binding a second cleavage is initiated by ADAM10 and a final cleavage by the γ-secretase complex. The cleaved C-terminal receptor fragment, known as the NOTCH Intracellular Domain (NICD), translocates to the nucleus where it binds the repressive CSL protein (named for its orthologs: CBF1/Su(H)/Lag1 also known as *RBPJ,* the official human gene)[202].

The NICD/CSL complex recruits co-activators such as Mastermind-like (MAML1/2/3) and p300 which trigger a switch from repression to activation of the classic NOTCH target genes of the hairy and enhancer of split (HES) family: *HES1-7* and *HEY1/2/L*[204]. After activating transcription, the NICD fragment is quickly degraded and the HES/HEY transcriptional repressors typically function in negative feedback by repressing their own genes, thus critically controlling the temporal regulation of NOTCH. NOTCH/CSL also directly activates transcription of other targets, including *p21/CDKN1A* and *MYC* [205]. While there is overlap, the four different receptors appear to have some differential preferences for ligands and downstream targets, though these details are not thoroughly resolved[202,206,207]. Adding to the complexity, NOTCH and CSL are reported to have some independent functions and do not always require each other for signaling[208-211]. In addition, there are further mechanisms of NOTCH regulation, such as

endosomal and proteosomal turnover of the receptor as well as post-translational modifications of the ligands and receptors[202,204,212].

ii. Role in cancer

The NOTCH pathway is misregulated in many cancers, though the type of misregulation is tumor and cell-type specific[213,214]. The most studied model is T-cell Acute Lymphoblastic Leukemia (T-ALL), where NOTCH signaling is over activated in the majority of tumors[215-217]. Conversely, in other cancers such as cutaneous and lung squamous cell carcinoma NOTCH is understood to be a tumor suppressor[218]. *Notch1* loss drives skin cancer progression in mice in a non-cell autonomous matter due to loss of barrier cell function, which triggers an immune and growth cytokine response within the microenvironment[219].

Within the prostate cancer field there are conflicting reports about whether the NOTCH pathway is tumor suppressive or oncogenic[201,220,221]. Supporting the case for NOTCH as a tumor suppressor, Belandia and colleagues reported that HEY1 and HEYL are excluded from the nucleus upon the transition from benign to carcinoma in human prostate samples[222,223] (**Table 5**). Furthermore, the same group showed that HEY1 and HEYL bind to AR and potentially function as AR co-repressors in LNCaP cells[223]. Other studies similarly found a decrease in NOTCH1 and HEY1 protein in human PCa tumors compared to normal tissue[224,225].

Conversely, several reports demonstrate increased levels of JAG1 and NOTCH1 protein in high grade PCa tumors, implicating NOTCH as an oncogene[126,127,226,227] (**Table 5**). Bin Hafeez et al. observed higher NOTCH1 protein staining in more aggressive prostate tumors. Moreover, knockdown of *NOTCH1* in PC3 cells decreases metastatic gene expression and decreases invasion *in vitro*[127]. Furthermore, knockdown of *CSL*, which ablates downstream NOTCH activity, leads to decreased proliferation in PC3 prostate cancer cells[228]. Other groups reported that siRNA knockdown of *NOTCH1* or *JAG1* in PC3 cells decreases PC3 growth and colony formation, in part due to an increase in cell death[229,230].

% HEY1 Nuclear [a]	Tumor Type	Method	Citation
93	BPH	IHC	Belandia, 2005[222]
20	Primary	IHC	Belandia, 2005
% HEYL Nuclear [a]	**Tumor Type**	**Method**	**Citation**
100	BPH	IHC	Lavery, 2011[223]
22	Primary	IHC	Lavery, 2011
JAG1 Protein[b]	**Tumor Type**	**Method**	**Citation**
1.0	BPH	IHC	Zhu, 2013[126]
2.1	HG-PIN	IHC	Zhu, 2013
0.9	Primary (LG)	IHC	Zhu, 2013
3.0	Primary (HG)	IHC	Zhu, 2013
3.8	Met	IHC	Zhu, 2013
1.0	BPH	IHC	Santagata, 2004[226]
1.2	Primary	IHC	Santagata, 2004
1.6	Met	IHC	Santagata, 2004
NOTCH1 Protein[b]	**Tumor Type**	**Method**	**Citation**
1.0	BPH	IHC	Zhu, 2013[126]
1.4	HG-PIN	IHC	Zhu, 2013
1.0	Primary (LG)	IHC	Zhu, 2013
2.2	Primary (HG)	IHC	Zhu, 2013
4.4	Met	IHC	Zhu, 2013
NICD1 Protein[b]	**Tumor Type**	**Method**	**Citation**
3.6	Normal - Basal	IHC	Whelan, 2009[225]
2.7	Normal - Luminal	IHC	Whelan, 2009
1.1	Primary	IHC	Whelan, 2009
% NOTCH3hi	**Tumor Type**	**Method**	**Citation**
23	Primary (GG <3)	IHC	Danza, 2013[231]
95	Primary (GG >4)	IHC	Danza, 2013

Table 5: NOTCH signaling in PCa. Summary of publications. [a]percentage of tumors with nuclear staining. [b]relative to benign samples. [c]percentage of tumors with high staining. Abbreviations: LG, low grade; HG, high grade; Met, metastasis; GG, Gleason Grade

While most research has focused on NOTCH1 or overall NOTCH activity, there are also a few papers reporting a specific role for NOTCH3 in PCa. Using prostate tumors with known patient outcome, Long et al. found *NOTCH3* mRNA levels positively correlate with PCa recurrence[232]. Moreover, of a 12-gene mRNA panel, *NOTCH3* has the 2nd highest prognostic ability for recurrence[232]. Ross et al. reported that *NOTCH3*, *JAG2*, and *PSEN1* (a catalytic subunit of the γ-secretase complex) mRNA transcripts are upregulated in high grade prostate tumors [167]. NOTCH is also implicated in PCa via a role in hypoxia. Exposure of LNCaP, PC3, and DU145 cell lines to prolonged hypoxia leads to down regulation of *NOTCH1/2* mRNA and protein but has no effect on *NOTCH3*[233]. A follow up report found that hypoxia also induces changes in cholesterol and lipid rafts in the cell membrane, which increases colocalization of NOTCH3 and γ-secretase and in turn activated NICD3[231]. The study also measured NOTCH3 protein levels in PCa tumor sections and found NOTCH3 protein levels correlate positively with Gleason grade, thus supporting the *NOTCH3* mRNA correlation reported by Long et al.[231,232].

iii. Role in differentiation

When it comes to cell fate decisions, NOTCH signaling is critical across most cell types. The NOTCH pathway has been studied in the prostate to some extent, but knowledge about specific mechanisms and signaling pathways is lacking. Many studies have been conducted in the mouse which, as discussed earlier, has some significant structural differences from the human. Treatment of rat prostates *ex-vivo* with a γ-secretase inhibitor prevents lumen formation and treatment with the inhibitor *in vivo* prevents prostate regeneration following castration[229]. A similar finding was reported for mouse prostates treated with γ-secretase inhibitors[234]. As for receptor-specific studies, *NOTCH1* has been the most studied. Wang et al. used an interesting model where they made a transgenic mouse with a lethality gene (bacterial nitroreductase) under control of the *Notch1* promoter, which would only be lethal in the presence of an inducing chemical[229]. They took early developing mouse prostates and grew them *ex vivo* with or without

the inducer and found that ablation of *Notch1*-expressing cells prevents proper organoid development and differentiation[229]. In a follow up study, they utilized γ-secretase inhibitors and an interferon-inducible *Notch1* mouse (Mx-Cre/Notch1^{flox}) to study the effect of *Notch1* loss on prostate development[224]. They found that induced *Notch1* knockout (in all cells of the prostate including the stroma) leads to increased proliferation and prostatic hyperplasia as well as co-expression of basal and luminal keratins[224]. Moreover, Wu et al. utilized transgenic mice to investigate NOTCH in prostate development, reporting that Nkx3.1-Cre driven *Csl* knockout leads to decreased proliferation and differentiation defects in the prostate[235]. Conversely, *Notch1* constitutive activation (via Pb-Cre or Nkx3.1-Cre driven NICD1) in the mouse prostate causes increased proliferation and hyperplasia[235]. Both of these studies suggest that NOTCH signaling is required for proper differentiation, while *NOTCH1* specifically appears to be crucial for maintenance of a proper and distinct basal layer. *NOTCH1* also regulates *p63*, which is a classic basal marker in the prostate and a regulator of cell adhesion, including integrins[236-238]. Therefore it is intriguing to consider that NOTCH signaling during prostate differentiation may need to strike a balance between downregulating adhesion through p63 while NOTCH1 must also maintain homeostatic basal cells. The balance between multiple NOTCH receptors and downstream targets may be crucial for regulating the decision to stay basal or differentiate.

Studies on other NOTCH receptors in the mouse prostate are limited; though there are some studies in other tissues. *Notch3* knockout mice develop normally, suggesting its loss can be compensated[239]. Also, the NICD3 appears to be a weaker activator of downstream signaling than NICD1 and may actually antagonize NICD1 by competing for CSL[240]. Dang et al. reported that constitutive *Notch3* expression (via NICD3) in mouse lung epithelium prevents terminal differentiation and causes metaplasia and reduced epithelial branching[241]. In esophageal differentiation, NOTCH1 activates *NOTCH3*, which in turn activates *HES5* and drives differentiation[242]. In skin differentiation, NOTCH1/2/3 have all been detected in the interfollicular epidermis, but there is a shift in ligands from JAG2 in the basal layer to JAG1 in the upper

layers[243]. Moreover, in the hair follicle NOTCH1 is expressed primarily in the bottom of the niche, while the upper regions mainly express NOTCH2 or NOTCH3[243].

Due to the structural differences in the mouse vs. the human prostate and the highly context-specific nature of the NOTCH pathway, further studies are needed to understand the role of NOTCH in human prostate tissue. For example, in mouse skin Notch1 and Notch2 are mainly expressed in the upper layers; however, in human skin NOTCH1 is expressed in all layers and NOTCH2 is mainly restricted to the basal layer[244]. There have been few reports clearly and uniformly demonstrating which components of the NOTCH pathway are expressed at the protein level in the normal human prostate[201]. However, Wang et al. reported mRNA for all four receptors and most *HES/HEY* genes are expressed in human prostate samples, but only *NOTCH1* and *HEY1* levels are altered in PCa tumors[224]. *NOTCH1* is the most well studied receptor in the prostate and it is found predominantly in basal cells of both mouse and human prostates[227,245]. Research on the other receptors is much less common but has been done recently, showing *NOTCH3* higher in the luminal layer and the surrounding stroma[246,247]. Recently, one study investigated *NOTCH2* and *NOTCH3* expression in PCa progression. They found low levels of NOTCH3 staining in normal prostate sections and decreased NOTCH2 expression with increasing tumor grade but did not report whether they detected NOTCH2 in normal prostate tissue[231]. In a mouse model, Notch2 and Dlk1 protein were detected in developing mouse prostate stroma but not the epithelium[234]. Understanding the specific role for each NOTCH receptor in prostate will require further investigation.

iv. Conclusions

Though clearly important, the exact role of NOTCH in prostate differentiation and cancer is still ambiguous. The field is still working to define clear roles for the various ligands, receptors, and downstream targets. Moreover, any resolved mechanism is likely to be tissue and cell specific[244]. The lack of an NICD3-specific antibody makes identifying its contribution difficult to

assess. Additionally, the transient nature of NICD activation and turnover makes it difficult to detect endogenous NICD via histology or immunoprecipitation[202]. Additionally, many studies rely on γ-secretase inhibitors, which fail to distinguish the function of specific NOTCH receptors. The same applies to studies that use knockdown of *CSL* to ablate NOTCH signaling. The limitations of γ-secretase inhibitors or *CSL* knockdown are apparent in a study from Yong et al. which saw differential effects depending on which technique they used[228]. Such discrepancy are likely due to γ-secretase involvement in other NOTCH-independent functions and CSL-independent NOTCH signaling[210,211]. Specific knockdown of individual NOTCH components is more arduous but allows for a better understanding of the pathway.

There is conflicting data about whether NOTCH is acting as a tumor suppressor or an oncogene in PCa. While the role of *NOTCH1* in normal prostate differentiation has been investigated, specific mechanisms remain elusive. NOTCH1 is known to transcriptionally upregulate *MYC* in T-ALL, which may explain how NOTCH signaling can function as an oncogene[248]. The link between NOTCH-mediated repression of p63 could also explain why prostate tumors show loss of p63[237]. NOTCH may function as a tumor suppressor through *HEY2/L* expression, which acts as an AR co-repressor. NOTCH function as an oncogene or tumor suppressor may be dependent on which receptors and downstream transcription factors are being activated. For example, upregulation of *MYC* would be oncogenic but increasing *HEYL* may be tumor suppressive. Due to the complexity of the NOTCH pathway, merely looking at a small selection of the ligands, receptors, or downstream factors may only be providing a small piece of the overall puzzle. As is seen with skin, temporal changes in NOTCH ligand expression are characteristic of differentiation[243]. Perhaps the status of the NOTCH pathway in prostate tumors can be indicative of the cell of origin or be used to grade relative differentiation status. More thorough investigations of NOTCH signaling may help clarify its function in differentiation and resolve some of the conflicting findings about its role in oncogenesis and tumor progression.

CHAPTER 2 — REFINEMENT OF THE pLKO TET-INDUCIBLE SYSTEM

A. Background

i. Rationale for use of inducible, lentiviral shRNA

Knockdown of gene expression at the mRNA level via RNA interference (RNAi) is a common method for investigating gene function. For transient knockdown in mammalian cell culture, small interfering RNA (siRNA) is often favored. The benefits of siRNA include commercially available RNA oligos for nearly any gene that can be transfected into cells for quick and efficient knockdown. However, siRNA becomes less useful when using cell types with low transfection efficiency or when experiments require prolonged gene knockdown[249]. Another common method for utilizing RNAi is via short-hairpin RNA (shRNA), which are synthetic non-coding RNA genes that share microRNA machinery used by cells for post-transcriptional regulation. Though not as simple to use as siRNA, shRNA can avoid concerns of low transfection efficiency and temporary knockdown by using retroviral delivery and selection for stable genomic integration[250-252].

Lentiviral shRNA vectors are popular due to their ability to infect nearly any cell type and integrate into the genome of both dividing and non-dividing cells. In 2006, the BROAD institute established the RNAi Consortium, which sought to identify and clone multiple shRNA candidate sequences for every gene in the mouse and human genomes[253]. The consortium cloned the shRNA sequences into the pLKO lentiviral vector backbone and has made them available for distribution from Fisher Thermo Scientific and Sigma-Aldrich. The shRNAs were not all functionally validated, but they were given a computationally calculated score for predicated efficiency and specificity.

In 2009, Dmitri Wiederschain and colleges built upon the pLKO vector and made multiple changes, the two most significant of which were the inclusion of the Tet-Repressor gene (TetR) and an H1/TetO promoter to drive shRNA expression. Together, these

modifications allow transcription of an shRNA upon the addition of tetracycline, or its analogue doxycycline (Dox), to sequester TetR and relieve repression at the Tet Operator sequence[253,254]. This vector combines the benefits of lentiviral delivery and inducible gene knockdown, providing many advantages over siRNA or constitutive shRNA. By combining inducible vectors with the list of candidate shRNA sequences by the RNAi consortium, it is now possible to inducibly knockdown nearly any gene in virtually any cell type.

ii. Rationale for improving pLKO system

The Tet-pLKO-Puro vector is a potentially powerful tool, but the process of designing and cloning shRNAs into the vector is not without challenge. In an effort to improve this tool even further I made some modifications to the vector to make it more amenable for cloning. Such modifications include shrinking the stuffer region and changing the 5' cloning site. Furthermore, I established clear and improved protocols for designing and cloning shRNAs into the vector. As part of this protocol, I demonstrate the importance of loop design in terms of both making easier screening and using mismatches to optimize shRNA efficiency. With this modified vector (EZ-Tet-pLKO-Puro) and detailed description for designing and cloning of shRNAs, I aim to make it easy for anyone to quickly adopt and utilize this tool for whatever gene or cell type they wish to investigate.

B. Results

i. Vector modifications

I started with the Tet-pLKO-Puro vector and modified it to make it more amenable for molecular cloning, terming my version EZ-Tet-pLKO-Puro. First, I used mutagenesis to delete the large stuffer region (~1.9kb), leaving a smaller stuffer of ~200bp (**Fig. 2A**). Second, I mutated the 5' AgeI cloning site to an NheI sequence to ameliorate some occasional difficulties with inefficient AgeI+EcoRI co-digestion. The smaller stuffer allows easier purification of cut vector, in particular size-selective DNA precipitation via polyethylene glycol (PEG)[255] **(Fig. 2B)**. Compared to alcohol precipitation and gel extraction, PEG precipitation is faster, provides cleaner DNA, and avoids concerns of potential DNA damage from ethidium bromide and UV exposure[256,257]. To compare precipitation methods, cut DNA (3µg) was precipitated with isopropanol, 8% PEG, or 6% PEG. The 6% PEG precipitation removed most of the 200bp stuffer, though it did so at the cost of lowest DNA recovery **(Fig. 2B).** Together, the combination of vector modifications and utilization of PEG precipitation provides a simplified method for preparing and purifying cut vector for molecular cloning.

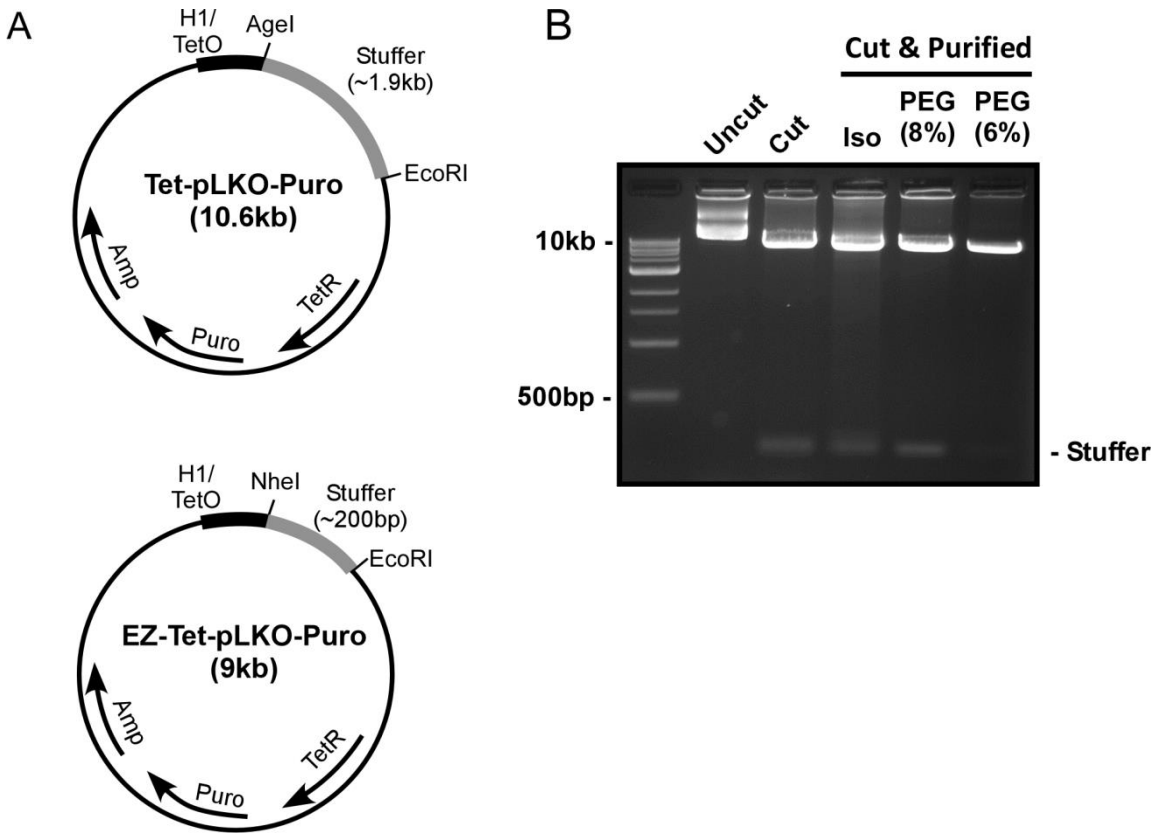

Figure 2: EZ-Tet-pLKO vector map and purification with PEG. (**A**) Basic vector maps for the original Tet-pLKO-Puro vector and my modified version, EZ-Tet-pLKO-Puro. Modifications include shrinking the stuffer region (from 1869bp to 221bp) and the mutation of the AgeI cloning site to NheI. (**B**) Agarose gel electrophoresis comparing DNA precipitation methods. 10µg of EZ-Tet-pLKO vector DNA was co-digested with NheI/EcoRI. The digest was then split into 3x 3µg reactions and precipitated with isopropanol (Iso) or polyethylene glycol 8000 (PEG) at 6% or 8% concentration. 1µg of uncut and cut DNA was run along with 1/3 of the precipitated DNA samples.

ii. shRNA design and cloning

Developing functional shRNA constructs often requires testing many targeting sequences. To reduce this time commitment I developed a method to improve shRNA efficiency and streamline the screening process. Targeting sequences were selected as described in the methods section and used to generate sense and antisense shRNA oligos **(Fig. 3A).** shRNA oligos contain the following elements: 5' overhang, sense targeting sequence, loop, reverse-complement targeting sequence, transcriptional terminator sequence, and 3' overhang. The antisense oligo is a reverse complement of the sense oligo, with opposite and complementary overhangs. The loop sequence includes a SpeI restriction site which allows restriction digest screening of ligated clones. The inclusion of mismatches in the loop region aids hairpin formation by stabilizing the loop and maintaining proper DICER binding and efficient mRNA cleavage[258,259]. Without the mismatch, a 6nt palindrome loop is predicted to collapse to a 4bp loop **(Fig. 3B)**. Immortalized prostate epithelial cells (iPrECs) were infected with shRNA lentivirus and pools were selected with shRNAs (sh-p38δ) containing the same targeting sequence with alternate mismatch loops. Immunoblot showed very efficient knockdown of p38δ with the 7nt loop and no knockdown with the 6nt loop after 72h of Dox treatment (**Fig.3C)**. Probing for TetR showed that both pools were infected with the lentivirus and had similar expression levels of the lentiviral construct, demonstrating the only difference between the pools was a single mismatch in the shRNA loop sequence.

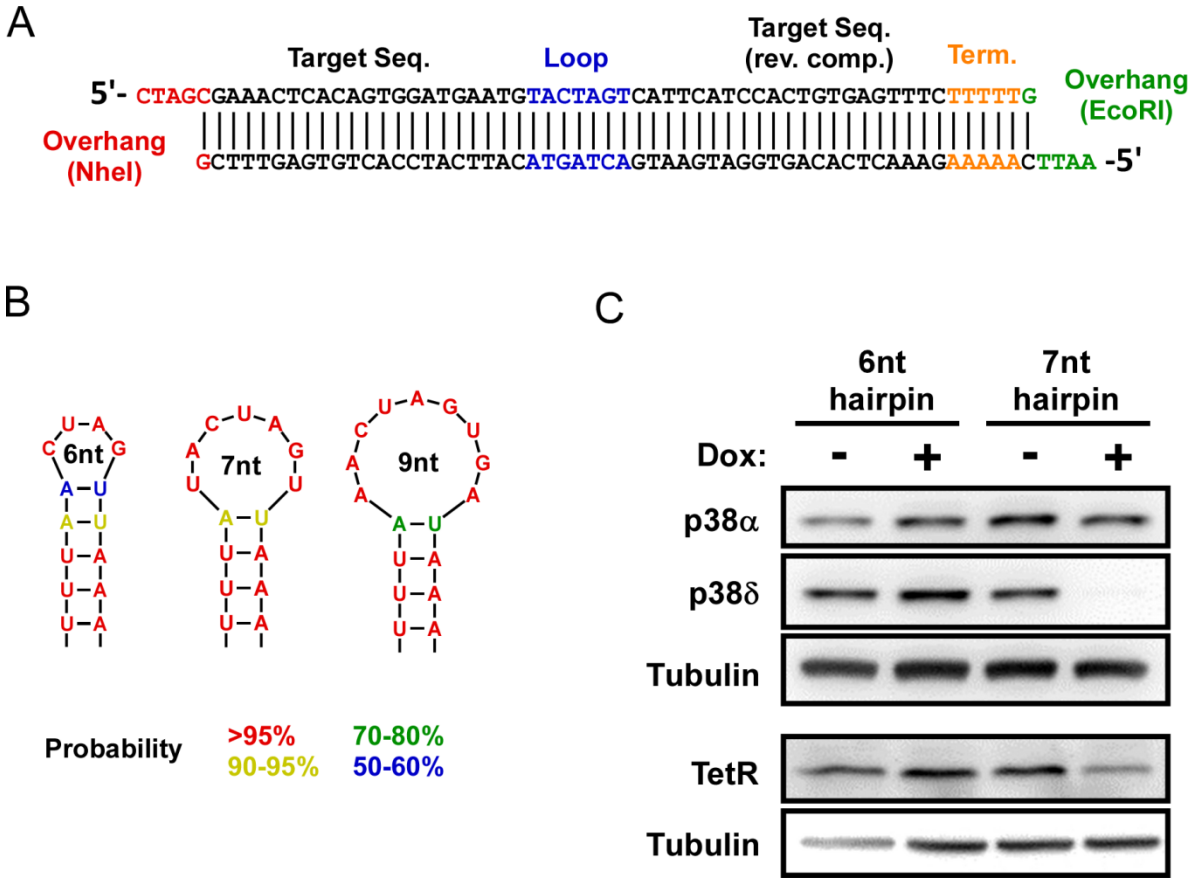

Figure 3: shRNA oligo design. (**A**) Format for shRNA design. shRNA must contain: 5' NheI overhang, matching mRNA target sequence, loop sequence, reverse complement targeting sequence, transcription terminator sequence, and 3' EcoRI overhang. (**B**) Diagram of shRNA loop structure, with and without mismatches, using a core SpeI loop (ACTAGT). Colors indicate computationally probability of 2º RNA structure. (**C**) Immunoblot showing two different pools of iPrEC cells, with the only difference being a single mismatch in the loop sequence of the sh-p38δ vector. Cells were treated -/+ Dox (100ng/mL) for 72h. p38α blot shows shRNA specificity, TetR shows pLKO integration, and Tubulin is the loading control.

iii. Streamlined colony screening

After ligation and transformation into competent *E. coli*, bacterial colonies must be screened for proper clones. Colony-PCR is a quick way to use small amounts of bacteria directly as template in a screening PCR reaction. I designed primers to span the insert region, producing a 450bp band for positive clones and a 620bp band for background vector with retained stuffer **(Fig 4A)**. PCR product was visualized by agarose gel electrophoresis, which produced clearly identifiable bands for true clones and background colonies **(Fig. 4B)**.

Additionally, clones can be further validated by restriction enzyme digest (RE) screening, which requires a miniprep step to isolate plasmid DNA. The original Tet-pLKO-Puro protocol recommended using an XhoI loop in the hairpin[254,260]. When running an RE screen with XhoI, the primary indication of a positive clone is the loss of a ~400bp band and gain of very small bands (~1-2% of total DNA) that are difficult to visualize on agarose (**Fig. 4C).** To resolve this issue I chose a SpeI site for my loop design. When visualized on agarose, a SpeI RE screen produces a clear band ~500bp, which is ~5% of total DNA (**Fig. 4C)**. To demonstrate this improvement I digested two vectors designed with either the XhoI or SpeI loop and ran 1µg of each digest by agarose gel electrophoresis. The SpeI digest produced the clear presence of a ~500bp band, as opposed to the XhoI screen where a positive clone was mainly identified by the loss of a ~300bp band since the smaller fragments were barely detected **(Fig. 4D)**. Positive clones can then be sent for sequencing validation using the same pLKO-fwd primer as used in the PCR screen. The combination of colony-PCR as a quick and cheap primary screen with RE digest as a secondary screen provides a streamlined process for identifying positive clones.

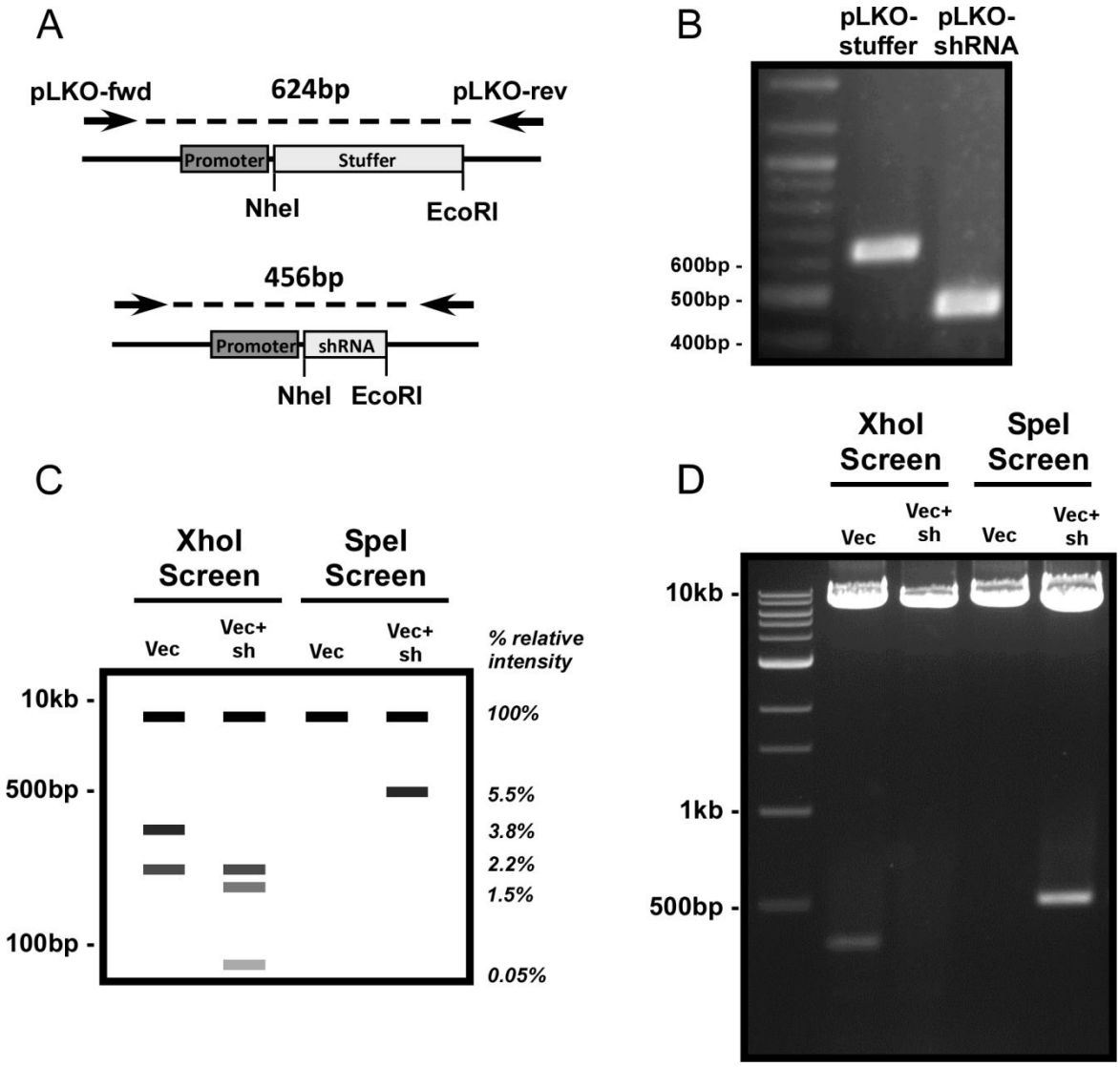

Figure 4: Ligation screening techniques. (**A**) Diagram showing expected products from PCR screening pLKO colonies. The pLKO-fwd and pLKO-rev primers will amplify a 456bp product for a positive clone (inserted shRNA oligo) or a 624bp product for a negative clone (background/re-ligated pLKO). (**B**) Agarose gel (2%) with a positive and negative PCR product. (**C**) Diagram showing expected DNA fragments and estimated band intensity from using either XhoI or SpeI loop designs and RE screening. (**D**) Agarose gel with either XhoI or SpeI shRNAs (or backbone vector) and the proper digest screens. 2µg of DNA was digested with the indicated enzyme and half the digest was run on 1.5% agarose. The <200bp fragments from the XhoI screen are very faint and could only be seen with a very high exposure (not shown).

iv. Dox titration and recovery validation

Next I validated the efficacy of the EZ-Tet-pLKO-Puro vector in cell culture using iPrEC cells. Cells were infected with lentivirus and pools were selected with puromycin (1-2µg/mL). I performed a titration with Dox and found that as little as 10ng/mL was sufficient to induce the shRNA (sh-p38α) and target knockdown **(Fig. 5A)**. Typical protein knockdown was achieved in 48-72h. Furthermore, the target protein can be recovered after removal of Dox. Cells with sh-p38α were treated with Dox for 72h and then split. Dox was removed and samples were harvested over a recovery time course **(Fig. 5B)**. Recovery p38α protein began 4 days after removal of Dox and was recovered by 8 days. Thus, the system is both inducible and reversible.

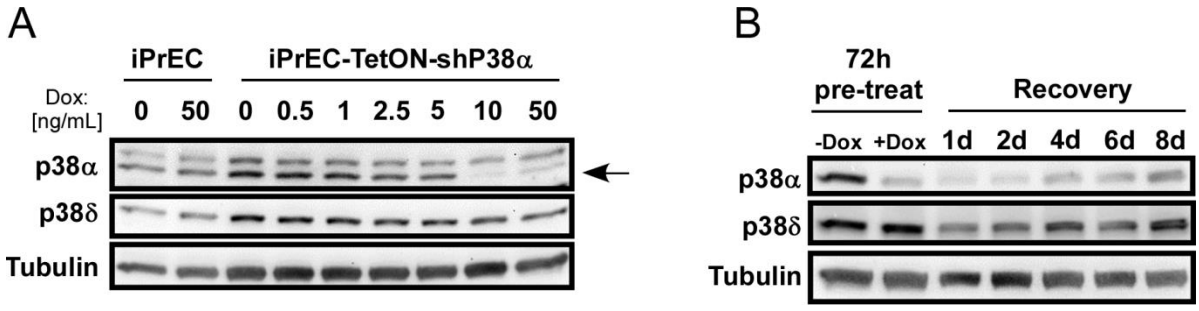

Figure 5: Dox titration and recovery. (**A**) Immunoblot showing Dox titration (0-50ng/mL) on TetON-shP38α cells. Cells were treated for 72h. First two lanes are cells without the shRNA insertion. Note: the lower band (arrow) is p38α. (**B**) The same shRNA cells were treated -/+Dox (100ng/mL) for 72h. At that time, two samples were lysed while others were split and allowed to recover without Dox for 1-8 days.

C. Materials and methods

***pLKO vector mutagenesis*.** The Tet-pLKO-Puro plasmid was ordered from the Addgene repository (Addgene plasmid 21915)[254]. Mutagenesis was performed using the QuikChangeII Site Directed Mutagenesis kit (Aligent). Bases 222-1869 of the stuffer region between the AgeI and EcoRI cloning sites were deleted. The deletion was performed by inserting an EcoRI site at base 222 of the stuffer (primers: 5'-GCTACTCCA-CCACTTGAATTCCTAAGCGGTCAGC and 5'-GCTGACCGCTTAGGAATTCAAGTGGTGG-AGTAGC). The vector was then digested with EcoRI and re-ligated, and clones were screened for those that ligated the new EcoRI site directly to the 3' cloning site, thus excising the bulk of the stuffer region and preserving the 3' cloning site. Mutagenesis was then used to mutate the AgeI restriction site to an NheI sequence (primers: 5'-TATCAGTGATAGAGACGCTAGCG-TGTTGTAAATGAGCA and 5'-TGCTCATTTACAACACGCTAGCGTCTCTATCACTGATA). Vector sequence was confirmed by Sanger sequencing. A caveat on sequencing: shRNA hairpin sequences can cause early termination when read by Sanger sequencing and may require the use of specialized sequencing protocols for dealing with RNAi constructs[261,262].

shRNA oligo design. shRNA targeting sequences were chosen from the BROAD RNAi Consortium database (http://www.broadinstitute.org/rnai/trc)[253]. Oligos were ordered from Integrated DNA Technologies. The RNA hairpin diagram in Fig.3 was created using an RNA folding tool by Reuter et al[263].

***shRNA oligo preparation*.** Sense and antisense shRNA oligos were suspended at 100µM in duplex buffer (100mM Potassium Acetate, 30mM HEPES, pH 7.5). Next, 20µL (2 µ-mol) of each oligo were combined and annealed by using a thermal cycler (Labnet TC9600-G) with a program set to start at 95 degrees and drop 5 degrees every minute down to room temperature. Alternately, DNA can be annealed by placing in a beaker of boiling water and allowed to cool to room temperature. The annealed oligos were then diluted with water to 400µL total and precipitated with isopropanol. DNA was centrifuged for 30m at 15,000 RCF in a

benchtop centrifuge (Eppendorf 5415D), washed twice with 70% ethanol, and suspended in water. Annealed oligo DNA was then quantified with a Nanodrop spectrophotometer (ND-1000, Thermo Scientific) and treated with T4 poly-nucleotide kinase (NEB) according to the manufacturer's protocol to phosphorylate the ends.

Vector digest and PEG precipitation. Vector was prepared by co-digesting EZ-Tet-pLKO-Puro DNA with NheI and EcoRI (NEB). A typical digest consisted of 5µg of vector DNA with 20u of each enzyme in a 50µL digest volume for at least 3h at 37°C. The cut vector was then dephosphorylated with Antarctic Phosphatase (NEB) using the manufacturer's protocol and supplementing the 50µL digest reaction with AP buffer, enzyme, and water to make a 60µL reaction volume. The vector was then diluted with water to a 200µL volume. PEG was then used to precipitate the DNA and exclude the 200bp excised stuffer by first preparing a 2X stock of 12% (w/v) PEG-8000 / 20mM Magnesium Chloride and adding that 1:1 to the DNA sample. The DNA/PEG mixture was gently mixed by inverting the tube and left to sit at room temperature for 1h. After the incubation, the DNA was centrifuged at 15,000 RCF for 40m. The length of the incubation and spin are critical; less time can greatly decrease recovery. Supernatant was carefully decanted, leaving a small volume of liquid behind to avoid sucking up the DNA pellet. Next, 500µL of 70% ethanol was added to wash the DNA pellet, which was spun again for 5m. The ethanol was aspirated and the wash repeated once more. After the washes the DNA pellet was allowed to air dry and then suspended in water (typically ~50µL). Prepared vector was then quantified by Qubit (Invitrogen) to get a highly accurate concentration reading, which is important for proper ligation ratios.

***Ligation and transformation*.** Prepared vector was diluted to a working concentration of ~20-100ng/µL. Prepared oligos were diluted to a 1ng/µL working concentration. Ligations were performed using the LigateIT rapid ligase kit (Affymetrix) with 100ng vector DNA and a 7:1 insert:vector molar ratio. A vector-only ligation was also prepared to control for incompletely digested and/or re-ligated vector derived colonies. Following a 15m incubation, 2µL of the

ligation reactions were transformed into Stbl3 (Life Technologies) or NEB-Stable (NEB) chemically competent E. coli. These strains are recommended for their ability to minimize unwanted recombination due to lentiviral LTR sequences. Competent cells were incubated on ice for 30m with the ligation DNA, then heat shocked at 42ºC for 40s and returned to ice for 1m. 1mL of LB media was then added to the cells and they were allowed to recover at 37ºC for 30m, after which time 200µL was plated on LB-agar plates containing 100µg/mL ampicillin and incubated 12-16h at 37 degrees.

***PCR screen*.** Colony-PCR was used to screen bacteria for successfully ligated clones. Primers used were as follows: pLKO-Fwd 5'- ATTAGTGAACGGATCTCGACGG; pLKO-rev 5'-AACCCAGGGCTGCCTTGG. Successful clones will produce a 624bp product while background colonies that retained the stuffer region amplify a 456bp product. To set up the PCR reactions, first 15µL of water was added to PCR tubes. Colony inoculation was performed by touching a pipette tip to a colony, mixing it in the desired PCR tube with the water, and then dotting ~1uL on a labeled fresh agar plate to keep track of the colony. PCR master mix was made containing (per reaction): 2.5µL of 10X Taq Buffer and 0.2µL of Taq enzyme (TP-100, Syzygy Biotech), 2µL of $MgCl_2$ (25mM), 0.2µL of each primer (100uM), and 3.9µL water. Then, 10µL of the master mix was added to each tube with 15µL of inoculated water which serves as the template (thus making a 25µL final reaction). Thermalcycler settings used were as follows: Initial step: 1x (95°C, 5m); amplification steps: 30x (95°C for 30s; 55°C for 30s; 72°C for 30s); final extension 1x (72°C for 1m). PCR product was run on 2% agarose with 100bp ladder (NEB).

***Restriction enzyme digest screen*.** Clones were minipreped by alkaline lysis and DNA was precipitated with isopropanol[264]. DNA was digested using SpeI restriction enzyme (NEB). A standard reaction condition contained ~3µg of DNA digested with 10u of enzyme in a 50µL reaction for at least 1h at 37ºC. 10-20µL of digest was then run out on a 1.2% agarose gel with 1kb ladder (NEB). Negative colonies are cut once by SpeI and create a band ~9kb, while clones with shRNA containing a SpeI loop sequence will produce bands at ~8.5kb and ~500bp.

***Virus production and infection*.** pLKO constructs were used to make lentivirus in HEK 293FT cells. Proper viral safety protocols should be followed when working with lentivirus. 293FT cells were seeded in T75 flasks coated with 1µg/mL PolyD lysine in PBS for 1h at 37ºC or overnight at 4ºC. Cells were transfected with packaging plasmids (pLP1, pLP2, pVSV-G) (Thermo Fisher) and the desired pLKO construct. Per T75 flask 4µg of each plasmid was used along with 48µL of Lipofectamine2000 transfection lipid (Life Technologies). 24h following transfection, media was changed on 293FT cells to the target cell media, i.e. the media for the cells you wish to infect. Note: target cell media should not contain antibiotics and if serum is needed, it must be heat-inactivated to prevent immune complement interference. 293FT cells were incubated for 48h at 37ºC in target cell media to produce viral particles. Viral media was harvested by transferring into 15mL conical tubes which were then centrifuged for 10m at 1500 RPM in a swinging bucket bench top centrifuge (Megafuge 1.0R) to pellet cell debris. Next, the viral media was filtered by syringe through a 0.45µM, low protein binding filter (28145-505, VWR). Cells were typically infected by first adding half the volume with normal growth media (no antibiotics, heat inactivated serum) and half volume with the filtered viral media plus polybrene to a 5µg/mL final concentration to improve infection rate[265]. Infected cells were incubated 48-72h and then given fresh growth media for 24h-48h before beginning puromycin selection (1-2µg/mL). Remaining virus can be snap frozen in liquid nitrogen and stored at -80ºC. Thawed virus is still effective but loses ~50% infectivity each thaw cycle.

Immunoblot. Cells were lysed in MAPK lysis buffer (50mM Tris, pH7.5, 0.5mM EDTA, 50mM NaF, 100mM NaCl, 50mM β-glycerol phosphate, 5mM Sodium Pyrophosphate, 1% TritonX100) or RIPA lysis buffer (10mM Tris, pH7.5, 1mM EDTA, 158mM NaCl,, 0.1% SDS, 1% Sodium Deoxycholate, 1% TritonX100). Cells were chilled, washed, and then lysis buffer was added and plates sat for 30m on ice. Cells were then scrapped, centrifuged, and protein was quantified by BCA assay (Pierce). Equivalent amounts of 30-50µg of denatured protein per sample was run on Novex SDS polyacrylamide tris-glycine gels (Life Technologies). Protein was

then transferred onto PVDF membrane and blocked in 5% BSA/TBST for 1h at room temp. Primary and secondary antibodies were diluted in blocking buffer. Primary antibodies were probed either 2-3h at room temp or overnight at 4ºC while all secondary antibodies were probed 1h at room temp. Luminol chemiluminescence was used with a Bio-Rad Chemi-Doc imaging system with CCD camera to image blots and analyzed on Quantity One software v4.5.2. Detailed antibody information can be found in **Table S1**, Appendix A.

***Cell culture*.** iPrEC cells were grown in Keratinocyte Serum Free media (Life Technoliges) and 30u/mL Pen/Strep (Life Technologies). HEK293FT cells were maintained in DMEM (11995, Life Technologies) plus 2mM L-glutamine, 10% fetal bovine serum (Gemini), and 30u/mL Pen/Strep (Life Technologies). During viral production and infection cells were grown without antibiotics and with heat inactivated fetal bovine serum (heated 30m at 56°C). Cells were maintained at 37 ºC with 5% CO2.

D. Discussion

i. Importance of loop design

When designing the loop sequence for shRNAs, the length and makeup of the nucleotides can potentially make an impact on the efficiency of the shRNA. miRNAs can have loops from 3-17nt long[266]. For the sake of simplicity, shRNA design guides often suggest using a 6nt palindrome restriction enzyme sequence. RNA folding programs predict that a 6nt loop has a risk of collapsing to a 4nt loop[258,263]. However, in my experience sometimes the basic 6nt RE sequence was sufficient for solid knockdown. Regardless, the use of a 7-9nt loop containing at least one mismatch maximize the chances of getting an efficient shRNA construct and can even enhance the efficiency of an existing 6nt-loop shRNA[267].

ii. Caveats for use of doxycycline

At high doses (>1µg/mL) doxycycline can have detrimental effects on cell viability via disruption of mitochondrial function[268]. However, typical cell culture concentrations of as low as 10-100ng/mL are sufficient for knockdown induction; well below reported toxic levels. In my experience, prolonged treatment (>4 days) at 500ng/mL began to cause effects on cell viability in culture (not shown). However, typical use of 50ng/mL had no obvious effects on cell health, even when used for two weeks continuously. As an extra control, the parent cell line (without lentiviral infection) can be treated with Dox to check specifically for effects on cell viability. For most cases a 10-50ng/mL dose of Dox should be well tolerated but that should be tested by the end user as a precaution.

iii. Dox titration and recovery

The use of titratable amounts of Dox should in theory allow partial vs full knockdown if shRNA expression can be properly tuned. For some experiments a partial knockdown may

actually be desired, e.g. testing for haploinsufficiency. In my titration experiment I was not able to find a dose of Dox that gave only partial knockdown. At 5ng/mL I saw no effect and at 10ng/mL knockdown was near complete. However, depending on the target gene and cell type it may still be possible to find an effective dose for partial knockdown.

For most genes 72h is sufficient to see knockdown at the protein level. However, this is highly dependent on protein stability. For example, longer-lived membrane proteins or stable housekeeping proteins may take up to a week for proper knockdown. Likewise, protein recovery will be very dependent on the transcription rate of the gene so that lower expressed genes will take longer to recover. Furthermore, cell confluency and proliferation rate will also affect the rate of protein synthesis and turnover, thus affecting Dox knockdown and recovery timing. All these factors need to be considered when designing carefully timed experiments and will be cell line and context specific.

vi. Additional inducible systems

In addition to the Tet inducible system, there are other inducible shRNA vectors that can prove useful and are commercially available, such as Cumate or IPTG-inducible vectors[269,270]. With some creativity and strategy it is possible to create cells with multiple shRNAs, each activated by different inducers. Moreover, inducible shRNAs can be combined with inducible cDNA expression systems to test overexpression and knockdown simultaneously or sequentially[271]. Use of inducible vectors greatly opens the door for greater quantity and variety of questions that can be addressed with molecular biology.

v. Conclusions

Inducible shRNAs are a very powerful tool. Though I have focused on a particular modified pLKO vector, the principles of shRNA design and screening are broadly applicable. Additionally, though I have focused on *in vitro* use, the pLKO system can also be useful *in vivo*.

For example, tumor cell lines can be modified *in vitro* and then xenografted into an animal where knockdown can be induced temporally upon addition of Dox to the food or water.

There are many ways to manipulate gene expression, including the recent advent of CRISPR/Cas9. The potential of gene editing is great but not without limitation, including the inability to study genes with lethal knockout phenotypes. Additionally, CRISPR knockout can be poorly efficient in cell culture and relies on selecting clonal populations[272]. Lentivirus allows efficient infection and selection for pools or clones of cells. With this streamlined protocol and refined vector the Tet-pLKO system can be used with greater ease and efficiency by all.

CHAPTER 3 —p38-MAPK REGULATION OF NOTCH IN DIFFERENTIATION

A. Background

i. Rationale

One common characteristic of tumor cells is their ability to avoid terminal differentiation and maintain an unregulated proliferative state. To understand how tumors make this proliferative switch it is essential to appreciate the underlying differentiation program. The vast majority of prostate tumors are adenocarcinomas, arising from the epithelial compartment. Prostate epithelium consists of basal and luminal cell types, with various mutually exclusive markers such as Androgen Receptor (AR) in the luminal layer and Integrin α6β4 in the basal layer[71,273]. Each layer contains a subset of self-regenerating cells in addition to a population of basal cells that differentiate into luminal cells as part of normal gland homeostasis[274]. Moreover, lineage tracing in the developing mouse prostate has revealed populations of uni- and bi-potent progenitors that retain the ability to differentiate into either luminal or basal cells[79,275]

The definitive cell of origin for human prostate cancer is complicated[276,277]. Mouse models suggest that oncogenes driven by basal or luminal promoters can give rise to tumors, though basal driven tumors require partial luminal differentiation before becoming fully proliferative[90,278]. A more recent understanding is that there are varying types of progenitors in prostate tumors, which may or may not be the same as the cell of origin[276,279,280]. Understanding both the cell of origin and the cell of propagation for prostate tumors will be critical for classification and treatment strategies.

Human prostate tumors show co-expression of basal and luminal markers (e.g. AR and integrins) which suggests a defect in differentiation[78,79]. Moreover, many of the commonly altered genes in prostate cancer (e.g *MYC*, *AR*, *ERG*, *PTEN*) are also implicated in differentiation[273]. However, the specific mechanisms by which these genes drive differentiation or tumorigenesis are not well resolved. Previous work from our group demonstrated that

manipulation of differentiation regulators, i.e. *MYC*, *PTEN*, and *ING4*, results in tumor formation in normal human prostate epithelial cells[102].

p38-MAPK is a known driver of epithelial differentiation in various tissues, including skin and lung[152]. p38-MAPK can regulate a wide range of targets, including other kinases and phosphatases, transcription factors, and RNA binding proteins[152]. FGFR2b is crucial for epithelial differentiation in the skin and prostate and is an upstream activator of p38-MAPK[71,281,282]. However, a specific role for p38-MAPK in prostate epithelial differentiation, including its relevant targets, remains undefined.

In addition to being overexpressed in the majority of prostate tumors and a driver of tumorigenesis in mice, *MYC* is also a regulator of skin and prostate differentiation[24,102,142]. *MYC* can potentially regulate thousands of genes via its activity as a transcription factor with many targets being tissue and context specific[106,283]. Moreover, regulation of *MYC* is complex and can occur at many different levels, including transcription, RNA stability, protein stability, and post-translational modification[284].

Another key differentiation pathway in the prostate is NOTCH, which is associated with regulation of cell fate, stemness, survival, and differentiation[285]. Mammals contain four NOTCH transmembrane receptors (*NOTCH1-4*), five transmembrane ligands (*JAG1/2*, *DLL1/3/5*) and ten classic downstream targets (*HES1-7*, *HEY1/2/L*). Cell-cell contact that joins ligand and receptor triggers proteolytic cleavage by the γ-secretase complex which releases the active intracellular domain (ICD) of the receptor into the nucleus to activate transcription[202]. Work with mouse models has demonstrated the importance of the NOTCH pathway in prostate development[286,287]. NOTCH can regulate cell cycle arrest and de-adhesion from the matrix, both of which are essential for luminal differentiation[288-290]. However, there are conflicting reports as to whether the NOTCH pathway is oncogenic or tumor suppressive in prostate cancer and the specific functions of each receptor in prostate epithelial differentiation have not been defined[291].

ii. Hypothesis

To further investigate the process of prostate epithelial differentiation, I utilized an established model of *in vitro* differentiation which uses human basal prostate epithelial cells (PrEC)[71,102]. This model allows considerable pharmacologic and genetic manipulation to study specific genes and their role in luminal differentiation. In this study I utilized our model to test the hypothesis that p38-MAPK upregulation of *NOTCH3*, via *MYC*, is required for prostate epithelial differentiation. I identified two novel mechanisms of *NOTCH3* regulation by p38-MAPK at the transcriptional and post-transcriptional level, both of which are required for differentiation of prostate basal epithelial cells into luminal cells. This knowledge improves our understanding of prostate epithelial differentiation and will inform future investigations into how specific manipulations in these signaling pathways may drive tumorigenesis.

B. Results

i. MAPK isoforms p38α and p38δ are required for prostate epithelial differentiation

To induce differentiation of human basal prostate epithelial cells (PrEC) into luminal cells, I treat with KGF/FGF7 and synthetic androgen (R1881) for two weeks[71]. This results in a stratified epithelium consisting of luminal cells sitting atop basal cells. p38-MAPK is a known downstream target of KGF-FGFR2 signaling and this pathway has been implicated in epithelial differentiation in several tissue types, including prostate[71,282]. There are four different genes encoding p38 isoforms: *MAPK14*/p38α, *MAPK11*/p38β, *MAPK12*/p38γ, and *MAPK13*/p38δ. p38α is the most ubiquitously expressed, while the other isoforms are typically more tissue specific[152]. From RNA-seq data of basal cells I found p38α and p38δ to be the predominantly expressed isoforms (**Fig. 6A**). Consequently, p38α and p38δ protein were readily detectable by immunoblot (**Fig. 6B**).

To assess p38-MAPK activation during differentiation, cell lysates from differentiating cells were collected over a two week time course, and p38α activity was measured by immunoblotting with a phospho-specific antibody. On the terminal day of differentiation, the newly formed luminal (L) layer was separated from the basal (B) layer, allowing separate assessment of basal and luminal cells. I compared primary cells (PrECs) to immortalized cells (iPrECs)[102]. In primary cells, activated p38α was elevated at day 4 and remained elevated (**Fig. 6C**). In immortalized cells, which take 4 days longer to reach full differentiation, p38α was activated at day 8 (**Fig 6D**).

To determine if p38-MAPK is necessary for differentiation, iPrECs were differentiated for 16 days in the presence of two different p38 inhibitors (SB202190, BIRB796) or Tet-inducible shRNA. The concentration of each p38-MAPK inhibitor that effectively blocked CREB1 phosphorylation by constitutively active MKK6 was subsequently used for this study (**Fig. S1A**, Appendix B).

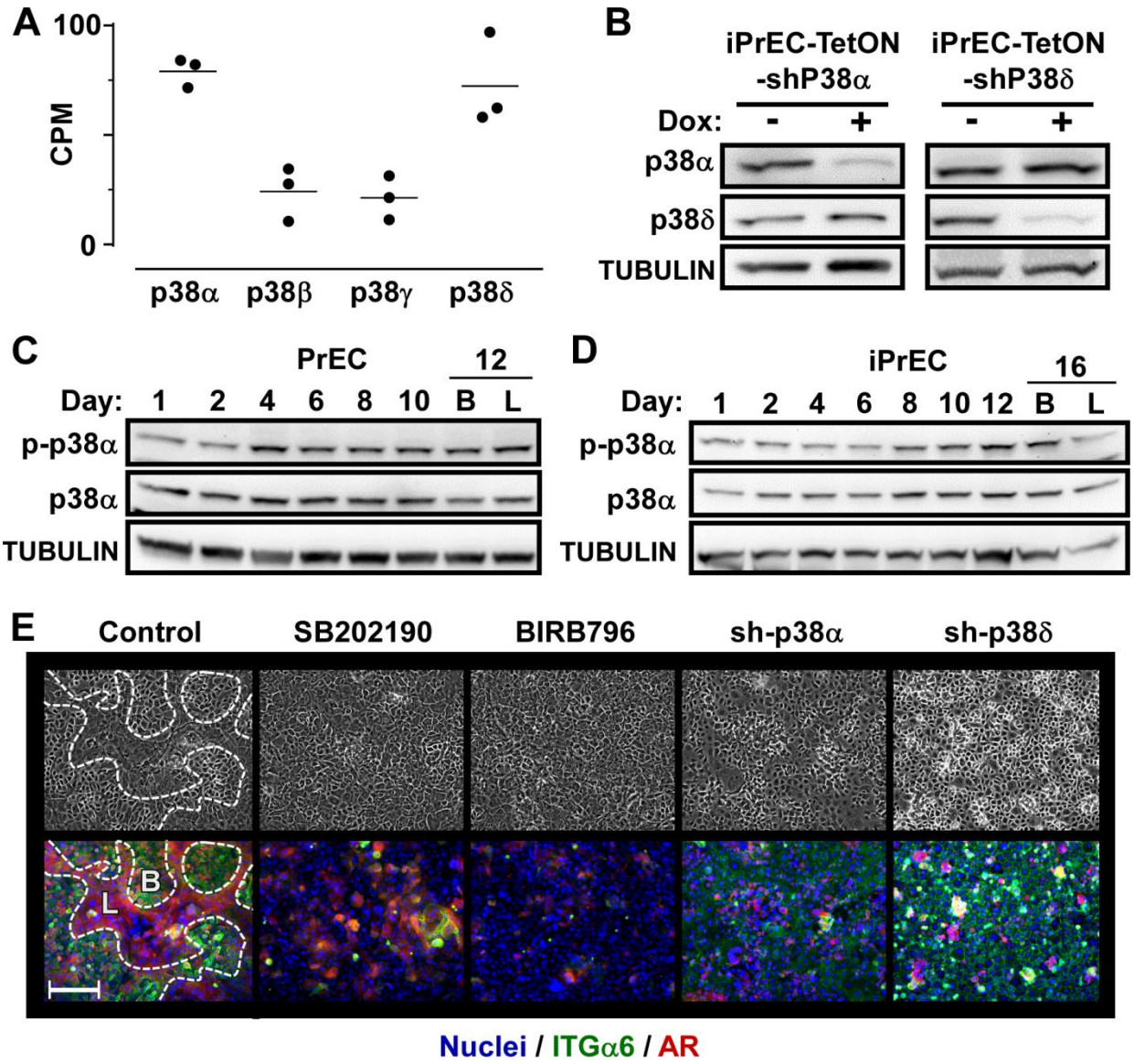

Figure 6: p38α- and p38δ-MAPK are required for differentiation. (A) Plot showing Counts Per Million (CPM) reads for the four p38-MAPK isoforms taken from RNA-seq data of basal iPrECs. Data are from biological triplicates. **(B)** Stable pools of iPrECs expressing Tet-inducible p38α or p38δ shRNAs were treated with 50ng/mL doxycycline (Dox) for 72h and probed by immunoblot. **(C,D)** Primary (PrEC) and immortalized (iPrEC) human basal prostate epithelial cells were differentiated with KGF and R1881. Cell lysates were collected at indicated time points and the luminal cells (L) were separated from the basal cells (B) at the final time point before lysis. Levels of p38α and phospho-p38α were measured by immunoblotting. TUBULIN served as the loading control. **(E)** iPrECs were treated with DMSO + Dox (Control), 1μM SB202190, or 0.1μM BIRB796 while inducible shRNA lines were treated with 50ng/mL Dox over 16 days of differentiation. Cells were then fixed and visualized by immunofluorescence. Top row images show phase contrast microscopy while the bottom row shows merged epifluorescence images of Hoescht-stained nuclei (blue), Androgen Receptor (red) as a luminal marker, and Integrin α6 (green) as a basal marker. Luminal layer is outlined (dashed line) in control cells; (L) is the luminal layer and (B) is the basal layer. Scale bar = 200μm.

Effective knockdown of p38α or p38δ in shRNA lines was achieved by 72h with Dox treatment (**Fig. 6B**). Differentiation was monitored by microscopy using phase-contrast and immunofluorescence for Integrin α6 (ITGα6) and Androgen Receptor (AR), which mark basal and luminal cells, respectively. Control cells (DMSO plus Dox) differentiated normally as typified by the presence of a large patch of luminal cells (AR+/ITGα6-) with some non-differentiated underlying basal cells (AR-/ITGα6+) (**Fig. 6E**). Treatment with 1μM SB202190 or 0.1μM BIRB796 completely prevented formation of a luminal layer. Moreover, Dox-induced knockdown of p38α or p38δ in shRNA lines also prevented luminal cell formation. Nuclear staining of nonpermeabilized cells with propidium iodide detected virtually no cell death, indicating a block in differentiation rather than decreased survival (**Fig. S1B**, Appendix B). Thus, p38α and p38δ are each required for PrEC differentiation.

ii. NOTCH1 and NOTCH3 are induced during differentiation.

A hallmark of luminal cell differentiation is the loss of integrin expression. NOTCH is known to negatively regulate integrin expression and is generally required for epithelial differentiation[24,273,288]. Therefore, I sought to determine which NOTCH receptors are important for human prostate epithelial cell differentiation. *MYC* also controls integrin expression[142]. We previously demonstrated *MYC* is required for prostate luminal cell differentiation[102]. In some contexts *MYC* is a direct downstream target of NOTCH[205]. To decipher the roles of *MYC* and NOTCH, cell lysates from differentiating iPrECs (**Fig. 7A**) or primary PrECs (**Fig. S2A**, Appendix B) were collected over a two week time course and protein expression was measured by immunoblot. MYC expression and activation (as measured by phosphorylation) is initially elevated and wanes as basal cell proliferation subsides, but is transiently elevated again around day 8 (**Fig. 7A**). A similar response was observed in primary cells but occurring 4 days earlier (**Fig. S2A**) consistent with the more rapid differentiation of primary cells compared to immortal cells as noted in Figure 6.

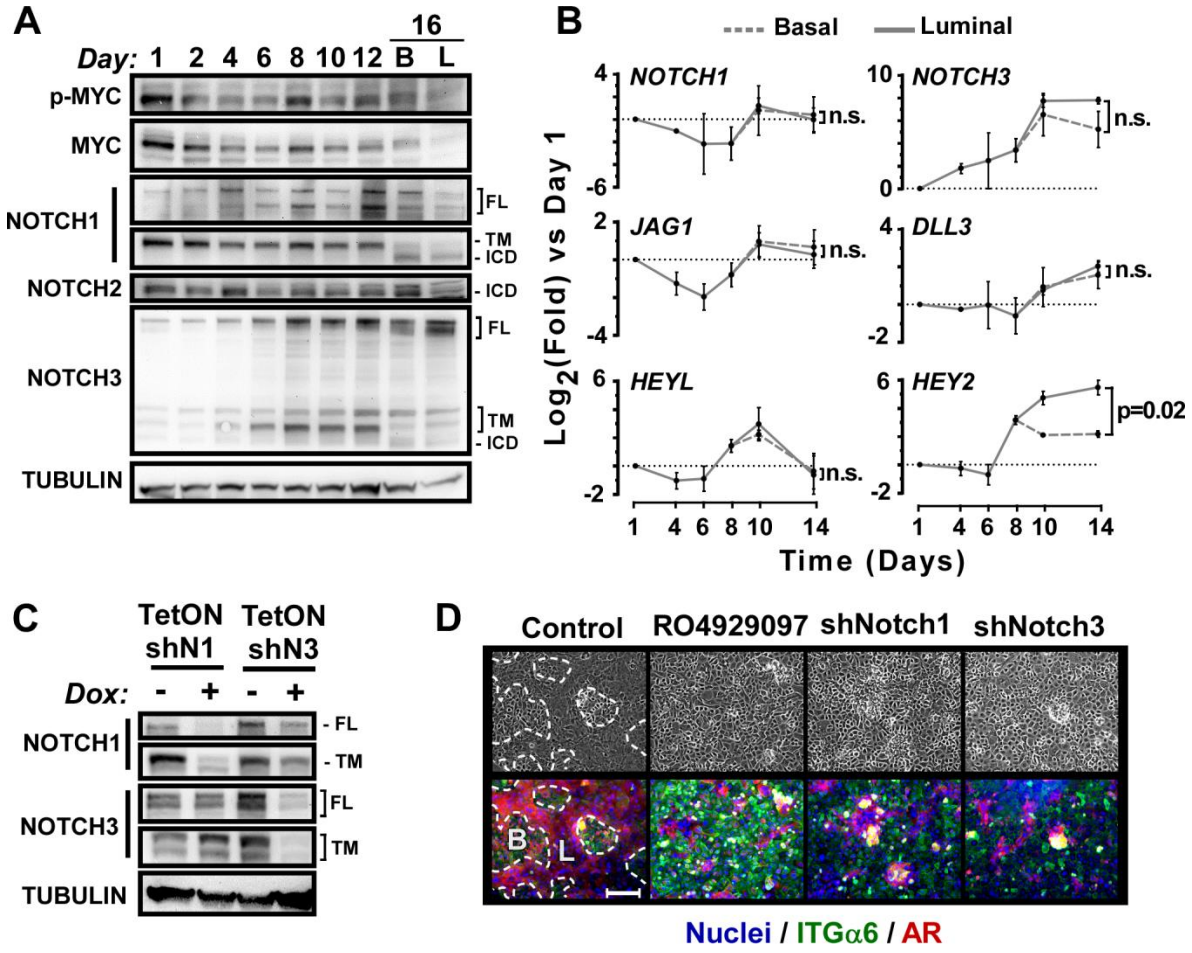

Figure 7: *NOTCH1* and *NOTCH3* are required for differentiation. (A) iPrECs were differentiated for the indicated days and cell lysates collected for immunoblotting as in Fig.6D. MYC and p-MYC (T58/S62) were probed along with three NOTCH receptors (NOTCH1,2,3). NOTCH2 antibody is ICD-specific, while NOTCH1 and NOTCH3 target the C-terminus and recognize all three fragments: full length (FL), transmembrane (TM), and intracellular domain (ICD). TUBULIN served as loading control. **(B)** RNA was collected from iPrECs differentiated for the indicated days and the levels of mRNA for several ligands and downstream targets of the NOTCH signaling pathway were measured by qRT-PCR. Luminal (L) cell were separated from basal (B) cells at days 10 and 14; dashed lines shows basal, solid line shows luminal. Error bars show standard deviation of biological triplicates. *p*-values were determined by paired, two-tail t-test between d14 basal and luminal samples; n.s. = non-significant (p>0.2). Data were standardized to *18S* and *GAPDH*. Y-axis shows ΔΔCT values relative to day 1, which is equal to Log_2(fold change). **(C)** iPrEC pools expressing TetON-shRNA (shNOTCH1 or shNOTCH3) were treated with 50ng/mL Dox and differentiated for 4 days. Levels of NOTCH expression were measured by immunoblotting. **(D)** iPrECs were treated with DMSO + Dox (Control) or 1μM RO4929097 while Inducible shRNA lines were treated with 50ng/mL Dox over 16 days of differentiation. Cells were then fixed and stained by immunofluorescence. Top row shows phase contrast while the bottom row shows merged epifluorescence images of Hoescht-stained nuclei (blue), AR (red) as a luminal marker, and ITGα6 (green) as a basal marker. Luminal layer is outlined (dashed line) in control cells; (L) is the luminal layer and (B) is the basal layer. Scale bar = 200μm.

Of the four NOTCH receptors in mammals, I was only able to detect significant expression of NOTCH1, 2, and 3 (**Fig. 7A**). Expression of NOTCH2 remained essentially unchanged during differentiation. NOTCH1 protein was initially high early in differentiation but decreased and later recovered. In contrast, NOTCH3 protein expression was very low in basal cells but increased dramatically with time during differentiation; moreover, significant induction occurred at day 8 (**Fig. 7A**), when p38α and MYC activity (**Fig. 6D**) were also maximal. A similar time course and pattern distribution was observed in primary PrECs, occurring 4 days earlier with significant induction coinciding with p38α and MYC activation (**Fig. S2A**, Appendix B).

Induction of *NOTCH1* and *NOTCH3* mRNA, as well as NOTCH ligands and *HES/HEY* downstream targets, was measured by qRT-PCR over the same differentiation time course. *NOTCH1* and *NOTCH3* mRNA expression paralleled their protein expression; *NOTCH1* dipped and recovered to baseline, while *NOTCH3* increased dramatically and ultimately was higher in the luminal cells than the basal cells (**Fig. 7B**). *NOTCH3* mRNA appeared to increase in two phases; first a steady climb increasing ~10-fold over the first eight days, then a more dramatic increase, up ~220-fold (vs day 1) in the luminal cells (**Fig. 7B**). NOTCH ligands displayed two distinct expression profiles; *JAG1* (**Fig. 7B**) and *DLL4* (**Fig. S2B**, Appendix B) showed initial decreases but then recovered by day 10, following the pattern of *NOTCH1* expression. Meanwhile, *DLL3* held flat and began to increase after day 10, paralleling the increase in *NOTCH3* mRNA expression (**Fig. 7B**). *HEY2*, *HEYL* (Fig. 2B), *HES1*, *HES6*, and *HEY1* (**Fig. S2B**, Appendix B) all increased during differentiation, with day 8 being a key inflection point. *HEY2* was unique in that not only did it show a large spike at day 8 (increasing ~8 fold), but it segregated into the luminal population (up 45-fold vs day 1) similar to *NOTCH3*. Although it initially increased, *HEYL* eventually decreased after day 10. These data show that the day 8 to day 10 window is critical for activation of the NOTCH pathway, as ligands and downstream targets are induced during that time. This window correlates with the visual appearance of an emerging luminal layer and integrin mRNA downregulation (**Fig. S2B**, Appendix B).

iii. NOTCH1 and NOTCH3 are required for differentiation.

To examine the requirement of NOTCH for differentiation, iPrECs were differentiated and treated with either a γ-secretase inhibitor (RO4929097) or Dox to induce expression of *NOTCH1* or *NOTCH3* shRNA. Efficient knockdown of *NOTCH* in the shRNA lines occurred 4 days after Dox treatment (**Fig. 7C**). Control cells differentiated well as indicated by formation of an AR-positive luminal layer, while treatment with RO4929097 greatly ablated differentiation (**Fig. 7D**). Knockdown of *NOTCH1* or *NOTCH3* by shRNA each led to disruption of the luminal layer, though some small clumps of cells were visible in the upper layer. Propidium iodide staining indicated that these clumps of cells were dead (**Fig. S2C**, Appendix B). Thus, *NOTCH1* and *NOTCH3* are each required for prostate differentiation. However, unlike with p38-MAPK inhibition, the NOTCH-antagonized cells began detachment to form a luminal layer but were unable to survive.

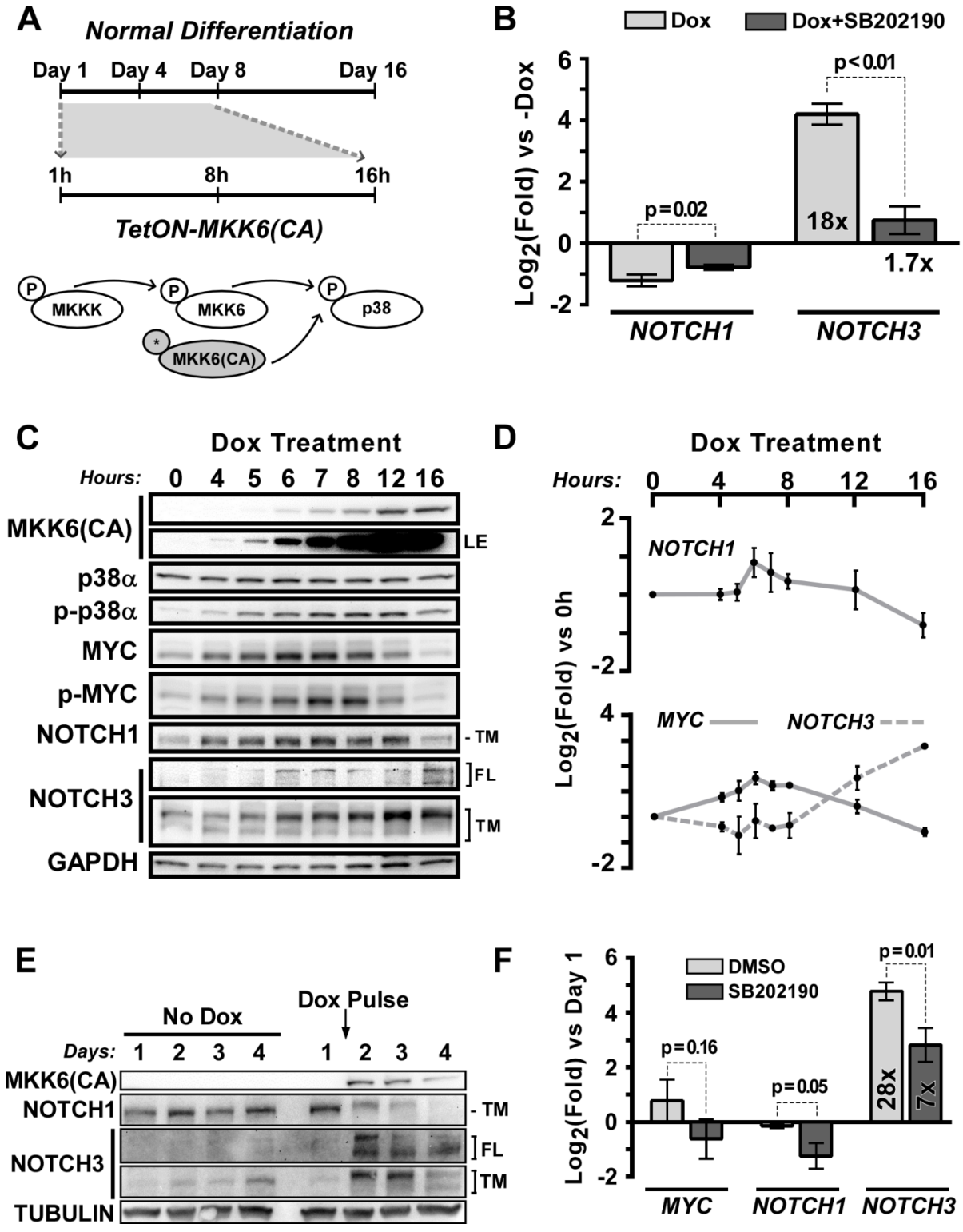

Figure 8: p38-MAPK induces *NOTCH3*.

Figure 8 (cont'd)

(A) Diagram explaining the MKK6(CA) model. iPrECs were engineered to stably express a Dox-inducible constitutively active MKK6 mutant: iPrEC-TetON-MKK6(CA). The classic MAPK phosphorylation cascade involves MKKK, MKK, and MAPK factors. p38-MAPK activation is usually moderate and occurs over the course of days in the differentiation context. However, MKK6(CA) overcomes the bottleneck of upstream activation and constitutively phosphorylates all p38 isoforms upon its induction by Dox. **(B)** iPrEC-TetON-MKK6(CA) cells were treated with Dox (5ng/mL) for 16h with or without 5μM SB202190. *NOTCH1* and *NOTCH3* mRNA expression was analyzed by qRT-PCR. Data were standardized to *18S* and *GAPDH*. Y-axis shows ΔΔCT values relative to untreated (DMSO only) cells, which is equal to Log_2(fold change). Error bars show standard deviation of biological triplicates and *p*-values were determined by paired, two-tail t-test. Text within bars is rounded to fold change. Text within bars is rounded fold change. **(C)** iPrEC-TetOn-MKK6(CA) cells were treated with Dox (2ng/mL) for up to 16h and harvested at indicated times with lysates analyzed by immunoblot. Myc-tagged MKK6(CA) was recognized with a MYC antibody (LE = long exposure). **(D)** iPrEC-TetON-MKK6(CA) cells were treated and collected as in (C), but qRT-PCR was used to measure *MYC*, *NOTCH1*, and *NOTCH3* mRNA. Data were standardized to *18S* and *GAPDH*. Y-axis shows ΔΔCT values relative to 0h samples. Error bars show standard deviation of biological triplicates. **(E)** iPrEC-TetON-MKK6(CA) cells were differentiated for 1-4 days, with or without a Dox pulse between day 1 and day 2 (5ng/mL for 4h). Lysates were collected and levels of MKK6(CA), NOTCH1, and NOTCH3 were analyzed by immunoblotting. TUBULIN served as a loading control. **(F)** iPrECs were differentiated for 4 days with DMSO or 5μM SB202190. qRT-PCR was used to measure *MYC*, *NOTCH1*, and *NOTCH3* mRNA expression. Data were standardized to *18S* and *GAPDH*. Y-axis shows ΔΔCT, or Log_2(fold change), values relative to day 1. Error bars show standard deviation of biological triplicates and *p*-values were determined by paired, two-tail t-test. Text within bars is rounded to fold change.

iv. MKK6-induced p38 recapitulates differentiation-induced MYC and NOTCH3

To determine the relationship between p38-MAPK and *NOTCH3*, I engineered an iPrEC line with a Dox-inducible constitutively active MKK6 mutant[292], MKK6(CA), which directly phosphorylates and activates p38-MAPK. During differentiation p38-MAPK activation is moderately elevated over several days (see **Fig 6A**), but when MKK6(CA) is induced, the signaling events that naturally occur over days are condensed into hours (**Fig. 8A**). Although prolonged constitutive p38-MAPK activation leads to stress and cell death, the Dox-inducible system allows me to tightly control induction and measure downstream signaling over a short time period. A 16h treatment of iPrEC-TetON-MKK6(CA) cells with Dox led to an 18.4-fold increase in *NOTCH3* mRNA that was blocked by a p38-MAPK inhibitor (**Fig. 8B**). Conversely, MKK6(CA) induction decreased *NOTCH1* by 2.3-fold.

iPrEC-TetON-MKK6(CA) cells were then treated with Dox and cell lysates evaluated for induction of p38, MYC, and NOTCH at various time points (**Fig. 8C**). Induced MKK6(CA) could be detected as early as 4 hours after dox, at which time a corresponding increase in active p-p38α and MYC began. NOTCH3 levels began to increase at around 6 hours with a greater increase after 12h. A similar time course was used to measure induction of *MYC* and *NOTCH* mRNA. As with the protein, *MYC* mRNA induction preceded *NOTCH3* and *NOTCH1* was decreased (**Fig. 8D**). Furthermore, a short pulse of Dox after one day of differentiation with the iPrEC-TetON-MKK6(CA) cells was sufficient to induce NOTCH3 at day 2 (**Fig. 8E**), 3-6 days earlier than NOTCH3 is normally induced (see **Fig. 7A**). Thus, constitutive activation of p38-MAPK is sufficient to induce p38 and MYC phosphorylation, increased *NOTCH3* expression, and downregulated *NOTCH1*. Thus, the MKK6(CA) model mimics regulation of these genes as in the standard differentiation assay. Consequently, differentiation of iPrECs for four days in the presence of a p38-MAPK inhibitor suppressed *MYC* induction and dampened *NOTCH3* upregulation to 7-fold vs 27.5-fold in control cells (**Fig. 8F**).

v. MYC is required for p38-MAPK regulation of NOTCH3.

MKK6/p38 can regulate transcription by post-translational activation of transcription factors. Thus, downstream transcription induced by p38-MAPK could be due to either direct activation of an already expressed transcription factor or subsequent upregulation of a secondary factor. To investigate which mechanism was required for *NOTCH3* I utilized cyclohexamide (CHX) to block protein synthesis at various times after Dox induction of MKK6(CA) and measured the effect on *NOTCH3* mRNA. iPrEC-TetON-MKK6(CA) cells were treated with Dox, and CHX was added at 6h, 8h, or 10h with samples harvested at 12h. Addition of CHX at 6h blocked *NOTCH3* mRNA upregulation, while addition of CHX at 8h or later did not (**Fig. 9A**, **Fig. S3A**, Appendix B). Thus, synthesis of an intermediate protein must occur after 6h but before 8h following Dox treatment. This window of 6h-8h fits the timing of maximal MYC induction and activation (**Fig. 8C**). To test the dependency of *NOTCH3* induction on *MYC*, iPrEC-TetON-MKK6(CA) cells were transfected with siRNA against *MYC* or a non-targeting control sequence and then induced with Dox for 12h. *MYC* mRNA was knocked down ~80% and though *NOTCH3* mRNA induction was not completely prevented, it was diminished ~50% compared to the control cells (2.1 fold difference, p=0.01) (**Fig. 9B**). To further address the dependency of *NOTCH3* induction on *MYC*, I utilized a MYC-MAX antagonist, 10058-F4[293]. iPrEC-TetON-MKK6(CA) cells were treated with Dox and increasing concentrations of 10058-F4 for 16h and *NOTCH3* mRNA and protein were measured. Treatment with as little as 5μM 10058-F4 suppressed the induction of NOTCH3 protein to the same level as control cells **(Fig. 9C**), whereas 20μM was required to suppress *NOTCH3* mRNA (**Fig. S3B**, Appendix B). These doses for 10058-F4 are at or below common usage[294,295]. Thus *MYC* contributes to and is required for full p38-MAPK-induced upregulation of *NOTCH3*.

To determine whether *MYC* is sufficient for *NOTCH3* upregulation, I generated a Dox-inducible *MYC* expressing cell line: iPrEC-TetON-Myc. MYC induction occurred after 2h of Dox treatment and NOTCH3 protein gradually increased slightly and peaked at 6h (**Fig. 9D**). However, there was no change in *NOTCH3* mRNA at 8h (**Fig. S3C**, Appendix B). I then tried MYC induction after differentiating cells for 5 days to allow some expression of NOTCH3 and induced MYC above what is normally seen at this time. I observed an increase in NOTCH3 protein expression that peaked at 24h after MYC induction compared to untreated controls at 24h (**Fig. S3D**, Appendix B). Thus, *MYC* is not sufficient in this context to induce *NOTCH3* mRNA, while the protein effect may be explained by upregulation of translation machinery[113].

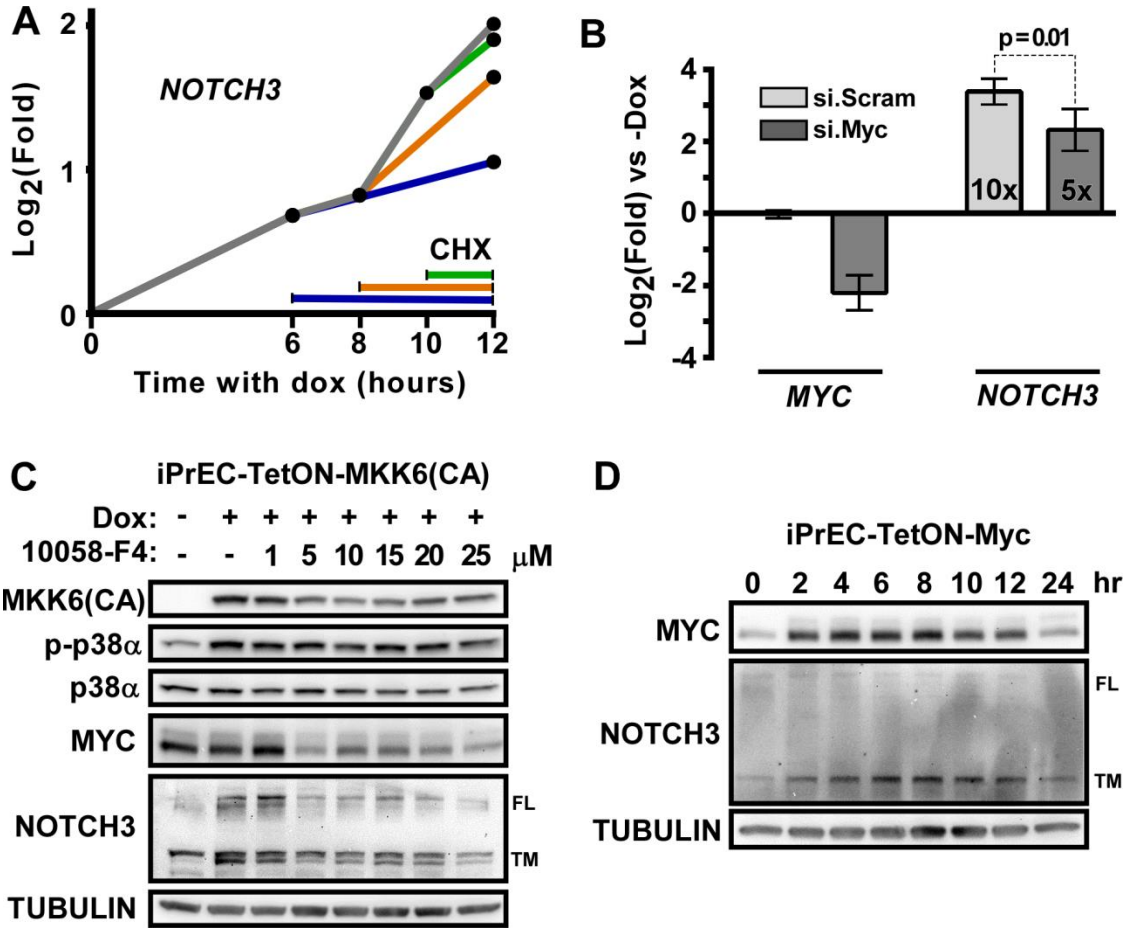

Figure 9: MYC is an intermediate for p38-MAPK induction of *NOTCH3*.

Figure 9 (cont'd)

(A) iPrEC-TetON-MKK6(CA) cells were induced with 5ng/mL Dox, then 10µg/mL Cyclo-hexamide (CHX) was added at 6h, 8h, or 10h after Dox treatment. *NOTCH3* mRNA was measured by qRT-PCR. Samples were standardized to *18S* and *GAPDH*. Y-axis shows ΔΔCT values relative to 0h. Dashed lines show expression after CHX addition (6-12h, 8-12h, or 10-12h). **(B)** iPrEC-TetON-MKK6(CA) cells were transfected with siMyc or siScram for 24h, then induced with Dox (5ng/mL) for 12h. qRT-PCR was used to measure *MYC* and *NOTCH3* mRNA expression. Error bars show standard deviation of biological triplicates and *p*-values were determined by paired, two-tail t-test. Text within bars is rounded to fold change. Data were standardized to *18S* and *GAPDH*. Y-axis shows ΔΔCT values relative to non-transfected, untreated controls. Text within bars is rounded to fold change. **(C)** iPrEC-TetON-MKK6(CA) cells were treated 16h with Dox (5ng/mL) plus DMSO or increasing doses of 10058-F4 MYC inhibitor. p38α, p-p38α, MYC, and NOTCH3 levels were measured by immunoblot. **(D)** iPrECs expressing Dox-inducible MYC (iPrEC-TetON-Myc) were treated with Dox (10ng/mL) for 0-24h and MYC and NOTCH3 levels were analyzed by immunoblot.

vi. NOTCH3 is transcriptionally regulated via a MYC-binding enhancer.

The *NOTCH3* promoter contains a CpG island and no TATA sequence within 2kb upstream of the start codon[296]. To investigate the transcriptional regulation of *NOTCH3* during prostate epithelial differentiation, I sought to identify the regulatory regions involved. A 2kb region of the *NOTCH3* upstream proximal promoter was not sufficient to induce a luciferase reporter after 6 days of differentiation, even though the endogenous gene was induced ~25-fold (**Fig. 10A**). I took two approaches to define enhancers that could control *NOTCH3* expression. The first made use of a specialized RNA-Seq approach called UV-BrU-Seq[297,298]. This technique enriches for short transcripts near sites of active transcription. iPrEC-TetON-MKK6(CA) cells were treated with or without Dox for 10h and subjected to the UV-BrU-Seq protocol. Dox induction dramatically increased *NOTCH3* reads (RPKM) that accumulated near the start site (**Fig. 10B**). Strikingly, there was also a peak of reads from the plus strand (non-coding) within the second intron, a region previously reported to contain a *NOTCH3* enhancer[238,299]. The gene for MKK6 (*MAP2K6*) served as a positive control, showing induction only upon Dox treatment with reads mapping only to the exons generated from the cDNA construct (**Fig. S4A**, Appendix B). Other controls include *CALB1* and *TRIM22*, genes which increased and decreased their expression, respectively, upon MKK6 induction and did not show any reads from the non-coding strand outside the promoter (**Fig.S4A**, Appendix B).

My second approach used a combination of DNAse hypersensitivity, histone patterns (K27Ac + K4me1/2), and ChIP-seq data from ENCODE to identify potential promoter and enhancer elements[296,300]. Five different elements were chosen based on ENCODE patterning and confinement between neighboring genes. Elements were then cloned into a pNL1.1-miniTK luciferase reporter vector and tested for their ability to be induced by Dox in the iPrEC-TetON-MKK6(CA) cells (**Fig. S4B**, Appendix B). Two candidate enhancer elements (En1 and En3) were upregulated 7- and 5-fold, respectively, after 16h of Dox (**Fig. 10C**). A positive control

vector with 5 tandem CREB response elements was upregulated ~3.5-fold. Meanwhile, En2.1, En2.2, and the promoter displayed negligible induction. En1 is ~10kb upstream of the promoter, while En3 is in the second intron. En3 corresponds to the site identified with bidirectional transcripts in UV-Bru-Seq.

Deletions within En1 and En3 that eliminated all or most of the predicted *MYC* binding sites completely ablated the ability of the En1 reporter to be induced but had only a small effect on En3 reporter activity (**Fig. 10C**). To determine if *MYC* can bind these enhancers, MYC ChIP was carried out in iPrEC-TetON-MKK6(CA) cells. Two primer sets were designed per element: set (1) is more upstream, set (2) more downstream, flanking *MYC* sites in the area if possible. ChIP with a MYC antibody confirmed that MYC is inducibly bound to En1 (both primer sets) and En3 in the 3' end; the region retained in ΔEn3 (**Fig. 10D**). To further link *MYC* to these enhancers, the luciferase assays were repeated in the presence of the MYC inhibitor 10058-F4. Again the En1 deletion abrogated induction, but the MYC inhibitor had little if any effect on the induction of the full En1 reporter (**Fig. 10E**). As seen before, the En3 deletion only minimally inhibited induction, but inhibition of MYC dramatically reduced En3 reporter activity in both En3 and En3Δ constructs. Thus, the first 360bp of En1 are absolutely required for induction by MKK6(CA) and are bound by MYC; however, En1 is still upregulated in the presence of a 10058-F4, which suggests other factors are likely sufficient. Furthermore, En3 appears to be regulated by MYC utilizing the 3' region of the element as the 5'-truncated En3Δ construct was still induced by MKK6(CA) but not in the presence of MYC inhibitor.

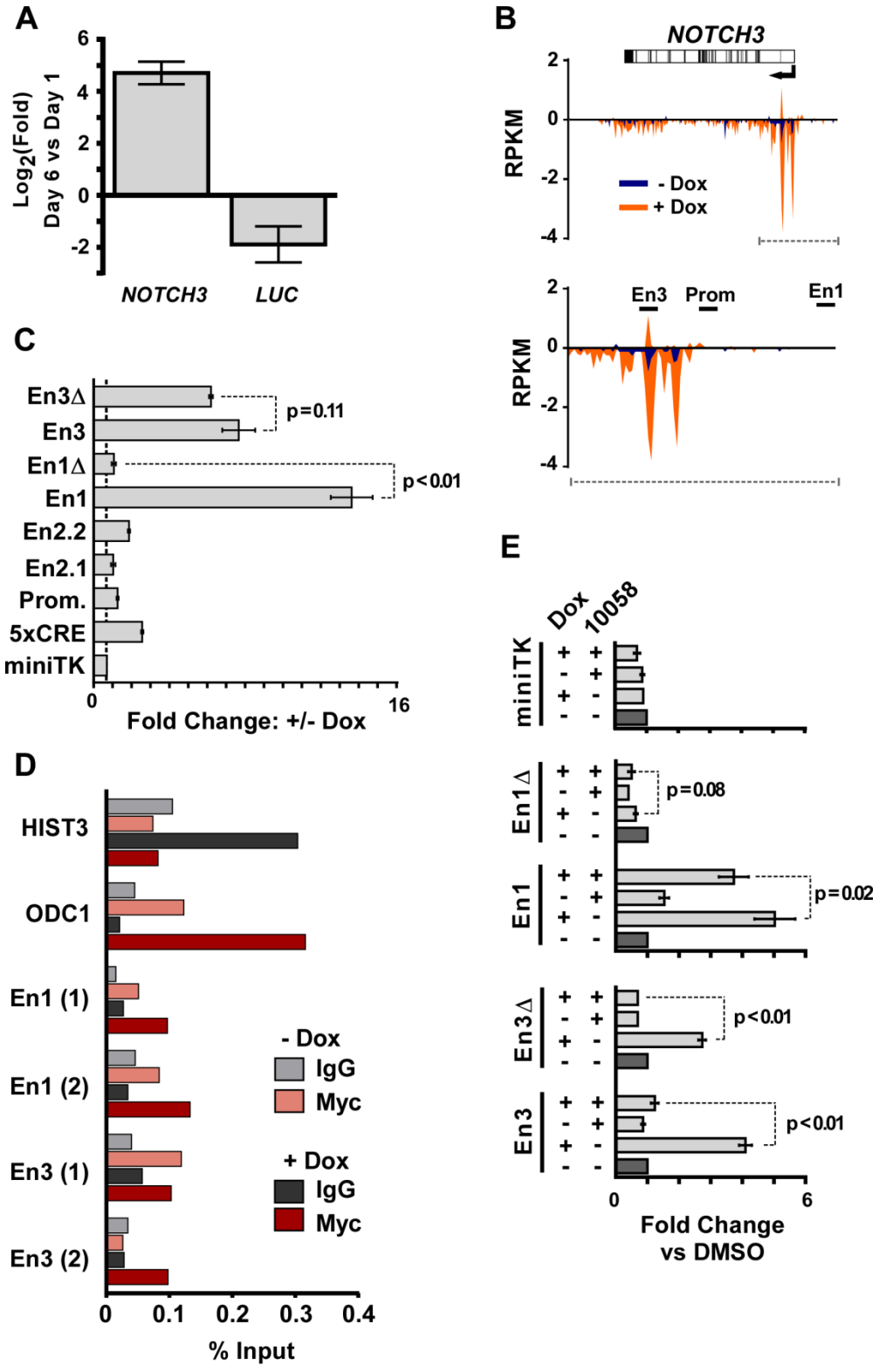

Figure 10: *NOTCH3* transcription requires a MYC-driven enhancer element.

Figure 10 (cont'd)

(A) iPrECs were transfected with a selectable pGL4.15 vector containing 2kb of *NOTCH3* upstream sequence. A stable pool of cells was differentiated for 1 or 6 days and *NOTCH3* and *LUCIFERASE* mRNA expression were analyzed by qRT-PCR. Samples were standardized to *18S* and *ACTB*. Y-axis shows ΔΔCT values relative to day 1 samples. Error bars show standard deviation of biological triplicates. **(B)** iPrEC-TetON-MKK6(CA) cells were treated with 5ng/mL Dox for 10h and processed for UV-BrU-Seq. Graphs show RNA reads across gene locus (bin = 300bp). Lower region is an enhanced view, marked by dashed grey lines. Y-axis is RPKM (reads per kilobase of transcript per million mapped reads). Plus strand reads are (+) values, minus strand reads are (-). Blue = -Dox samples and orange = +Dox. *NOTCH3* gene diagram shows exon mapping (black regions). Note: *NOTCH3* is on the minus strand. **(C)** iPrEC-TetON-MKK6(CA) cells were transfected with reporter constructs and run in luciferase assay. After transfection, each pool of cells was split and treated -/+ 5ng/mL Dox for 16h. Error bars show standard deviation of technical triplicates and *p*-values were determined by paired, two-tail t-test. pNL1.1-miniTK served as negative control and pNL1.1-5xCRE-miniTK (5 tandem CREB binding elements) served as a positive control. Vertical line was drawn at miniTK level as baseline. **(D)** iPrEC-TetON-MKK6(CA) cells were treated -/+ 5ng/mL Dox for 8h. MYC binding to specific enhancer regions was assessed by ChIP and qRT-PCR. IgG served as negative IP control. Positive and negative control MYC loci were *ODC1* and *HIST3*, respectively. En1 and En3 elements had two primer sets each, with set (1) being more 5'. **(E)** Same experiment as in (D) except that transfected pools were split into four wells and treated 16h with DMSO, Dox (5ng/mL), 10058-F4 (20μM), or a combination. Each group was normalized to DMSO treatment. p-values were calculated by 2-way ANOVA with Turkey's multiple testing correction.

vii. NOTCH3 expression is also controlled by mRNA stability.

NOTCH3 contains an AU-rich element in its 3' UTR (**Fig. S5**, Appendix B) and p38-MAPK is known to regulate RNA binding proteins so I tested whether it may be regulated in part by mRNA stability[152]. ActinomycinD (ActD) was used to halt transcription and nine time points were taken to measure mRNA decay[301]. The half-lives of *MYC*, *NOTCH1*, and *NOTCH3* mRNAs were measured in iPrECs at day 1 and day 4 of differentiation (**Fig. 11A, Table 6**). The *MYC* half-life, 0.8h, was similar to previous reports[302]. *MYC* and *NOTCH1* half-lives remained essentially the same at day 4. However, *NOTCH3* mRNA half-life nearly doubled on day 4 (11.5h vs 5.9h), along with an 8.5 fold increase in total expression. Alternately, a similar experiment was performed using iPrEC-TetON-MKK6(CA) cells. Cells were treated with Dox for 16h and then followed with the ActD time course (**Fig. 11B, Table 7**). Acute p38-MAPK activation had a small effect on *MYC* mRNA half-life. Both *NOTCH1* and *NOTCH3* mRNA half-lives more than doubled: 3.3h to 8.8h for *NOTCH1* and 7.6h to 17.6h for *NOTCH3*. However, the overall mRNA level of *NOTCH1* decreased ~4 fold upon Dox treatment while *NOTCH3* increased ~9 fold (**Table 7**). Thus, differentiation and acute p38-MAPK activation both lead to increased *NOTCH3* mRNA half-life, indicating that *NOTCH3* is also regulated post-transcriptionally through mRNA stabilization.

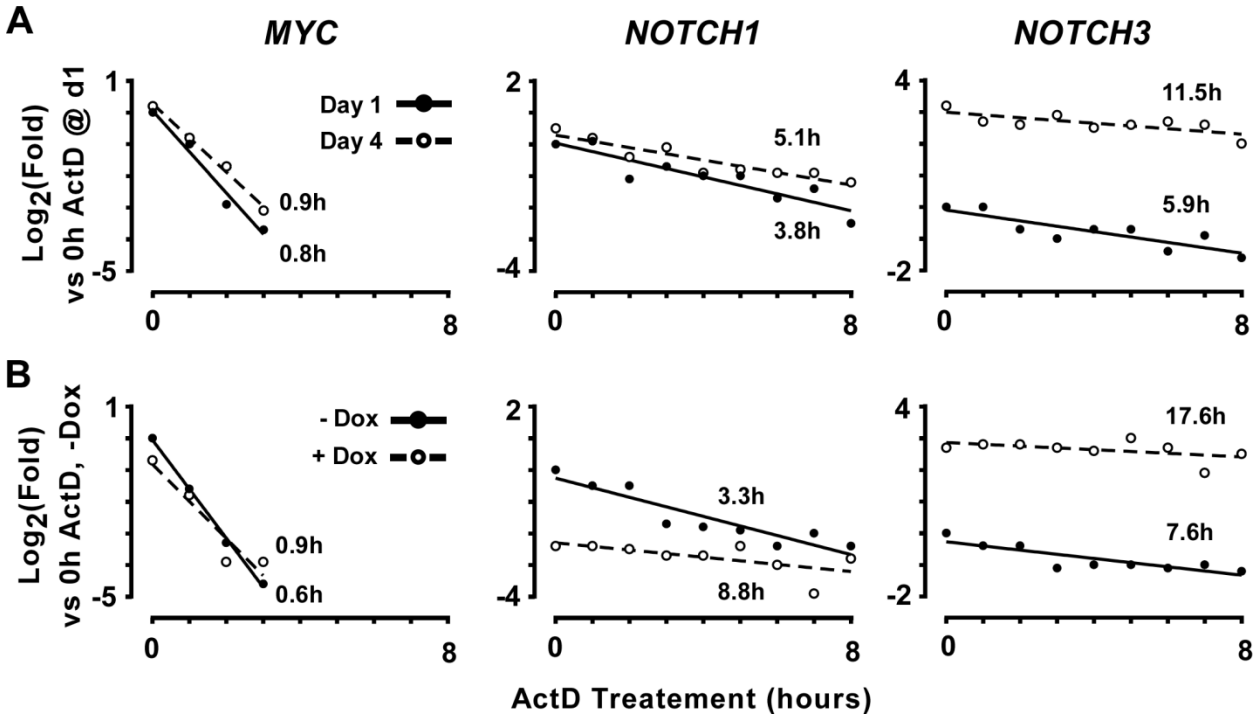

Figure 11: p38-MAPK upregulates *NOTCH3* mRNA stability. (A) iPrECs were differentiated for 1 or 4 days and at each time were treated with ActinomycinD (5µg/mL) for 0-8h. RNA samples were harvested each hour and qRT-PCR was used to measure *MYC*, *NOTCH1*, and *NOTCH3*. Samples were standardized to *18S* rRNA. Y-axis shows ΔΔCT values relative to the Day1, 0h sample. Closed circles/solid line = day 1 samples; open circle/dashed line = day 4. For *MYC*, only 1-4h time points were used to maintain a linear range. **(B)** The same experiment as in (A) but using the iPrEC-TetON-MKK6(CA) model. Cells were treated -/+ Dox (5ng/mL) for 16h and then treated 0-8h with ActD. Samples were normalized to the -Dox, 0h sample. Closed circles/solid line = +Dox samples; open circle/dashed line = -Dox.

		Line Equation Y= mx+b	*r ²	Half Life (1/m)	p-value (m1 vs m2)	Overall Expression
MYC	**Day1**	Y= -1.30x + 0.05	0.98	0.8h	0.25	+ 1.2 fold
	Day4	Y= -1.08x + 0.27	0.99	0.9h		
NOTCH1	**Day1**	Y= -0.267x + 0.03	0.82	3.8h	0.23	+ 1.2 fold
	Day4	Y= -0.197x + 0.29	0.85	5.1h		
NOTCH3	**Day1**	Y= -0.170x - 0.10	0.74	5.9h	0.11	+ 8.5 fold
	Day4	Y= -0.0867x + 2.99	0.55	11.5h		

Table 6: Day 4 vs Day 1 mRNA half-life calculations. *r^2 values indicate how well the 9 data points fit each linear regression line. p-value between slopes was determined by ANCOVA.

		Line Equation Y= mx+b	*r ²	Half Life (1/m)	p-value (m1 vs m2)	Overall Expression
MYC	**-Dox**	Y= -1.55x - 0.05	1.00	0.6h	0.50	+ 1.7 fold
	+Dox	Y= -1.17x - 0.82	0.90	0.9h		
NOTCH1	**-Dox**	Y= -0.302x - 0.26	0.85	3.3h	0.02	- 4.1 Fold
	+Dox	Y= -0.113x - 2.30	0.42	8.8h		
NOTCH3	**-Dox**	Y= -0.132x - 0.27	0.73	7.6h	0.14	+ 8.8 fold
	+Dox	Y= -0.057x + 2.86	0.25	17.6h		

Table 7: MKK6(CA) -/+ Dox mRNA half-life calculations. *r^2 values indicate how well the 9 data points fit each linear regression line. p-value between slopes was determined by ANCOVA.

C. Materials and methods

Cell Culture. Human primary prostate basal epithelial cells (PrEC) and an E6/E7+hTert immortalized variant (iPrEC) were used for this study[102,303]. Cells were grown in Keratinocyte Serum Free Media (Life Technologies) plus penicillin/streptomycin at 30u/mL (Life Technologies). Differentiation was induced as previously reported with recombinant KGF/FGF7 from Cell Sciences at 2.5ng/mL and R1881 from Perkin Elmer at 10nM with fresh media changes every 24h[71]. Luminal cell layer separation was achieved using calcium/magnesium-free PBS with 1mM EDTA to loosen cadherin junctions as previously described[71]. HEK 293FT cells were used for lentivirus production and were grown in DMEM (11995, Life Technologies) with 10% fetal bovine serum and 2mM L-glutamine. Cell lines were regularly tested and confirmed to be mycoplasma free. Cells were maintained at 37^{o}C in 5% CO_2.

Molecular Cloning and Stable Cell Line Construction. iPrEC lines were engineered with doxycycline (Dox)/tetracycline-inducible shRNAs via the Tet-pLKO-Puro vector[254]. shRNA oligos were designed using targeting sequences from the BROAD RNAi consortium[304]. Lentivirus was made in 293FT cells and iPrECs were selected with 1-2µg/mL puromycin. Dox was used at 50-100ng/mL to induce shRNA expression. shRNA targeting sequences can be found in **Table S2**, Appendix A.

Expression cDNAs were PCR subcloned with Q5 polymerase (NEB) into the pENTR3C gateway vector (Life Technologies) between SalI and NotI sites and then recombined with LR Clonase II (Life Technologies) into pLenti-CMV/TO-Puro-DEST, a gift from Eric Campeau (Addgene plasmid 17293)[305]. The constitutively active MKK6-DD (MKK6(CA)) mutant was subcloned from a plasmid gifted by Angel Nebreda[292]. The *MYC* cDNA was subcloned from pBabe-Myc, a gift from Beatrice Knudsen. TetR lines were established using pLenti-CMV-TetR-Blast, a gift from Eric Campeau (Addgene plasmid 17492)[305]. iPrECs were selected in 5µg/mL in blasticidin and 1-2µg/mL puromycin after infection. Dox was used at 2-10ng/mL to induce cDNA expression.

siRNA and Inhibitors. A mixed pool siRNA against *MYC* and non-targeting siRNA (siScram) was purchased from Origene (SR303025). Cells were transfected with siLentfect reagent (Bio-Rad). Cyclohexamide was used at 10µg/mL and ActinomycinD at 5µg/mL (both from Calbiochem). The p38 inhibitors SB202190 and BIRB796/Doramapimod plus the MYC-MAX inhibitor 10058-F4 were purchased from Cayman Chemical. The γ-secretase inhibitor RO4929097 was purchased from Apex Bio.

Immunoblotting. Cell lysates were prepared as previously described[303]. In summary, cells were chilled on ice and lysed with RIPA lysis buffer. Cells were then scrapped, centrifuged, and protein was quantified by BCA assay (Pierce). Equivalent amounts of 20-50µg of denatured protein per sample was run on Novex SDS polyacrylamide tris-glycine gels (Life Technologies). Protein was then transferred onto PVDF membranes and blocked in 5% BSA/TBST for 1h at room temp. Primary antibodies were probed either 1-3h at room temp or overnight at 4ºC while all secondary antibodies were probed 1h at room temp. Luminol chemiluminescence was used to image blots with a Bio-Rad Chemi-Doc imaging system with CCD camera. Images were analyzed using Quantity One software (v4.5.2). Detailed antibody information can be found in **Table S3**, Appendix A.

qRT-PCR. RNA was harvested and extracted with Trizol following the manufacturer's protocol (Life Technologies). cDNA was synthesized with M-MuLV reverse transcriptase (NEB) using a mix of poly-d(16)T and random hexamer primers (4µM:1µM). qRT-PCR was performed using SYBR Green Master Mix (Roche) and an ABI 7500 thermalcycler (Applied Biosystems). Primers were synthesized by Integrated DNA Technologies. Detailed primer information is available in **Table S4**, Appendix A.

Immunostaining. Cells were fixed, permeablized, and stained as previously described[102]. ITGα6 and AR were co-stained overnight at 4ºC with each at 1:200 dilutions (ITGα6: 555734, BD Biosciences / AR: sc-815, Santa Cruz). For Propidum iodide staining, cells were fixed with 4% paraformaldahyde, treated with RNaseA (10min, 100ng/mL), washed with

PBS, and then stained with propidum iodide (5min, 100ng/mL) (Sigma). Nuclei were stained with Hoescht33258 (Sigma) for 10min at 10µg/mL. Epifluorescence microscopy was performed on a Nikon TE300 using Nikon Elements software (v4.11.00).

Luciferase assay and constructs. Putative *NOTCH3* regulatory elements were PCR subcloned from the RP11-937H1 BAC library (Life Technologies) using Q5 or LongAmp polymerase (NEB). The *NOTCH3* 2kb promoter element was ligated into pGL4.15-Hygro (Promega). Hygro selection was done at 25µg/mL. Candidate regulatory elements were ligated into pNL1.1 (Promega) after first cloning in a miniTK promoter at the HindIII site. Cloning primers and miniTK sequence information can be found in **Table S5**, Appendix A. Deletion mutants were made using the QuickChange II Mutagenesis kit (200524, Stratagene,). Deletion primer sequences are in **Table S6,** Appendix A.

Luciferase assays were performed using the NanoGlo Dual-Luciferase Reporter kit (Promega). pGL4.15-miniTK-Luc was used as the transfection control. pNL1.1-miniTK served as the negative reporter control and pNL1.1-5xCRE-miniTK served as a positive control for p38-MAPK activation (5 tandem CREB response elements). 5xCRE sequence can be found in **Table S5**, Appendix A. Luminescence was measured on a BioTek Synergy Neo II plate reader with Gen5 software (v2.04.). pNL constructs were transfected into iPrEC-TetON-MKK6(CA) cells using XtremeGeneHP reagent (Roche). Luciferase assays were run 16h after Dox (~48h after transfection). Cells were lysed using Passive Lysis Buffer (E1941, Promega) and lysates were transferred to a 96-well plate and assayed in triplicate. Data were standardized to the pGL4.15-miniTK control (NanoLuc/FireflyLuc).

***Chromatin Immunoprecipitation*.** Cells (3 million) were fixed with 1% formaldehyde (Thermo Scientific) for 1-5min. Cells were washed 3X with ice cold Calcium-Magnesium Free PBS (CMF-PBS) plus protease inhibitors. Pelleted cells were treated with swelling buffer (5 mM PIPES pH 8.0, 85 mM KCl, 0.5 % IGEPAL/CA-630) on ice for 30min. Nuclei were dounce homogenized and pelleted at 4000rpm for 10min, 4^{o}C (Eppendorf 5415d). Sonication buffer

(0.1% SDS, 10 mM EDTA, 50 mM Tris-HCl pH 8.1) was added to nuclei and incubated on ice for 10min prior to sonication. Chromatin was sheared at 4°C using the Covaris E220 Ultra Sonicator following manufacturer's suggested settings of 2% Duty Cycle, 105 Watt Peak Intensity, 200 Cycles/Burst. In order to achieve 300-500bp fragments, samples were sonicated for 7min.

Chromatin immunoprecipitations were performed with 1.5-2 million cells per IP. The following antibodies were used: c-Myc (sc-764, Santa Cruz)] and Rabbit IgG (CST). 6µg of primary antibody was incubated with chromatin overnight at 4°C with rotation. Next, and 25µL of Protein A magnetic beads (NEB) was added to samples and incubated 6h at 4°C with rotation. Beads were then washed in the following buffers at 4°C for 10min with rotation: Triton Wash Buffer (50mM Tris-HCl pH 7.4, 150mM NaCl, 1% Triton X-100), followed by Lysis Buffer 500 (0.1% NaDOC, 1mM EDTA, 50mM HEPES pH 7.5, 500mM NaCl, 1% Triton X-100), LiCl Detergent buffer (0.5% NaDOC, 1mM EDTA, 250mM LiCl, 0.5% IGEPAL, 10mM Tris HCl pH 8.1), and Tris-EDTA pH 8.1. Protein was eluted from beads in Elution Buffer (10mM EDTA, 1% SDS, Tris-HCl pH 8.0) for 30min at 65°C. Samples were then treated with 20µg proteinase K and10µg RNase A, then NaCl (200mM) was added and incubated at 65°C over night to reverse cross-links. DNA was purified using phenol/chloroform extraction and ethanol precipitation.

qRT-PCR was performed as described in the qRT-PCR methods section. ChIP primer information can be found in **Table S7,** Appendix A. Percent input was calculated as $2^{\Delta CT}$x100 divided by the ratio of chromatin per IP to Input (75µL per IP, 25µL for Input). *HIST3* was used as a control locus not reported to be regulated by MYC and *ODC1* was used as a positive control for MYC binding[306].

mRNA half-life measurement. Cells were treated with 5µg/mL ActinomycinD for 0-8h. RNA and cDNA were prepared as described in the qRT-PCR methods section. Data were standardized to *18S* rRNA and normalized as ΔΔCT values vs the Day1 or –Dox 0h ActD sample. Linear regression curves, equations (y=mx+b), and r^2 values were calculated with

GraphPad PRISM software. Half-life was calculated as 1/m. Overall expression change was calculated as $2^{(b_2-b_1)}$. AU rich elements were identified using the ARE site (v1) online tool[307].

***Statistical analysis*.** Unless otherwise stated, p-values were calculated using paired, two-tailed t-tests on biological triplicates. For Fig. 10E p-values were calculated by 2-way ANOVA with Turkey's multiple testing corrections. For Tables 6 and 7 p-values were determined by comparing the slopes for either day1/day4 or –dox/+dox mRNA decay. Values were calculated by ANCOVA analysis using PRISM GraphPad software. For Fig. S3B one-way ANOVA was used with Greenhouse-Geisser correction and Dunnett's multiple comparison correction

***UV-Bru-Seq*.** iPrEC-TetON-MKK6(CA) cells were treated -/+ 5ng/mL dox for 10h, then UV treated (100J/m^2) using a Stratalinker UV Crosslinker 1800 (Stratagene) and labeled with 2mM 5-Bromo-deoxyuridine (sc-256904, SantaCruz) for 30min before washing with PBS and collecting RNA with Trizol (Life Technologies). BrU isolation, library prep, sequencing, and mapping was performed by Mats Ljungman and his lab[297,308]. Data were exported (bin size = 300bp) and graphed using GraphPad PRISM software.

D. Discussion

i. Differential regulation of NOTCH1 and NOTCH3 in differentiation.

NOTCH1 expression has been reported in basal cells of mouse and human prostate, while *NOTCH3* has been reported to be more luminal, though mostly in mouse studies and with conflicting reports[227,287,309]. My data found that *NOTCH1* and *NOTCH2* are the most abundantly expressed members in human basal cells, while *NOTCH3* is very low. NOTCH4 protein was detectable but at a very low level and did not increase during differentiation (not shown). Since NOTCH2 protein was unchanged during differentiation and NOTCH4 was barely detectable, I focused on *NOTCH1* and *NOTCH3*. Quite strikingly I found a dramatic induction of *NOTCH3* mRNA and protein during the course of luminal cell differentiation. In contrast, *NOTCH1* mRNA and protein did not increase and actually decreased before returning to its original levels. Over time our model becomes a mixture of basal and luminal cells, though it is only the luminal cells that are generated and increased with time. *NOTCH3* expression coincides with the appearance of luminal cells. Therefore, *NOTCH3* is likely the primary driver of luminal cell differentiation, while *NOTCH1* serves its previously described role in maintaining the basal population[227,287,309]. Until recently, the function of *NOTCH3* remained controversial. However, recent reports show that *NOTCH3* drives luminal differentiation of normal human airway basal cells and mammary epithelium[242,310-313]. Moreover, of the NOTCH receptors only *Notch3* is sufficient to drive hepatocyte differentiation in embryonic mouse liver cells[314]. Thus, my study provides support that *NOTCH3* defines a more luminal phenotype in prostate epithelium.

ii. Transcriptional regulation of NOTCH3 by p38-MAPK.

Part of the mechanistic insight from this work demonstrates that p38-MAPK can regulate *NOTCH3* transcription in a *MYC*-dependent manner. Although a relationship between p38-MAPK and NOTCH has previously been suggested, mechanistic details have not been clearly

established[315-318]. I found that the ability of *NOTCH3* to be induced by either MKK6(CA) or through KGF/androgen-induced differentiation depends on p38-MAPK. *MYC* has been reported as a potential downstream target of p38-MAPK and was previously shown to be required for PrEC differentiation[102,319]. Consequently I found that suppressing *MYC* expression by siRNA or blocking its ability to bind MAX with a pharmacological inhibitor, 10058-F4, suppresses the induction of *NOTCH3* by MKK6(CA). However, in both cases suppression was not complete. MYC on its own is not sufficient to induce *NOTCH3* mRNA. Thus, although *MYC* is required for full upregulation of *NOTCH3* by p38-MAPK, there are additional unidentified factors involved.

iii. Identification and validation of a novel NOTCH3 enhancer.

I investigated potential regulatory regions of the *NOTCH3* gene and found two elements capable of upregulating a luciferase reporter upon MKK6(CA) activation. One element lies ~10kb upstream (En1) and has not previously been identified, while the other is a previously reported region[238,299] within the second intron (En3). However, my report is the first to show functional validation of En3 in human cells. Either element is sufficient to drive a reporter, and the intronic En3 region produces eRNA upon p38-MAPK stimulation, as measured by UV-BrU-Seq. Bi-directional eRNA is a hallmark validating an active enhancer, though not all enhancers produce eRNA[320,321]. Furthermore, I was able to ChIP MYC on both elements and there are several predicted MYC binding sites in these elements[322]. However, deletions within these elements that eliminate all are nearly all predicted MYC binding sites did not always correlate with loss of induction. The intronic enhancer, En3, was still induced even when all known MYC sites were removed (En3Δ). However, both En3 and En3Δ induction was sensitive to MYC inhibition. Thus, there is likely to be another element within the remaining En3Δ region controlled by MYC –- either directly or indirectly. The upstream enhancer, En1, was severely compromised upon deletion of all but one of the MYC binding sites (En1Δ). However, it was insensitive to MYC inhibition. This suggests additional sites within the deleted region, not

dependent on MYC, are responsible for controlling *NOTCH3* expression from this enhancer. There are numerous predicted transcriptional elements in both of these enhancers[300,322]. A systematic detailed analysis will be required to define all the possible mechanisms by which *NOTCH3* mRNA transcription is regulated.

iv. NOTCH3 regulation via mRNA stability.

I also identified a post-transcriptional mechanism by which p38-MAPK regulates *NOTCH3*. *NOTCH1* expression is reported to be regulated by RNA stability through AU-rich elements in its 3' UTR and is modulated by p38-MAPK[317,323]. p38-MAPK is known to regulate mRNA stability through phosphorylation of mRNA binding proteins TTP and HUR[152]. *NOTCH3* also has predicted AU-rich elements in its 3' UTR[307]. I am the first to demonstrate that *NOTCH3* mRNA stability is regulated during epithelial differentiation and that this is mediated through p38-MAPK. Interestingly, short term p38-MAPK activation via MMK6(CA) increased both *NOTCH1* and *NOTCH3* mRNA half-life, but only *NOTCH3* maintained that stability at 6 days of differentiation. There are also reports of post-transcriptional NOTCH regulation by miRNAs[299,324,325]. Further research will be needed to fully comprehend the mechanisms of *NOTCH1* and *NOTCH3* post-transcriptional regulation.

v. Day 8 is a critical transition point in differentiation.

Temporal regulation of *NOTCH3* throughout differentiation is dynamic. I observed at least two phases of *NOTCH3* mRNA induction: an early steady increase up to day 8 followed by a more dramatic increase. Considering that *NOTCH3* mRNA is stabilized by Day 6, it could be that early upregulation is less dependent on transcriptional mechanisms and more so on message stability. Then again, I cannot rule out the possibility of other transcription factors with temporal regulation patterns. Formation of the luminal layer becomes noticeable around day 8, coinciding with induction of downstream targets *HES/HEY*. Additionally, it is at this transition

point that p38-MAPK is activated and MYC is transiently increased and activated. Thus, transcriptional induction of *NOTCH3* appears to fit best around this time may serve as the 2nd phase regulators of *NOTCH3* upregulation. Though there are still unsolved mechanisms, it appears that the window around day 8 is a key point for NOTCH activation and cell commitment to luminal transition.

vi. Modeling differentiation signaling with MKK6(CA).

Much of my detailed signaling mechanistic work was done with the iPrEC-TetON-MKK6(CA) cells. This model simplifies the effects of p38-MAPK signaling via constitutive activation and allows investigation of signaling events before toxic stress effects arise. Acute activation of p38-MAPK mirrors the same cascade of *MYC* and *NOTCH3* induction as seen during differentiation, but the timing is greatly compressed to hours instead of days. In normal differentiation there is bi-phasic *NOTCH3* mRNA upregulation, but with MKK6(CA) those phases are compressed. Though both En1 and En3 elements are upregulated after 16h with induced MKK6(CA) it is not known when they are active during differentiation and for how long. Furthermore, though I know p38-MAPK is required for differentiation, I cannot rule out the possibility of other upstream pathways which may not be represented in the MKK6(CA) model. Thus, MKK6(CA) is a great model for p38-MAPK signaling, which is a large component (but not necessarily complete representation) of total differentiation signaling.

vii. Potential downstream effects of NOTCH activity.

The direct effectors of NOTCH signaling are the canonical *HES/HEY* transcriptional repressor family. Though all these genes increase during differentiation, *HEY2* is unique in that it is much higher in the luminal layer upon terminal differentiation. Whether *HEY2* is preferentially increased by *NOTCH3* is unknown but may define a unique target for *NOTCH3* signaling. *NOTCH1* directly upregulates *MYC* in its function as a well-known oncogenic driver of

T-cell acute lymphoblastic leukemia[205]. However, I find *MYC* is upstream of *NOTCH3*. Despite the large increase in *NOTCH3* and *HES/HEY* late in differentiation I do not see an induction of *MYC* after Day 8. Thus, in a normal differentiation context *MYC* does not appear to be a downstream NOTCH target. Additional downstream pathways that NOTCH signaling can impact include *PTEN* and *E-CADHERIN*, both of which are critical for luminal cell survival[71,326]. Furthermore, NOTCH activity can downregulate adhesion genes, including integrins, which are required for basal cell detachment from the extracellular matrix[237,288,327]. There are also reports that NOTCH can upregulate *MKP1*, a phosphatase that targets p38-MAPK, thus providing a potential feedback mechanism in terminally differentiated cells to balance p38-MAPK activity[299,328]. Further extensive research will be needed to validate which downstream NOTCH targets are most relevant to prostate differentiation. Furthermore, the relationship between NOTCH and its targets may be very different in a prostate tumor cell, where many of these genes (especially integrins, *MYC* and *PTEN*) are misregulated.

viii. Conclusion.

My goal is to define the mechanisms that drive basal to luminal differentiation in the normal prostate epithelium. In this study, I report on a novel mechanism for crosstalk between p38-MAPK, MYC, and NOTCH. Moreover, I identify two distinct regulatory mechanisms for *NOTCH3* in the prostate: a two-pronged coordination of increased mRNA stability and increased transcription from multiple enhancer elements. These findings provide a better understanding for how these differentiation pathways are connected in normal prostate epithelium and open the door to defining how their dysregulation may impact prostate cancer development and progression.

CHAPTER 4 — UPSTREAM AND DOWNSTREAM REGULATORS OF NOTCH

A. Background

i. Upstream and downstream Notch regulation

In Chapter 3 I focused on investigating how p38-MAPK signaling regulates *NOTCH3* at the transcriptional and post-transcriptional level. However, NOTCH signaling requires more than just mRNA upregulation of the receptors. In Chapter 1 I described a variety of ways NOTCH signaling can be regulated, including pre-/post- transcription and translation. In addition to regulation of the receptors, NOTCH ligand expression is also required for pathway signaling. At the other end, downstream NOTCH signaling involves the HES/HEY family as well as a handful of other direct targets, such as and *MYC*. To thoroughly investigate the NOTCH signaling pathway, it is crucial to also understand the upstream (i.e. ligands) and downstream (i.e. HES/HEY) genes involved.

ii. Rationale for understanding ligand specificity

There are five canonical NOTCH ligands and four receptors, but until recently there had been little evidence to demonstrate that specific ligands showed any preference for one receptor or another[329]. Within the past five years reports have begun to elucidate that different ligands may have different functional consequences. Depending on the context (e.g. cell type, orientation, glycosylation state) ligands may be able to activate various combinations of NOTCH receptors. Despite such potential broad interaction, differential roles for the ligands are beginning to be revealed. For example, a report utilizing peptides and biochemical assays demonstrated that DLL4 has a much higher binding affinity to NOTCH1 than does DLL1[330]. Additionally, there have been reports that DLL3 may play a unique negative regulatory role by antagonizing NOTCH receptors[331,332]. In an alternate approach to tackle ligand specificity, Kangsamaksin et al. created NOTCH decoy peptides that sequestered either JAG or DLL

ligands[333]. They expressed these decoy proteins in endothelial cells and observed different physiological effects depending on whether they used the JAG or DLL decoy. These emerging studies are at the forefront of a new understanding of receptor-ligand interactions.

iii. Rationale for understanding receptor specificity, in particular NOTCH3

In addition to understanding specific ligand functions, there is also an effort to understand specific NOTCH receptor signaling profiles. *Notch1* or *Notch2* null mice are embryonic lethal, while *Notch3* or *Notch4* null mice survive and are fertile[239,334,335]. As may be expected due to the dramatic mouse phenotypes, earlier research largely focused on *NOTCH1*, while only more recently (within ~5-10 years) has attention been given to the other receptors. Though each NOTCH receptor likely has its own unique role, I have chosen to focus on *NOTCH3*, given my findings on its role in prostate differentiation. Despite being fertile, *Notch3* null mice do show defects in smooth muscle arterial cells[278] and thymocyte differentiation[336,337]. Moreover, *NOTCH3* gain of function is associated with the genetic disease CADASIL (Cerebral Autosomal Dominant Arteriopathy with Subcortical Infarcts and Leukoencephalopathy)[338] and is most studied in the cancer field as an oncogene in ovarian carcinoma[339]. Thus, despite compensation for loss of *Notch3* in knockout mice, its activation can drive unique physiological processes.

There are a variety of published reports to support the idea of *NOTCH3*-specific functions. A recurring theme from the literature is that *NOTCH3* is involved in downregulating cell cycle progression. A 2014 report by Ortica et al. investigated each of the four NOTCH receptors in the context of mouse liver differentiation[340]. They utilized bipotent embryonic mouse liver cells that are able to differentiate into either hepatocytes or cholangiocytes. While investigating the role of NOTCH signaling in their model the authors overexpressed each of the four NICD constructs and found that NICD3 alone halted proliferation and was sufficient to drive hepatocyte differentiation.

Moreover, the effect of *NOTCH3* on cell cycle and differentiation may also be relevant in cancer cells. Multiple papers using breast cancer cells reported that *NOTCH3* can drive cell cycle arrest in tissue culture[341,342]. Additionally, there was a report that *NOTCH3* aided luminal survival and evasion of apoptosis in an organoid model of HER2-driven ductal carcinoma in situ using MCF10A immortalized human mammary epithelial cells[343]. Cui et al. reported that NICD3 was sufficient to drive cellular senescence in fibroblasts and a variety of tumor lines (MDA-MB-231/breast, A375P/melanoma, T98G/glioblastoma) in part via upregulation of *p21*[344]. Most recently, a 2016 paper in *Nature Communications* found that *NOTCH3*, driven by IL-6, was required for survival of a sub-population of self-renewing hormone-therapy resistant breast cancer cells using tumor xenografts in mice[345]. Knockdown of *NOTCH3* by shRNA greatly decreased the number of resistant cells, though unfortunately the authors did not investigate the ligands or downstream effects of *NOTCH3* manipulation[345].

Another aspect by which *NOTCH3* may be unique among the NOTCH receptors is via its post-translational regulation. One study found that mice with genetic knockout of Lunatic Fringe (a NOTCH glycosyltransferase) had increased *Notch1/2/4* in the mouse prostate and decreased *Notch3*[346]. These mice also had expansion of both basal and luminal prostate layers and showed PIN lesions. Surprisingly, in the same study knockdown of Lunatic Fringe in the DU145 PCa cell line had the opposite effect and led to increased *NOTCH3* expression, which enabled increased sphere forming ability in 3-D culture[346]. Though the effect seems to vary *in vivo* and *in vitro*, there may exist some contextual specificity for *NOTCH3* by Lunatic Fringe which affects its stability and/or activity.

Though the NOTCH receptors are fairly conserved and share similar domain structure, there are some important differences[202]. A structural study found that NOTCH3 has a unique negative-regulatory region, which is the part of the transmembrane protein that is ‘pulled’ open by ligand binding, thus allowing cleavage[347]. The authors report that NOTCH3 has a weaker negative regulatory region and is more prone to spontaneous activation, i.e. translocation to the

nucleus without ligand present. Taking all these reports together, *NOTCH3* may not only have unique signaling abilities when it comes to cell cycle and differentiation, but its structure may also contribute to differential regulation at the post-translational level.

iv. Hypothesis

In order to begin investigating the upstream and downstream events of NOTCH signaling during prostate differentiation I ran some preliminary experiments. I proposed two hypotheses: 1) NICD3 and NICD1 will have differential effects on NOTCH target gene expression. 2) NOTCH ligands will be upregulated to coincide with NOTCH activation during differentiation. To test the first hypothesis I engineered iPrEC lines with Dox-inducible NICD1 or NICD3 and measured downstream expression of NOTCH target genes by qRT-PCR. For the second hypothesis I measured mRNA expression of NOTCH ligands during differentiation by qRT-PCR over a time course. With these experiments I expanded my investigation of NOTCH signaling and laid the ground work for additional experimentation.

B. Results

i. Construction and validation of inducible NICD1 and NICD3 cell lines

In order to study the effects of *NOTCH1* vs *NOTCH3* signaling in iPrECs, I first had to construct cell lines with inducible NICD1 or NICD3 expression. I first cloned NICD1 and NICD3 into a Dox-inducible lentivirus and selected cell lines using the Tet Repressor (TetR) system. I began by testing the TetR-NICD1 cell line by treating with a dox pulse for 8h and then waiting 24, 48, and 72h later to harvest samples and measure protein induction and turn-over. NICD1 expression was robust and detectable at 24h following dox pulse and then faded over time and was gone by 96h (**Fig.12A**). Next, I used the TetR-NICD3 cells and differentiated them to day 4 (when NOTCH3 is moderately expressed) and treated with Dox for 20h. Instead of seeing NICD3 appear at ~80kDa as predicted, I observed a series of bands between 45kDa and 55kDa (**Fig. 12B**). The addition of a proteasome inhibitor (MG132) restored NICD3 to the expected 80kDa size (**Fig. 12C**).

In an effort to create a more tightly controlled system I proceeded to clone the NICD constructs into a reverse tetracycline trans-activator (rtTA) system. Both the rtTA-NICD1 and rtTA-NICD3 cell lines induced expression of their respective constructs at the expected sizes (**Fig. 13A,B**). Moreover, the rtTA-NICD3 was titrated with increasing Dox and expression was increased dose-dependently (**Fig. 13C**). The rtTA-NICD3 pool does show a small amount of leakiness, which can be seen by the appearance of some 80kDa product without Dox in undifferentiated cells which normally express barely-detectable NOTCH3 (**Fig. 13B,C**). With these upgraded tools I can induce tighter, more controlled expression of NICD which will enable more reliable experimentation.

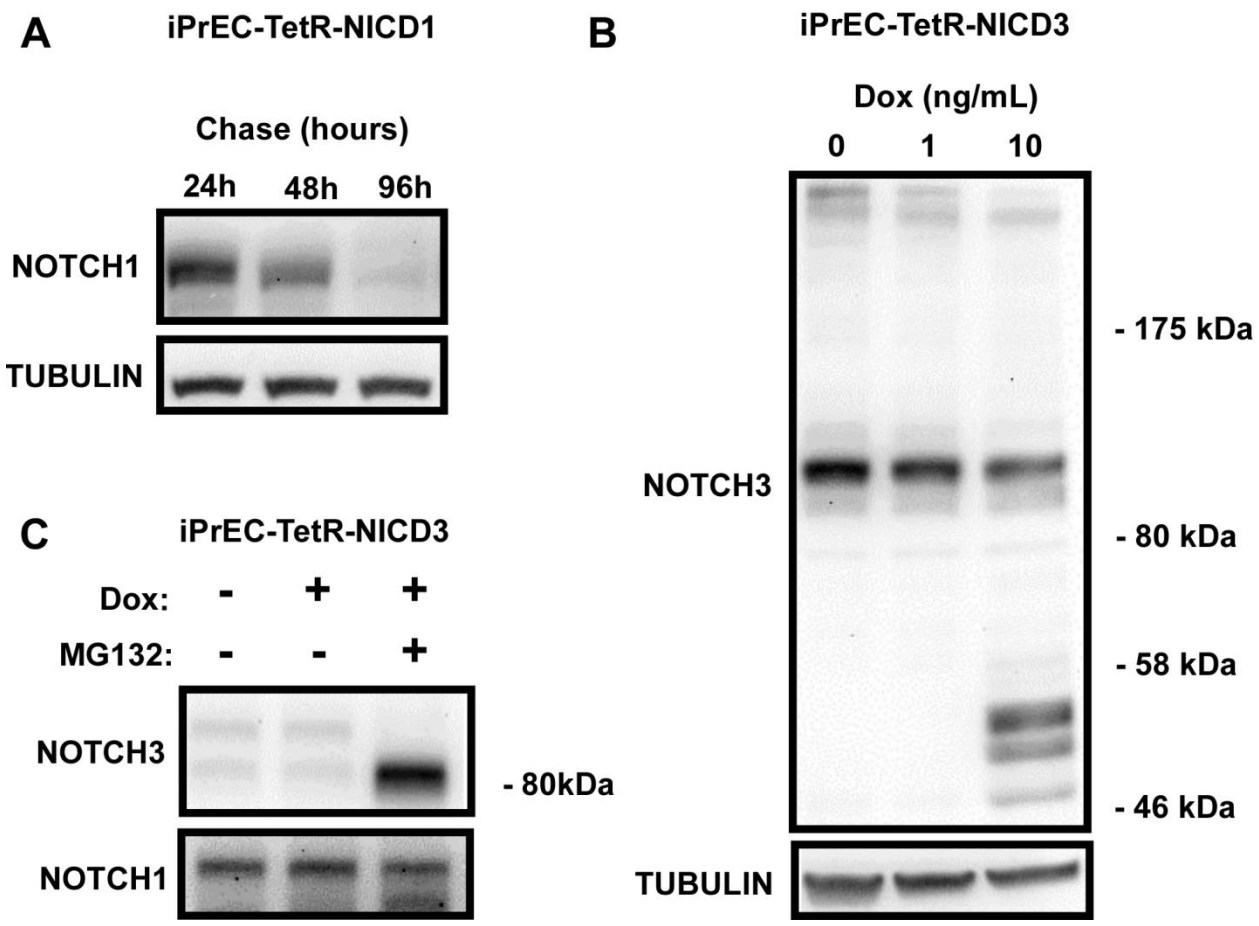

Figure 12: TetR-NICD cell line validation. (**A**) Immunoblot of iPrEC cells containing TetR-NICD1. Basal undifferentiated cells were treated with 10ng/mL Dox for 8h, then switched back to regular media and harvested at 24, 48, and 96h. NICD1 was detected with an ICD-specific antibody. (**B**) TetR-NICD3 cells were differentiated to day 4 and then treated 20h with Dox (0/1/10 ng/mL). Protein was measured by immunoblot with NOTCH3 antibody that detects the C-terminus. NOTCH3-ICD is predicted to appear at ~80kDa. (**C**) Undifferentiated TetR-NICD3 cells were treated 16h with Dox (5ng/mL) and MG132 (10µM) proteasome inhibitor.

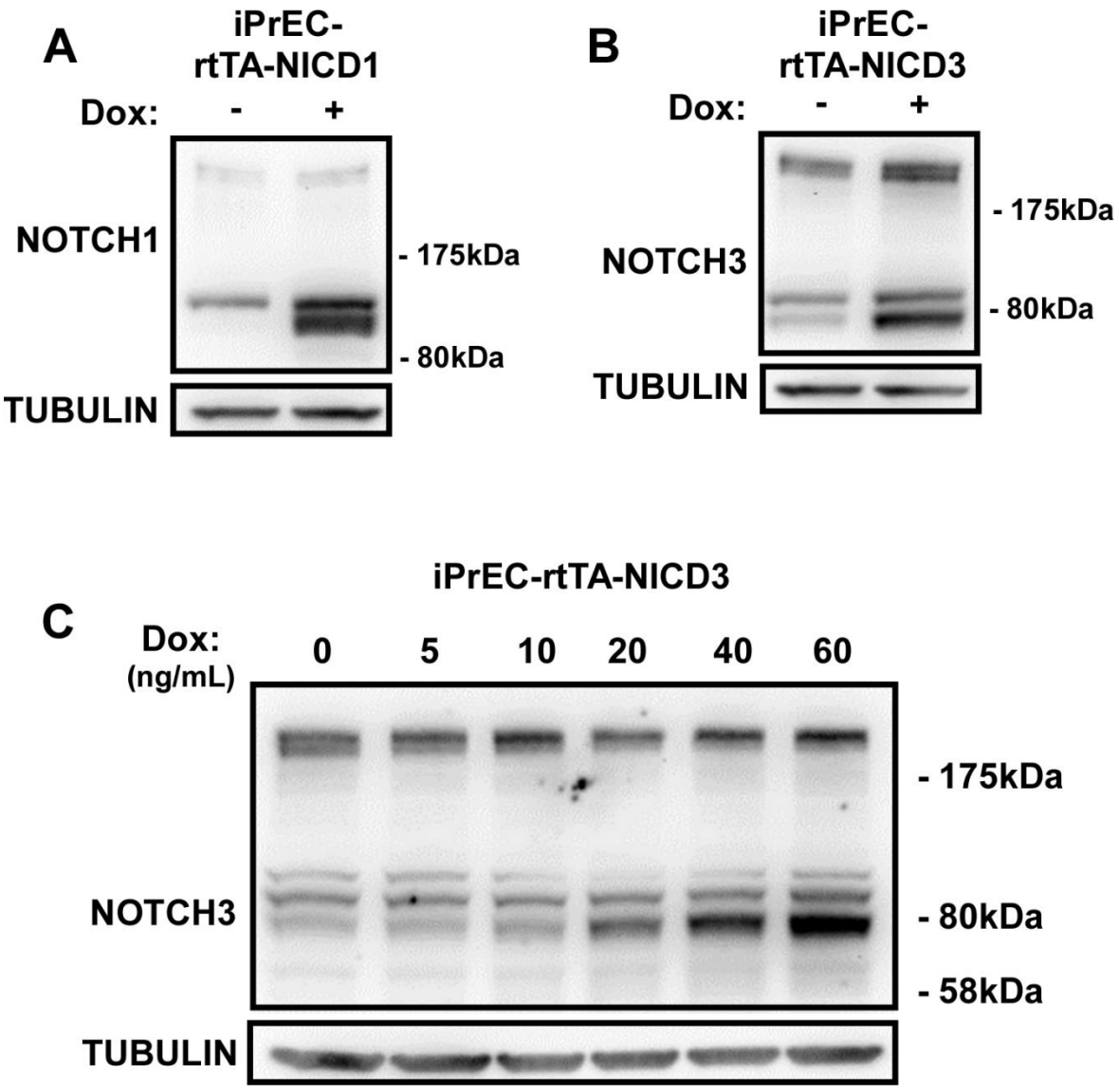

Figure 13: rtTA-NICD cell line validation. (**A**) Immunoblot of iPrEC-rtTA-NICD1 cells that were treated with 10ng/mL Dox for 16h. NOTCH1 was probed with a C-term antibody. TM = ~120kDa, ICD = ~110kDa. (**B**) Same experiment as (**A**) but with rtTA-NICD3 pool. NICD3 appears ~80kDa. (**C**) rtTA-NICD3 cells were treated 20h with 0-60 ng/mL Dox.

ii. NICD1 vs NICD3 target gene expression

Before I was able to make the rtTA-NICD cell lines, I ran a preliminary experiment comparing target gene expression between the TetR-NICD1 and TetR-NICD3 cells. Cells were treated -/+ Dox (and in the case of TetR-NICD3 +MG132) for 16h and mRNA expression was measured by qRT-PCR. NICD1 induction caused an increase in *HES1/2/4/5/6/7* (**Fig. 14A**) and *HEY1/2/L* (**Fig. 14B**) expression. NICD1 appeared to induce the HEY genes more dramatically than HES, with the exception of *HES5* which showed highest induction among the HES genes (~64 fold). NICD3 also induced expression of *HEY1/2/L*, though slightly less dramatically than NICD1 (**Fig. 14B**). To the contrary, NICD3 induction (+Dox, +MG132) decreased expression of all the HES genes. (**Fig. 14A**).

Expression of NOTCH ligands and some other genes of interest were measured as well. Both NICD1 and NICD3 decreased expression of the NOTCH ligands *JAG1*, *JAG2*, and *DLL1* (**Fig. 14C**). However, *DLL3* was unaffected and possibly slightly induced by both NICDs while *DLL4* was unchanged. Integrinβ4, a basal prostate marker lost with differentiation, was decreased by both NICD1 and NICD3 (**Fig. 14D**). *CDH1* (E-Cadherin) was slightly increased by NICD1 (~2 fold) but was equally decreased by NICD3. Additionally, *MYC* was increased by NICD1 (~4 fold) but similarly decreased by NICD3. These results suggest that *NOTCH1* and *NOTCH3* may have differential regulation of target genes in PrECs.

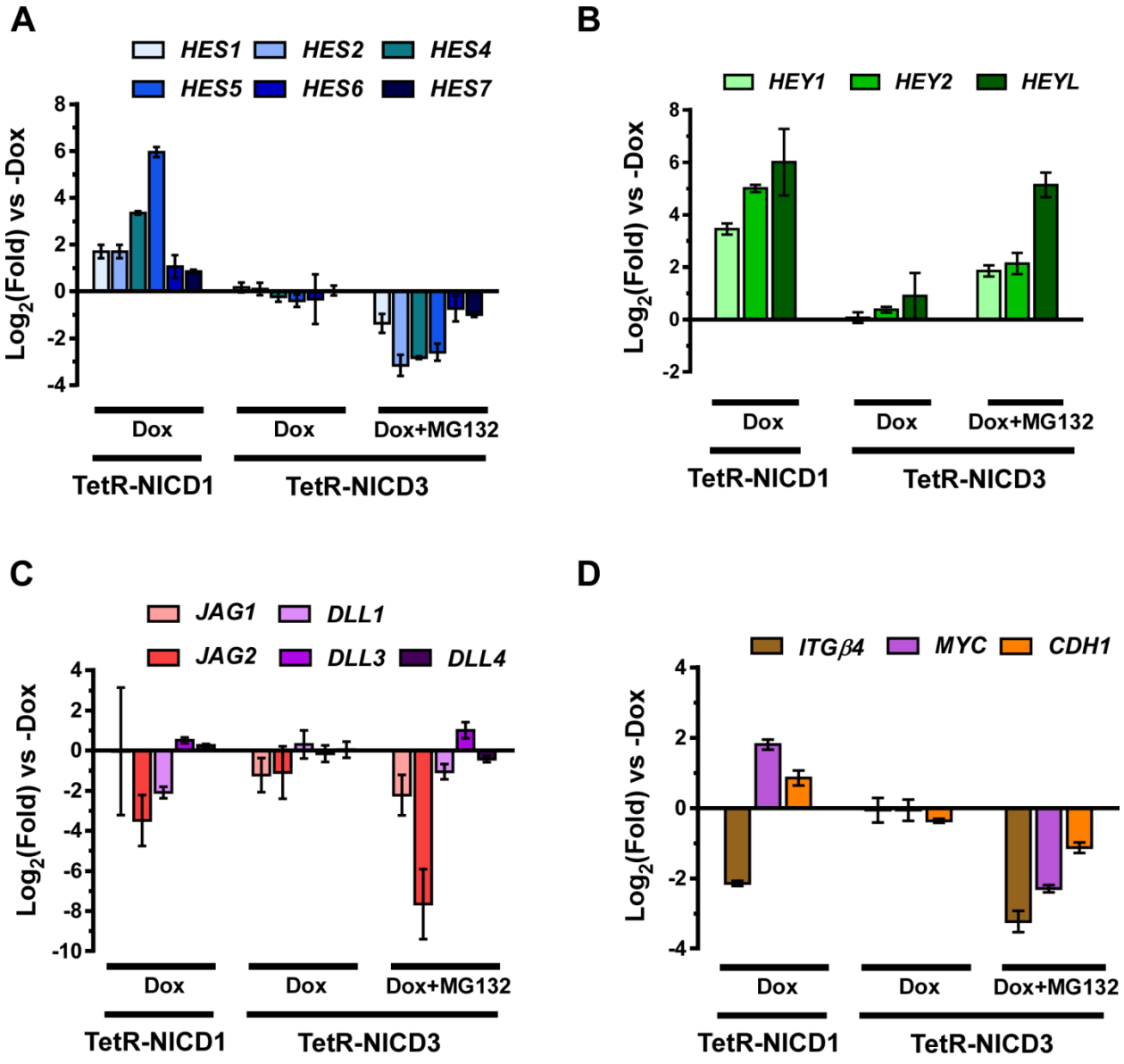

Figure 14: NICD1 vs NICD3 target gene expression. TetR-NICD1 and TetR-NICD3 cells were treated for 16h with water, Dox (10ng/mL), or Dox + MG132 (10µM). RNA was extracted and qRT-PCR was run. Error bars show standard deviation of biological triplicates. Data were standardized to *18S* and *RPL19* and normalized to –Dox samples. Y-axis shows ΔΔCT, which equals Log2(Fold). (**A**) HES genes. (**B**) HEY genes. (**C**) Ligands. (**D**) Other targets, including *Integrinβ4*, *MYC*, and *CDH1* (E-Cadherin).

iii. Ligand expression during differentiation

To investigate which ligands are involved in iPrEC differentiation cells were differentiated and analyzed by qRT-PCR. This data was also in Chapter 3 but scattered and is shown here unified (**Fig. 15**). Of the five ligands, three were examined: *JAG1*, *DLL3*, and *DLL4*. *JAG1* and *DLL4* followed a similar pattern while *DLL3* was different. JAG1 and *DLL3* decreased initially (down ~4 fold at d6) but then rebounded by d10 with no difference between the basal (bottom) and luminal (top) layers (**Fig. 15**). Alternately, *DLL3* remained flat until d10 and then began a slight increase (~2 fold at d10, ~4 fold at d14) with no difference between layers. Thus, there are at least two patterns of ligand regulation.

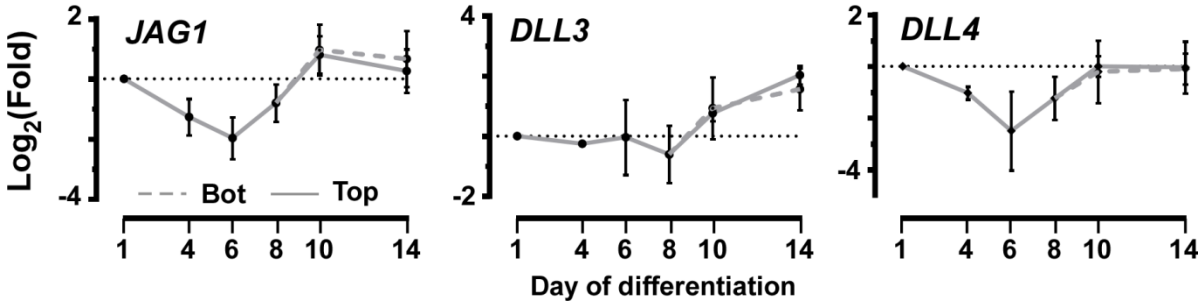

Figure 15: Ligand expression during differentiation. iPrECs were differentiated for 14 days and RNA was harvested for analysis by RT-PCR. Layers were separated at d10 and d14 into bottom(basal) and top(luminal) layers (dashed and solid lines, respectively). Error bars show standard deviation of biological triplicates. Data are standardized to *18S* and *GAPDH* and normalized to d1 samples. Y-axis shows ΔΔCT, which equals Log2(Fold).

C. Materials and methods

Cell culture, immunoblot, and qRT-PCR. Cell line maintenance, immunoblot, and qRT-PCR were all performed as previously described in Chapter 3. Antibody information is in **Table S3**, Appendix A. Primer information is in **Table S4**, Appendix A.

Lentiviral constructs. The NICD1 construct was PCR subcloned from EF-hICN1-CMV-GFP, a gift from Linzhao Cheng (Addgene plasmid 17623)[348]. NICD3 was PCR subcloned from pCLE-NICD3, a gift from Nicholas Gaiano (Addgene plasmid 26894)[349]. Both NICD1 and NICD3 were amplified with Q5 polymerase (NEB), cut with SalI and NotI (NEB), and then ligated into pENTR3C (Invitrogen) between SalI/NotI sites. pENTR plasmids were recombined with LR Clonase (Invitrogen) into pLenti-CMV/TO-Puro-DEST (for TetR system) and pLenti-CMVtight-Neo-DEST (for rtTA system), both gifts from Eric Campeau (Addgene plasmids: 17293 and 26432). A TetR line was made using pLenti-CMV-TetR-Blast (Addgene 17492) and an rtTA line was made using pLenti-CMV-rtTA3-Blast (Addgene 26429), both gifts from Eric Campeau[305]. Virus was generated as described in Chapter 3 methods. Antibiotic selection was used at the following doses: 2µg/mL puromycin, 5µg/mL blasticidin, and 500µg/mL G418.

D. Discussion

i. NICD3 dose effect

The dosage effect of NICD can make a significant difference in the physiological response of a cell[288,350]. When selecting pools for TetR-NICD3 I noticed some odd phenotypic variation and had difficulty getting a stable pool. The TetR system is known to have some leakiness, depending on the occupancy rate between TetR protein and TetOperator DNA sequences[351]. With TetR-NICD3 the leakiness appeared to be poorly tolerated by the basal iPrECs. In addition, when a stable pool was eventually selected (presumably from clones with the lowest amount of leakiness) the induction of NICD3 was promptly degraded by the cell via a proteasomal pathway that could be rescued with MG132. This suggests that basal iPrECs have mechanisms to ensure very low *NOTCH3* expression, which would be expected if *NOTCH3* is a potent driver of luminal differentiation. NOTCH receptors (and the NICD in particular) are known to be post-translationally regulated by a variety of E3 ubiquitin-ligases, including *ITCH*, *MDM2*, *FBW7*, and *MIB1*[352]. Thus, I suspect that one or more of these E3-ligases is upregulated in the TetR-NICD3 basal iPrECs as a mechanism to counter leaky NICD3 expression.

NICD1 expression was better tolerated by iPrECs as was NICD3 expression from the rtTA system. NOTCH1 is normally found in basal prostate epithelium, so NICD1 seems likely to be well tolerated. As for rtTA-NICD3, due to the tighter regulation[351] (compared to TetR) the selection of a stable pool did not have difficulties as was the case with the TetR-NICD3. Additionally, induction by rtTA was not as dramatic as with TetR. Thus, the decreased leakiness and lower induction of the rtTA system may explain why NICD3 was more tolerated.

NICD3 degradation in basal prostate epithelial cells was likely encountered by at least one other group[353]. They were using an NICD3 construct with basal prostate cells (different than our iPrECs) and were able to show induction of HES/HEY and NICD3 by qRT-PCR, but they did not show a single immunoblot of the 80kDa NICD3 induction. If this other group did in fact have

NICD3 degradation issues, then that supports the idea that this mechanism is probably biologically relevant and not an artifact of our cell line specifically.

ii. NICD1 vs NICD3 differential gene regulation

The results from the NICD1 vs NICD3 qRT-PCR experiment were somewhat unexpected. I expected there to be some differences between NICD1 and NICD3, possibly in terms of preferential activation of different HES/HEY genes. However, the downregulation of HES genes by NICD3 was surprising, considering that both HES and HEY increase dramatically during differentiation. This result may be explained by a 1999 report showing that NCID3 is a less potent transcriptional activator than NICD1 and can act as a NICD1-antagonist by occupying the CSL machinery at HES promoters[240]. CSL is normally a transcriptional repressor in the absence of NICD, so if NICD3 binds and competes with other ICDs but does not activate transcription, then the net effect is a decrease in target expression. However, the TetR-NICD3 cells did upregulate the HEY genes, which also require the downstream NOTCH machinery. Worth noting, the HEY genes were not yet discovered in 1999 so they were not included in the study showing NICD3 acted as an antagonist[240]. Nevertheless, *NOTCH3* is not always a repressor of HES genes and NICD3 has also been reported to upregulate HES genes in some studies[353,354]. The differential effect of NICD3 could possibly be due to dosage, orientation of CSL binding sites at specific promoters, or the expression level of other NOTCH receptors[202].

In addition to the HES/HEY expression, the differential effects by NICD1 and NICD3 on *MYC* and *CDH1* were intriguing. *MYC* is reported as a *NOTCH1* target in T-ALL, so its upregulation by NICD1 was expected though its downregulation by NICD3 was not. Based on my p38-MAPK mechanism from Chapter 3, *MYC* is upstream of *NOTCH3*; however, this data suggests it may also be downstream and differentially affected by NICD1 (positively) and NICD3 (negatively). Similarly, the NICDs decreased expression of NOTCH ligands, which also indicates a potential feedback loop. The NOTCH pathway is known to have many levels of self-

regulation and feedback, so these results are not entirely unexpected. Still, this particular observation of NICD3 decreasing *MYC* and both NICDs decreasing JAG/DLL expression has not yet been clearly established[355].

Likewise, the differential regulation of *CDH1* was also surprising (increased by NICD1 and decreased by NICD3). NOTCH has been reported to be a negative regulator (indirectly) of *CDH1* in tumor epithelial-to-mesenchymal transition[356,357]. However, considering that both *NOTCH3* and *CDH1* increase during luminal differentiation I expected *NOTCH3* to positively regulate *CDH1* (NICD3 had the opposite effect). Since the regulation of *CDH1* is not direct, these differential effects may be due to alternate regulation of mediator proteins.

Nonetheless, these experiments were not without some limitations. Firstly, there was not a MG132-only test for the TetR-NICD3 experiment. Thus I cannot eliminate the possibility that some of the NICD3 effect could be due to the proteasome inhibition which affects other post-translationally regulated genes such as *MYC*, *p53* and other NICD fragments. The other, more challenging caveat is with the NICD constructs themselves. The endogenous NOTCH ICD fragments are usually degraded very quickly after binding CSL and activating transcription[202]. Moreover, the dose and ratio of NICD fragments can be crucial. Thus, using these potent activators is an artificial situation which may provide both relevant and irrelevant biological effects. With the advance to the rtTA-NICD lines one could begin to untangle some of these concerns. An inducible system can help separate primary from secondary transcription effects based on timing of induction. Moreover, by using titrated Dox doses and pulses vs continuous treatment the signaling can be more tightly controlled to more physiologic levels. Though still not perfect, these upgraded rtTA-based tools will allow for better controlled and more biologically relevant experiments.

iii. Ligand expression during differentiation

Expression of *JAG1*, *DLL3*, and *DLL4* was measured at the mRNA level throughout differentiation. *JAG1* and *DLL4* followed the same pattern, thus suggesting they may be coordinately regulated. Day 6 is a key time point at which *JAG1* and *DLL4* expression rebound, perhaps setting up for the spike in NOTCH activation seen at d8-10. *DLL3*, however, was unchanged until after d10 when it increased slightly. This would be after downstream NOTCH signaling is induced. Considering that *DLL3* has been reported to play a negative regulatory role, its later upregulation may actually be serving to attenuate NOTCH activity in late differentiation[331,332]. Follow up experiments will be needed to measure the remaining ligands (*JAG2*, *DLL1*) and complete the picture, as will protein measurement by immunoblot to confirm whether the protein expression follows the mRNA. There are also non-canonical proteins that can serve as NOTCH ligands which may also warrant investigation[358]. Moreover, another question to address is whether the ligand expressing cells are signaling horizontally (basal-basal and luminal-luminal) or vertically (basal-luminal). In skin differentiation the signaling is vertical as keratinocyte layers differentiate, but it is not clear if this is the same in the prostate epithelial structure[359,360].

iv. Conclusions

In beginning to examine upstream and downstream NOTCH regulation, it is becoming clear that *NOTCH1* and *NOTCH3* each have a role to play in differentiation. To further investigate the downstream consequences of NOTCH signaling, experiments will have to be carefully planned to make use of inducible NICD1 and NICD3 expression. Experiments will need to be done at low vs high NICD induction and for multiple time points to properly interrogate differential downstream effects. Furthermore, the downstream effects will need to be tested to

see if they have a functional consequence in normal differentiation by knockdown or overexpression with and without NOTCH manipulation to establish necessity and/or sufficiency.

It will also be important to examine the remaining NOTCH ligands during differentiation and begin to test which are necessary for differentiation and whether the ligands show differential activation of NOTCH receptors. Even if the ligands may be differentially regulated it does not necessarily mean that they will have different effects on NOTCH receptors. Though investigating the upstream and downstream regulation of NOTCH in prostate differentiation is complex, it will be necessary to fully understand tumor differentiation status and rationally target the pathway in cancer patients.

CHAPTER 5 — CONCLUSIONS

A. Key findings

i. Dox inducible lentivirus as an important tool

In order to study differentiation and manipulate signaling pathways, I relied on lentiviral delivery to create stable cell lines with Dox-inducible gene regulation. This involved both Dox-inducible shRNA (via Tet-pLKO-Puro) as well as inducible cDNA via TetR or rtTA systems. I made modifications to the Tet-pLKO-Puro vector to make shRNA cloning easier. Furthermore, I created a detailed protocol for using this tool including a demonstration on the importance of designing shRNA loop sequences and efficient screening techniques.

The inducible cell lines eliminate variability of having to compare one stable pool of cells vs another, which will undoubtedly have some unintended differences. Furthermore, by being able to acutely induce a pathway, time courses were used to unravel regulatory cascades. In particular for MKK6(CA), this signaling would have been much harder to investigate by any other means; prolonged signaling is toxic and transfection efficiency in iPrEC cells is very poor. With the NICD constructs, dosage and timing are key to running physiologically relevant experiments. In these scenarios and many others, having controlled expression of a transgene is extremely valuable.

ii. A link between p38-MAPK, MYC, and NOTCH

This work sought to better understand how p38-MAPK was involved in prostate epithelial differentiation. During my research I discovered a mechanistic link between three major differentiation pathways: p38-MAPK, MYC, and NOTCH. I demonstrated that p38-MAPK and NOTCH are both required for differentiation, and more specifically that *p38α*, *p38δ*, *NOTCH1*, and *NOTCH3* are each necessary. Moreover, I showed that p38-MAPK regulates *NOTCH3* at multiple levels, including transcription via *MYC* and enhancer elements but also by mRNA

stability. Differentiation is a long and complex process with many different signaling events working in amazing coordination. This work shows how three of these pathways work together in this complex process.

iii. Differential regulation of NOTCH3

One of the primary mechanistic insights from this work was revealing multi-level regulation of *NOTCH3* that was distinct from other NOTCH receptors. *NOTCH3* expression increased dramatically during PrEC differentiation at both the mRNA and protein level. This was due to a combination of mRNA stabilization and transcriptional regulation. Transcriptional regulation of *NOTCH3* by p38-MAPK is largely, though not entirely, mediated through *MYC.* Knockdown or inhibition of *MYC* reduced the ability of MKK6(CA) to upregulate *NOTCH3*. However, *MYC* overexpression was not sufficient to upregulate *NOTCH3* mRNA.

Moreover, I identified and validated two *NOTCH3* enhancer elements that were able to upregulate a reporter upon p38-MAPK stimulation. Both enhancers showed MYC binding by ChIP, but only one was ablated by a MYC inhibitor (En3). This enhancer data, along with the fact that *MYC* is partly required but not sufficient, leads to the hypothesis that there must be additional transcriptional regulators activated by p38-MAPK that are required for the full *NOTCH3* upregulation. The most likely candidates would be ATF family members, such as *ATF1* and *CREB1*, which are known p38 targets and can be involved in differentiation as well[152].

Additionally, this work also revealed that *NOTCH3* is regulated via mRNA stability during differentiation and by MKK6(CA) induction. *NOTCH3* transcript half life about doubled by Day 4 or with MKK6(CA) stimulation. *NOTCH1* mRNA was also stabilized in the short term upon MKK6(CA) induction but that stability was lost by Day4. Further work will be needed to understand why *NOTCH3* maintains that stability when *NOTCH1* does not. Moreover, exactly how much mRNA stability and transcriptional induction each contribute to the >200 fold increase

in *NOTCH3* mRNA during differentiation is not yet clear, though both mechanisms are surely involved.

iv. Unique signaling by NOTCH3

Along with being uniquely regulated among receptors, *NOTCH3* may also be responsible for distinct regulation of a subset of NOTCH target genes. TetR-NICD3 induction was found to upregulate HEY genes but downregulate HES genes. Furthermore, *HEY2* is the only HES/HEY member to increase preferentially in the differentiating luminal cells. Thus, part of NOTCH3 function may be due to preferential upregulation of *HEY2*. Likewise, NICD3 had opposite effects on *MYC* and *CDH1*, both of which were increased by NICD1 and decreased by NICD3. Whether these effects have functional consequences or are repeatable with lower NICD expression will have to be determined. These findings support recent reports in the literature which have found that *NOTCH3* has a specific role in differentiation[340]. Moreover, this special function may also be relevant to tumors where NOTCH3 could be playing a unique role[343,344,357]. Further experiments will be needed to validate these initial findings and follow up on the consequences of NICD3 downstream effects during prostate epithelial differentiation.

B. Significance

i. Molecular tools

During my research I spent a great deal of effort designing and constructing molecular tools to allow controlled manipulation of signaling pathways. One of the benefits of my work is that others will be able to utilize these tools for their own experiments and benefit from my efforts. I created multiple lentiviral inducible shRNAs targeting p38α, p38δ, *NOTCH1*, and *NOTCH3*. In the process I also compiled detailed methods for my modified EZ-Tet-pLKO-Puro vector and instructions for how best to design, screen, and test shRNAs.

I also cloned MKK6(CA), MYC, NICD1, and NICD3 into lentiviral inducible vectors. Additionally, I have all these constructs in a Gateway pENTR3C vector, which allows quick recombination into any vector with attL/attR sites for *in vitro* recombination. Thus, these constructs can easily be cloned into other plasmids, such as Adenoviral or Retroviral vectors, or even other TetON lentiviral vectors with different selection markers. These tools will be made available to anyone who wishes to use them for their own research. A fellow lab mate has already begun using these tools for another project investigating how manipulation of NOTCH in prostate cancer cells affects bone metastasis in mice. These vectors and the knowledge I gained while learning how to make them will be a great resource upon which others can build.

ii. A mechanistic link between p38-MAPK and NOTCH

This work directly links three major differentiation pathways in a novel signaling mechanism. p38-MAPK regulation of the NOTCH pathway has not been well established, with only a handful of papers suggesting the link and very few mechanisms[316,318,361]. This work is the first to show that p38-MAPK signaling upregulates *NOTCH3* and does so via a combination of mRNA stability and upregulation of *MYC*.

Now that there are known interactions between these pathways, our understanding of tumor biology can begin to evolve. For example, *MYC* upregulation is common in most prostate tumors. My work suggests that p38-MAPK activation can drive MYC upregulation, as can NOTCH1 signaling. p38-MAPK and NOTCH1 are upregulated in some tumors but is not known if they drive *MYC* in a tumor context which may help to explain their oncogenic potential. In addition, *MYC* is required for full *NOTCH3* upregulation by p38-MAPK in PrECs, but *MYC* is not sufficient. Thus I would expect that tumors with a combination of p38-MAPK activation and *MYC* overexpression will have increased *NOTCH3*. If that is the case, it will be important to understand whether *NOTCH3* is tumor suppressive and prevents proliferation[344] or is oncogenic and aids cell survival to hormone ablation[345] as has been described in breast cancer.

iii. Novel regulation of NOTCH3

This work includes specific mechanisms for regulation of *NOTCH3* that have not been reported. Part of the transcriptional regulation of *NOTCH3* requires *MYC* and enhancer sequences. My data showed that the proximal *NOTCH3* promoter is not sufficient for driving *NOTCH3* transcription in prostate epithelial cells. I validated two enhancer elements, En1 (10kb upstream) and En3 (within the 2nd intron). En3 has been previously studied by two groups, but both were in mouse and neither involved *MYC*[238,299]. Furthermore, I am the first to show eRNA detected from this locus; moreover, I did so by utilizing a recent specialized RNA-seq method called UV-BrU-Seq in collaboration with Mats Ljungman and his group at the University of Michigan. The combination of eRNA, ChIP, and Luciferase reporter activity is the strongest evidence to date of this intronic *NOTCH3* enhancer. Furthermore, though En1 did not produce eRNA, it was able to upregulate a reporter upon MKK6(CA) induction. This is the first report to show that this region has enhancer activity and is responsive to p38-MAPK activation. Moreover, though p38-MAPK has many potential targets, understanding which of its

transcription factor targets are involved in a given context is difficult. With these enhancers we now have a tool to report p38-MAPK activity in prostate cells and maybe other cell types as well.

Lastly, my work is also the first to clearly show *NOTCH3* regulation by p38-MAPK via mRNA stability. Though acute p38-MAPK activation stabilized both *NOTCH1* and *NOTCH3*, only *NOTCH3* maintained that stability during differentiation. With a nearly doubled half-life, even moderate increases in transcription can lead to a large build up in mRNA. Thus, my work describes a new, multifaceted mechanism for p38-MAPK regulation of *NOTCH3* mRNA.

iv. New targeted therapies for NOTCH

Returning to the big picture, why does it matter which specific ligand and receptor is involved in NOTCH signaling? Beyond the desire for basic understanding of the pathway, these findings are highly relevant for cancer where the NOTCH pathway is often a target of therapeutic efforts. The most common approach has been to use γ–secretase inhibitors, which prevent cleavage of all NOTCH receptors as well as a variety of other proteins that utilize the protease complex[362]. Though γ-secretase inhibitors have had some success in clinical trials, targeting specific receptors could minimize off-target effects. Moreover, specific targeting may be especially important in tissues where NOTCH signaling has conflicting reports as to whether it is an oncogene and tumor suppressor, as it is with prostate cancer[273]. More rationale targeting of the NOTCH pathway will likely aid therapeutic efficiency.

In the effort to more specifically target the NOTCH pathway there have been some recent advances. Firstly, there has been great progress on the creation and application of receptor[363,364] and receptor-ligand[365,366] blocking antibodies. Currently available blocking antibodies include OMP-52M51 (NOTCH1) and OMP-59R5 (NOTCH2/3), both of which are in clinical trials[329]. There are also ligand-specific blocking antibodies, including one that specifically blocks DLL4-NOTCH interactions[367]. Lastly, though they are not in clinical trials yet, JAG or DLL ligand decoy peptides may also lead to a potential therapeutic strategy in the future[333].

C. Future directions

i. Further investigation of NOTCH3 vs NOTCH1 signaling

In order to more fully comprehend the role of NOTCH singling in PrEC differentiation, additional experiments will be required to investigate regulation of the ligands and differential downstream effects by *NOTCH1* or *NOTCH3*. Downstream signaling can be better measured using the rtTA-NICD cell lines. A key experiment will be to compare treatment with low vs high doses of Dox to test whether there is a dosage effect from the NICD constructs on differentiation or proliferation. Furthermore, since the rtTA-NICD3 line has some leakiness it can be considered a 'constitutive low expressing' NICD3 line and will need to be compared to the rtTA line (without the NICD3 inserted). This will eliminate the need to use MG132 as was the case with the TetR lines. Once again, expression of HES/HEY, *MYC*, and *CDH1* should be monitored. Concurrent treatment of NICD induction with a γ–secretase inhibitor may be useful to untangle any effect from endogenous NOTCH receptors, such as *NOTCH2* which is steadily expressed in these cells. Also, shorter timecourses and cyclohexamide treatment could be used to help separate primary vs secondary transcriptional effects of NICD expression. These experiments would help reveal specific targets for each NOTCH receptor in prostate epithelium.

To further explore the role of NOTCH ligands, first the remaining ligands (*JAG2* and *DLL1*) could be measured during differentiation. Additionally, immunoblot can be used to measure protein expression of the ligands. shRNA or blocking antibodies can be utilized to functionally test the role of specific ligands. Moreover, RNA expression by qRT-PCR can be used to measure HES/HEY expression at different time points during differentiation to see how downstream NOTCH signaling is affected by loss of a specific ligand. In order to further investigate the cell layer responsible for expressing the ligand, immunofluorescence and confocal microscopy can be used once the relevant ligand or ligands have been revealed.

Lastly, I hypothesize that regulation of the ligands is somewhere downstream of p38-MAPK. There has not been a clear link between p38-MAPK and JAG/DLL, though at least one report found that p38-MAPK in endothelial cells could positively regulate *JAG1*[318]. A key experiment would be to differentiate cells with p38 activation (via the MKK6(CA) cell line) or shRNA knockdown of p38 and use qRT-PCR or immunoblot to measure potential changes in JAG/DLL expression. Considering that *JAG1* and *DLL4* expression decrease until d6 and then recover, I would expect that a downstream p38-MAPK target, possibly MYC which rebounds at day 8, may be responsible for the *JAG1* and *DLL4* upregulation after d6.

These potential future experiments would serve to help understand both the specific upstream and downstream regulators of NOTCH in the prostate epithelium. Knowing which ligands are activating the NOTCH receptors, and then which target genes the different receptors regulate, will be key to understanding the NOTCH pathway in the prostate.

iii. Use of NOTCH1 and NOTCH3 to understand tumor differentiation status

As previously mentioned, understanding the aggressive potential of prostate tumors is very important for aiding prognosis and helping patients make very tough decisions. Prostate tumors typically show co-expression of various layer markers. With this new knowledge about *NOTCH1* and *NOTCH3* roles in differentiation, we can begin to make testable hypotheses about how NOTCH expression may indicate differentiation status of tumors more accurately than Gleason grade. Tumor micro arrays can be used to stain for proteins across a range of tumor sections, which sometimes even includes patient outcomes[368]. I would expect that using a comparison of NOTCH1 to NOTCH3 could help identify well-differentiated (high NOTCH3, low NOTCH1) from more poorly differentiated tumors. As with Gleason score, poorer differentiation is very likely to correlate with increased aggressive potential and higher morality.

Likewise, if specific downstream targets for *NOTCH1* and *NOTCH3* are validated, those too could serve as a way to decipher which receptor is predominant and thus how well

differentiated the tumor may be. For example, if *HES1* is upregulated by the other NOTCH receptors but downregulated by *NOTCH3*, then the ratio of *HEY2* to *HES1* may inform NOTCH receptor expression and in turn differentiation status. Of course, using just this one pathway may only be part of the picture. However, by combining genomic analysis with a better sense for overall differentiation (e.g. NOTCH status), our prognostic ability will hopefully improve.

iii. Impact of NOTCH on tumorigenesis

Finally, it is important to take this understanding of normal differentiation and tie it back to oncogenesis. Our lab has previously used genetically engineered iPrECs to orthotopically inject cells into the mouse prostate and measure effects on tumorigenesis *in vivo*[102]. We know that overexpression of *ERG* and *MYC* plus shRNA to decrease either *PTEN* or *ING4* will cause normal iPrEC cells to develop tumors in mice.

Using this model, we are now able to settle some lingering questions about whether NOTCH is a tumor suppressor or oncogene in PCa. Tumorigenic cells can be combined with the Dox-inducible NICD1 or NICD3 to test whether induction of either receptor is able to decrease or possibly increase tumor growth *in vivo*. Likewise, by treating with Dox either continuously or after tumor growth begins one could address specific questions about NOTCH contribution to tumorigenesis or tumor progression, two related but distinct processes.

My prediction is that NICD3 would drive luminal differentiation and decrease early tumorigenesis. Moreover, the HEY genes have been reported as AR co-repressors[223] and NICD3 seems may have a preference for *HEY2* in differentiation, which could further support the case for its role as a tumor suppressor. However, if the cells progress far enough to when *AR* begins driving a luminal proliferation program, as is typified by PCa tumors, then *NOTCH3* may be unable to decrease those strong proliferative signals. Furthermore, if NICD1 is in fact able to drive MYC expression, then I would expect that NICD1 plus *ERG* and shPTEN would be sufficient to drive tumorigenesis without direct *MYC* overexpression.

With the tools I have developed and the signaling pathways deciphered, future experiments will finally be able to start addressing the specific function of NOTCH signaling in prostate tumorigenesis. Such work will be greatly needed as NOTCH receptor and ligand targeting antibodies continue progressing through clinical trials. The era of targeting specific NOTCH ligands and receptors is just beginning. However, basic research must strive to keep up with that progress so that these tools can be wielded wisely and with the intended effects.

APPENDICES

APPENDIX A

SUPPLEMENTARY TABLES

Target	Species of origin	Company	Product no.	Dilution for WB
p38α	Rabbit	Cell Signaling	9218	1 : 2,000
p38δ	Mouse	Santa Cruz	sc-136063	1 : 1,000
TetR	Rabbit	Genetex	GTX70489	1 : 1,000
Tubulin	Mouse	Sigma	T9026	1 : 10,000

Table S1: Antibody information (Ch.2). List of antibodies used for immunoblot experiments in Chapter 2.

Target Gene	Target bp	Source		Sequence (sense_loop_antisense)
p38α	1971	TRCN0000196472	**5'**	GTACTTCCTGTGTACTCTTTA_AACTAGTGA_TAAAGAGTACACAGGAAGTAC
p38δ	993	TRCN0000197043	**5'**	GAAACTCACAGTGGATGAATG_TACTAGT_CATTCATCCACTGTGAGTTTC
NOTCH1	6258	TRCN0000350330	**5'**	CCGGGACATCACGGATCATAT_ACTAGT_ATATGATCCGTGATGTCCCGG
NOTCH3	1958	TRCN0000363316	**5'**	TTTGTAACGTGGAGATCAATG_TACTAGT_CATTGATCTCCACGTTACAAA

Table S2: shRNA information. Information for shRNA target sequences. Source column shows the RNAi Consortium ID used for the given target sequences. Target bp is the first base targeted by the shRNA based on consensus cDNA sequence. All shRNAs were cloned into the Tet-pLKO-Puro vector and included a terminator 3' sequence (5xT).

Target	Species of origin	Mono/Poly-clonal	Company	Product no.	Dilution for WB	Additional Info
AR	Rabbit	Poly	Santa Cruz	sc-815		
CREB1	Rabbit	Mono	Cell Signaling	4820	1 : 1,000	
p-CREB1	Rabbit	Mono	Cell Signaling	9198	1 : 1,000	pSer133
E-CAD	Mouse	Poly	BD	610181	1 : 5,000	
GAPDH	Mouse	Mono	Millipore	CB1001	1 : 10,000	
ITGB4	Mouse	Mono	BD	611232	1 : 1,000	
MYC	Rabbit	Poly	Millipore	06-340	1 : 1,000	
MYC	Mouse	Mono	Santa Cruz	sc-40	1 : 1,000	Used for myc-tag
p-MYC	Rabbit	Mono	Millipore	04-217	1 : 5,000	pThr58/pSer62
NOTCH1	Rabbit	Mono	Cell Signaling	3608	1 : 1,000	
NOTCH2	Rabbit	Poly	Millipore	07-1234	1 : 500	ICD-specific
NOTCH3	Rabbit	Mono	Cell Signaling	5276	1 : 1,000	
p38α	Rabbit	Poly	Cell Signaling	9218	1 : 2,000	
p-p38α	Rabbit	Mono	Epitomics	1229-1	1 : 2,000	pThr180/pTyr182
p38δ	Mouse	Mono	Santa Cruz	sc-136063	1 : 1,000	
TetR	Rabbit	Poly	Genetex	GTX70489	1 : 1,000	
TUBULIN	Mouse	Mono	Sigma	T9026	1 : 10,000	

Table S3: Antibody information (Ch.3). List of antibodies used for immunoblot experiments in Chapter 3.

Gene			Sequence	Source
18S	Fwd	5'	CCGCAGCTAGGAATAATGGA	
	Rev	5'	CGGTCCAAGAATTTCACCTC	
ACTB	Fwd	5'	CCCTCCATCGTGGGGC	
	Rev	5'	GACGATGCCGTGCTCGATG	
DLL3	Fwd	5'	GGCGGCTTGTGTGTCGGG	
	Rev	5'	GCAGTCGTCCAGGTCGTGC	
DLL4	Fwd	5'	AGGCCTGTTTTGTGACCAAG	Ding, 2012[369]
	Rev	5'	CTCCAGCTCACAGTCCACAC	
GAPDH	Fwd	5'	GATCATCAGCAATGCCTCCTGC	
	Rev	5'	CTTCTGGGTGGCAGTGATGGC	
HES1	Fwd	5'	AATGACAGTGAAGCACCTCCG	
	Rev	5'	ATGCACTCGCTGAAGCCG	
HES6	Fwd	5'	GAGGACGGCTGGGAGACG	
	Rev	5'	TCGCTCGCTTCCGCCTGC	
HEY1	Fwd	5'	AGAGTGCGGACGAGAATGGAAACT	Niessen, 2008[370]
	Rev	5'	CGTCGGCGCTTCTCAATTATTCCT	
HEY2	Fwd	5'	AAGATGCTTCAGGCAACAGGG	
	Rev	5'	GGATCCGAGGAGTCCAGGC	
HEYL	Fwd	5'	CAGGATTCTTTGATGCCCGAG	Adepoju, 2011[371]
	Rev	5'	GACAGGGCTGGGCACTCTTC	
ITGA6	Fwd	5'	GCTGGTTATAATCCTTCAATATCAATTGT	Lamb, 2010[71]
	Rev	5'	TTGGGCTCAGAACCTTGGTTT	
ITGB1	Fwd	5'	CTGGCAAATTCTGCGAGTGTG	
	Rev	5'	CACTCACACACACGACACTTGC	
ITGB4	Fwd	5'	AACGGCGGTGAGCTGCATC	
	Rev	5'	GAGTGCTCAAAGTGAAGGCGG	
JAG1	Fwd	5'	ATAAGTGCATCCCACACCCG	
	Rev	5'	AGACACGGCTGATGAGTCCC	
LUC	Fwd	5'	GGCCTGACAGAAACAACCAGCG	
	Rev	5'	GGACGCACAGCTCGCCGC	
MYC	Fwd	5'	TTCGGGTAGTGGAAAACCAG	Integrated DNA Technologies
	Rev	5'	AGTAGAAATACGGCTGCACC	
NOTCH1	Fwd	5'	CGCAGATGCCAACATCCAGG	
	Rev	5'	CCCAGGTCATCTACGGCGTTG	
NOTCH3	Fwd	5'	CGTGGCTTCTTTCTACTGTGC	
	Rev	5'	CGTTCACCGGATTTGTGTCAC	
RPL19	Fwd	5'	CGGCTGCTCAGAAGATACCG	
	Rev	5'	TTGTCTGCCTTCAGCTTGTGG	

Table S4: qRT-PCR Primer information (Ch.3). Detailed primer information.

Element			Flank_Restriction Enzyme_Target
Prom.2kb	Fwd	5'	ATTAT_CTCGAG_CCGGCCCCATGGCGGCC
(2kb)	Rev	5'	ATAAT_GCTAGC_GATACAGGGCTGGAGCCTTAGCC
Prom	Fwd	5'	ATTAT_AAGCTT_TGGGTCCATGAGCCTCTCAGG
(400bp)	Rev	5'	ATTAT_AAGCTT_TCCCTCCTTCCCTGGGC
En1	Fwd	5'	ATTAT_GGTACC_CTGGGTGTCTCAGGCAGAGGG
(600bp)	Rev	5'	ATTAT_GGTACC_GCCTAGAGTTCGAGACCAGCC
En2.1	Fwd	5'	ATTAT_AGATCT_CGCCTGGAGTCCTGGG
(1.4kb)	Rev	5'	ATTAT_AGATCT_CCTGTGGGTGTTCGTGA
En2.2	Fwd	5'	ATTAT_GCTAGC_GCTGGTCTCGAACTCCTGACC
(600bp)	Rev	5'	ATTAT_GCTAGC_TTCAGGGGTAATAGAAGGG
En3	Fwd	5'	ATTAT_CTCGAG_TCTCCCACTCGGGCTCACC
(1kb)	Rev	5'	ATTAT_CTCGAG_CCAGAGAGTCCAAGCTCCGCC
miniTK		5'	TTCGCATATTAAGGTGACGCGTGTGGCCTCGAACACCGA GCGACCCTGCAGCGACCCGCTTAA
5xCRE		5'	TGACGTCACTTGGTGACGTCACCTGGTGACGTCACGTGG TGACGTCACATGGTGACGTCA

Table S5: Enhancer element cloning primers and control regulatory sequences. Details for primers (including amplicon size) used to PCR clone *NOTCH3* regulatory elements and sequence for miniTK promoter and 5xCRE (5x CREB response elements: TGACGTCA)

Deletion			Mut Primer: Left Half_Right Half
En1	Fwd	5'	CCTAACTGGCCGGTACC_GTCACTGAGACCCAGG
Δ1-360	Rev	5'	CCTGGGTCTCAGTGAC_GGTACCGGCCAGTTAGG
En3	Fwd	5'	GCTCGCTAGCCTCGAG_ACGGTCTCAAATACTC
Δ1-350	Rev	5'	GAGTATTTGAGACCGT_CTCGAGGCTAGCGAGC

Table S6: Enhancer deletion primers. Details for primers used in deletion mutagenesis.

Target			Sequence
HIST3	Fwd	5'	CCGAACCAAGCAGACTGCG
(118bp)	Rev	5'	GCGGTGCGGCTTCTTCACG
ODC1	Fwd	5'	AACAGACGGGCTCTGATGACG
(119bp)	Rev	5'	GGGCTTTACATGTGCGTGGTC
En1 (1)	Fwd	5'	TCCTGGGTGGTAGGCATGACG
(94bp)	Rev	5'	GGGGCACACACTGACTCACGG
En1 (2)	Fwd	5'	TGGCCGGGAGTCACTGAGACC
(135bp)	Rev	5'	AGTTCCAGACTGCAGGGAGCC
En3 (1)	Fwd	5'	GGGCTCAGTCCTCCGAGTTGG
(109bp)	Rev	5'	GGGGGCATCCTTGAAAGGAC
En3 (2)	Fwd	5'	GGGACCAGCTATCCTCGGC
(99bp)	Rev	5'	TCCCGTCCCCTCCTCCAAGG

Table S7: ChIP primer information. Details for ChIP primers, including amplicon size (bp).

APPENDIX B

SUPPLEMENTARY FIGURES

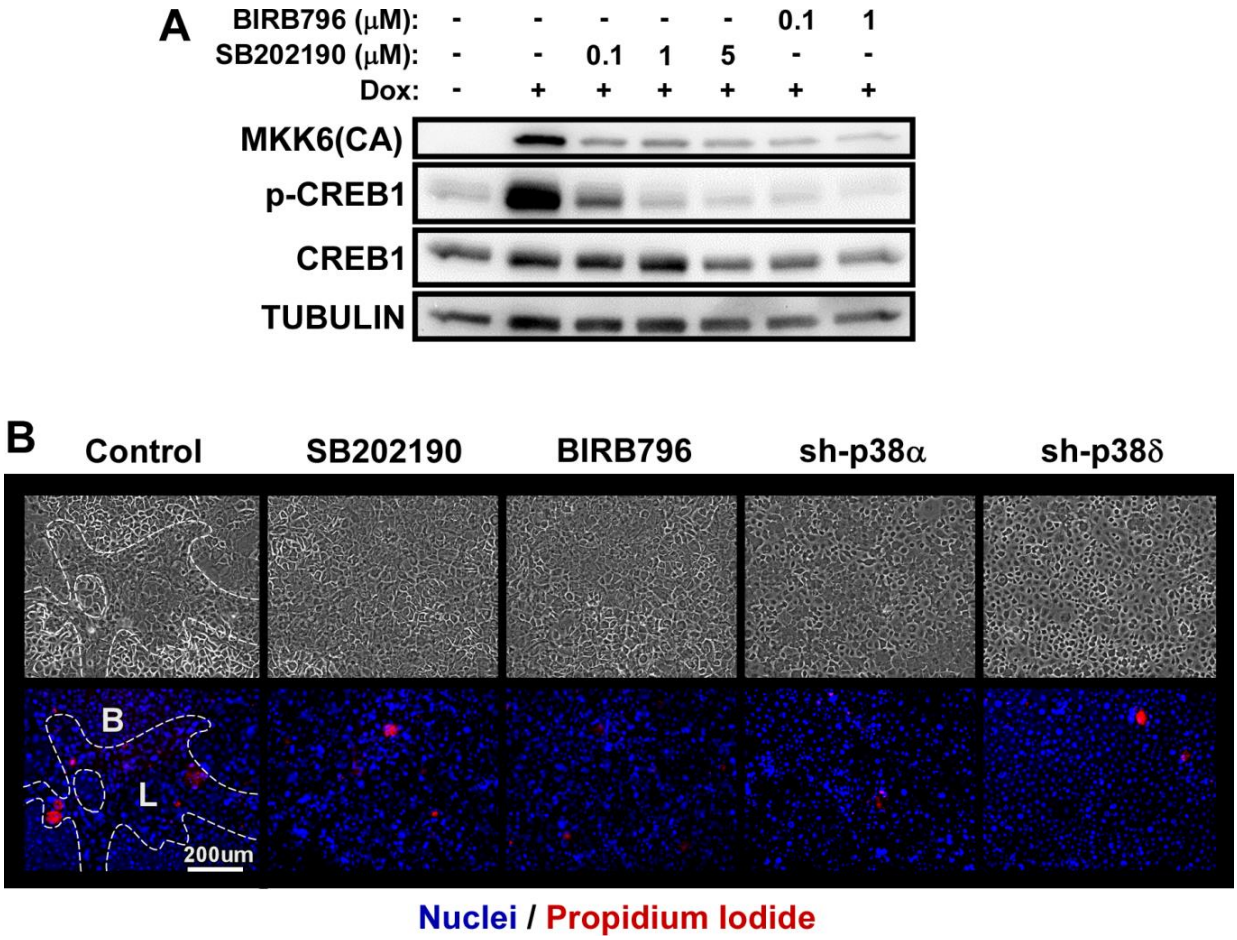

Figure S1: p38 inhibitor titration and propidium iodide staining. (A) iPrEC-TetON-MKK6(CA) cells were treated with doxycycline (Dox) at 5ng/mL for 6h in the presence of increasing concentrations of p38-MAPK inhibitors SB202190 or BIRB796, then lysed and probed by immunoblot. The Dox-induced constitutively active MKK6(CA) was detected via a Myc-tag and p-CREB1 was used as a target gene for readout of p38-MAPK activation. **(B)** iPrECs were treated with DMSO + Dox (Control), 1μM SB202190, or 0.1μM BIRB796 while inducible shRNA lines were treated with 50ng/mL Dox over 16 days of differentiation. Cells were then fixed and stained. Top row images show phase contrast microscopy while the bottom row shows merged epifluorescence images of Hoescht nuclei (blue) and propidium iodide (red), to which only dead cells are permeable. Luminal layer is outlined (dashed line) in control cells; (L) is the luminal layer and (B) is the basal layer. Scale bar = 200μm.

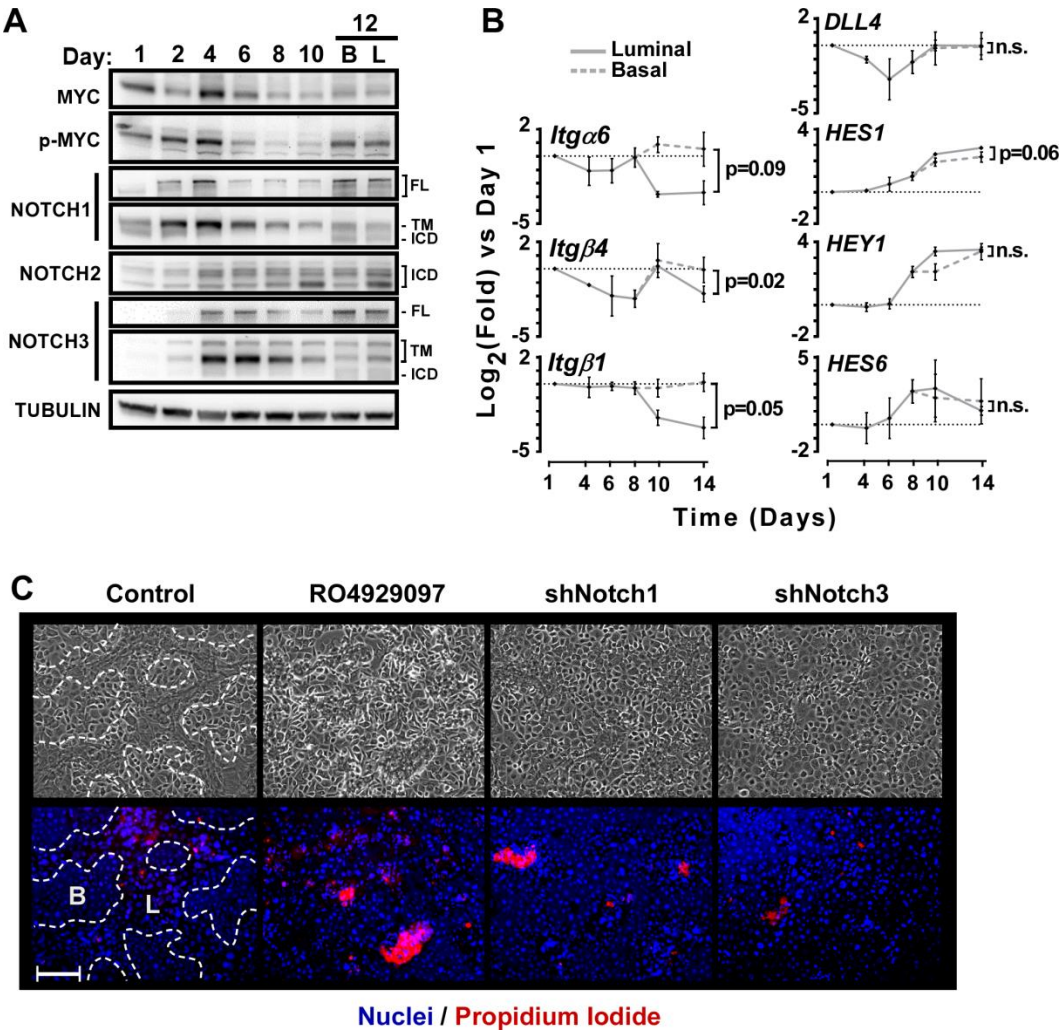

Figure S2: NOTCH signaling increases at day 8 and is required for survival. (A) Primary PrECs were differentiated for indicated days and cell lysates collected for immunoblotting. MYC and p-MYC (T58/S62) were probed along with three NOTCH receptors (NOTCH1,2,3). NOTCH2 antibody is ICD-specific, while NOTCH1 and NOTCH3 target the C-terminus and recognize all three fragments: full length (FL), transmembrane (TM), and intracellular domain (ICD). TUBULIN served as loading control. **(B)** RNA was collected from iPrECs differentiated for the indicated days and the levels of mRNA for several ligands and downstream targets of the NOTCH signaling pathway as well as integrins α6, β4, and β1 were measured by qRT-PCR. Luminal (L) cell were separated from basal (B) cells at days 10 and 14; dashed lines shows basal, solid line shows luminal. Error bars show standard deviation of biological triplicates. *p*-values were determined by paired, two-tail t-test between d14 basal and luminal samples; n.s. = non-significant (p>0.2). Data were standardized to *18S* and *GAPDH*. Y-axis shows ΔΔCT values relative to day 1, which is equal to Log_2(fold change). **(C)** iPrECs were treated with DMSO + Dox (Control) or 1μM RO4929097 while Inducible shRNA lines were treated with 50ng/mL Dox over a 16 day differentiation. Cells were then fixed and stained. Top row shows phase contrast; bottom shows merged epifluorescence images of Hoescht-stained nuclei (blue) and propidium iodide (red), to which only dead cells are permeable. Luminal layer is outlined (dashed line) in control cells; (L) is the luminal layer and (B) is the basal layer. Scale bar = 200μm.

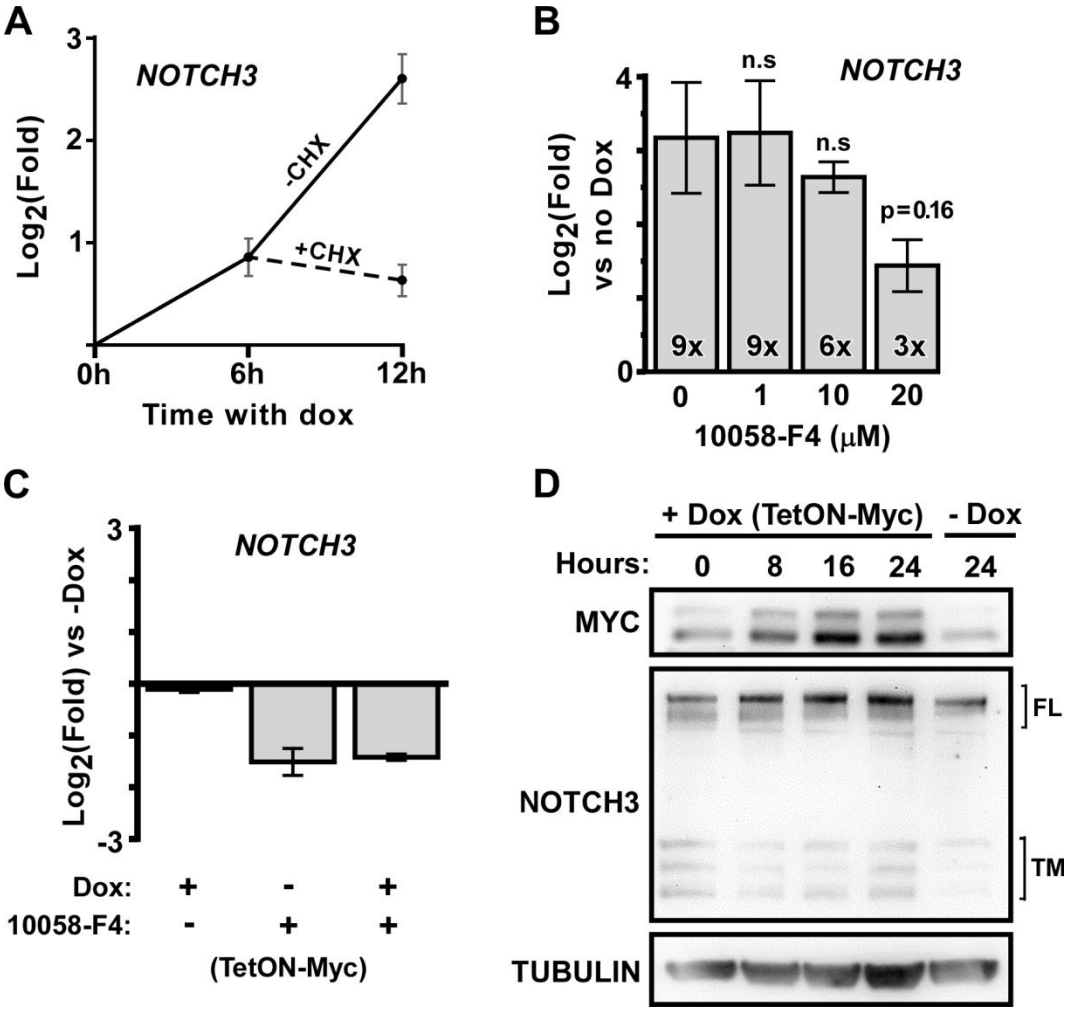

Figure S3: MYC is required but not sufficient for *NOTCH3* induction. (A) iPrEC-TetON-MKK6(CA) cells were induced with 2ng/mL Dox. After 6h Dox treatment one set of samples was harvested while the others were treated with 10µg/mL Cyclohexamide (CHX) or PBS control for 6h longer. *NOTCH3* mRNA was measured by qRT-PCR. Samples were standardized to *18S* and *GAPDH*. Y-axis shows ΔΔCT values relative to 0h. Error bars show standard deviation of biological triplicates. **(B)** iPrEC-TetON-MKK6(CA) cells were treated with 5ng/mL Dox for 16h plus DMSO or varying amounts of 10058-F4 MYC inhibitor. *NOTCH3* mRNA expression was measured by qRT-PCR. Error bars show standard deviation of biological triplicates. Statistical analysis vs 0µM (DMSO) was performed by one-way ANOVA with Dunnett's multiple comparison correction. n.s. = not significant (p>0.4). Data were standardized to *18S* and *RPL19*. Y-axis shows ΔΔCT values relative to untreated controls (no Dox, plus DMSO). Text within bars is rounded to fold change. **(C)** Basal, undifferentiated iPrEC-TetON-Myc cells were treated with Dox (10ng/mL) and/or 10058-F4 (10µM) for 8h and *NOTCH3* mRNA was measured by qRT-PCR. Control cells were treated with DMSO only. Error bars show standard deviation of biological triplicates. Data were standardized to *18S* and *RPL19*. Y-axis shows ΔΔCT values relative untreated controls (no Dox, plus DMSO). **(D)** iPrEC-TetON-Myc cells were first differentiated for five days without Dox. Then cells were treated with Dox (10ng/mL) for up to 24h and lysates collected to measure MYC and NOTCH3 by immunoblot. Control cells were treated with DMSO for 24h.

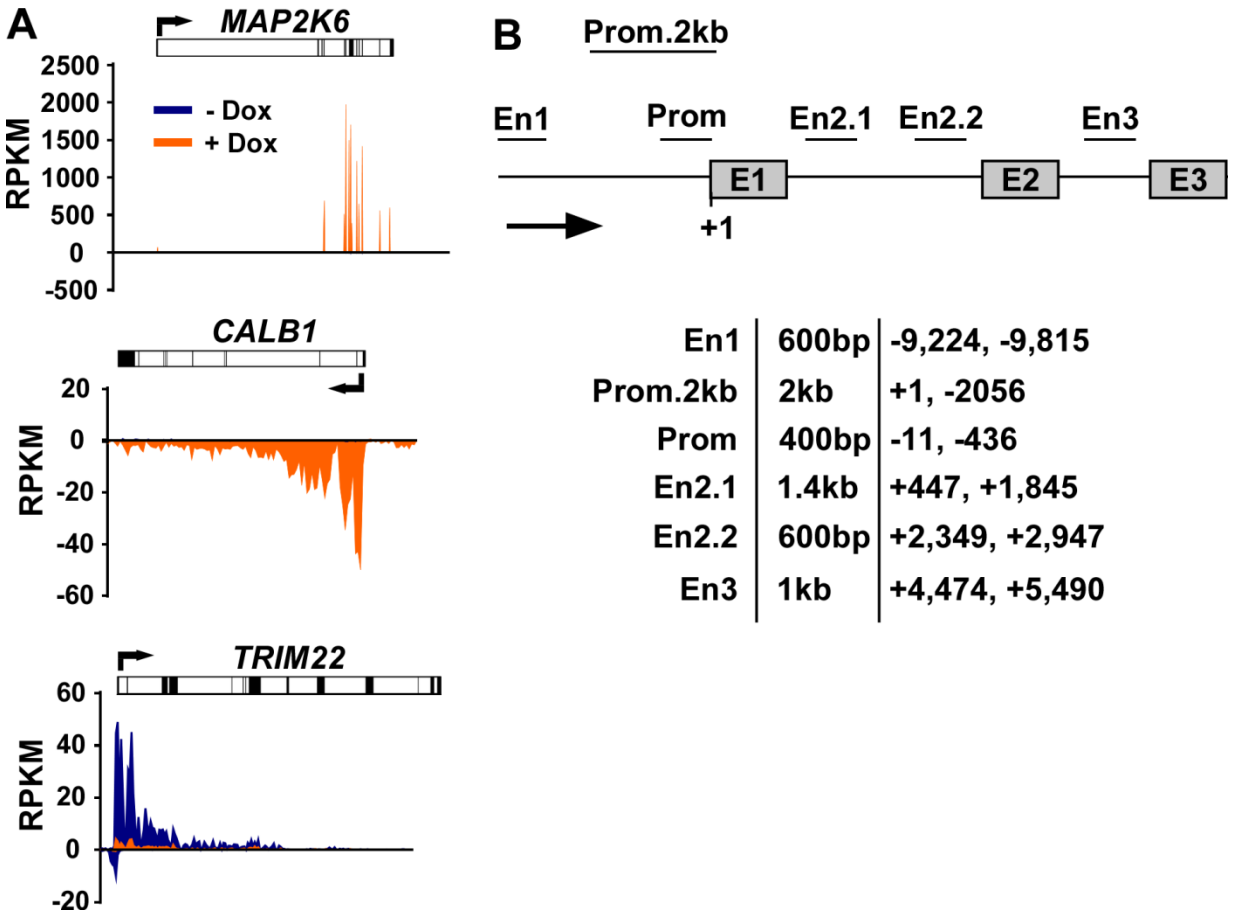

Figure S4: UV-BrU-seq controls and map of cloned regulatory elements. (A) Additional controls for the UV-BrU-seq data from Fig. 10B. iPrEC-TetON-MKK6(CA) cells were treated with 5ng/mL Dox for 10h and processed for UV-BrU-Seq. Graphs show RNA reads across gene locus (bin = 300bp). Y-axis is RPKM (reads per kilobase of transcript per million mapped reads). Plus strand reads are (+) values, minus strand reads are (-). Blue = -Dox samples and orange = +Dox. Gene diagrams show exon mapping (black region) and arrow indicates coding strand. **(B)** Diagram (not to scale) of the first three exons of *NOTCH3* and regions cloned for reporter assays. Note: *NOTCH3* is on the minus strand but is depicted here 5'>3'. The table shows the size of the cloned regions and their location in relation to the *NOTCH3* start codon (ATG = +1).

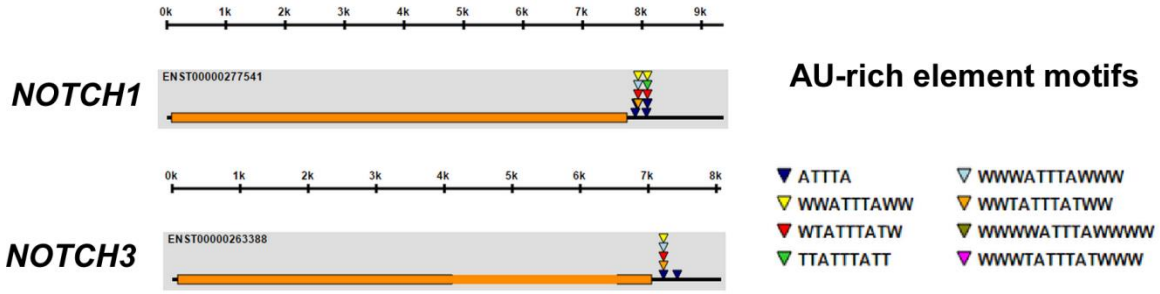

Figure S5: *NOTCH3* contains an AU rich element. The online tool ARE Site (v1) was used to search the *NOTCH3* transcript for common AU-rich motifs that are binding sites for RNA binding proteins. http://nibiru.tbi.univie.ac.at/cgi-bin/AREsite/AREsite.cgi.

BIBLIOGRAPHY

BIBLIOGRAPHY

1. Siegel R, Naishadham D, Jemal A. Cancer statistics, 2013. *CA Cancer J Clin.* 2013;63(1):11-30.

2. Attard G, Parker C, Eeles RA, et al. Prostate cancer. *Lancet.* 2016;387(10013):70-82.

3. Siegel RL, Miller KD, Jemal A. Cancer statistics, 2016. *CA Cancer J Clin.* 2016;66(1):7-30.

4. Ryan CJ, Smith MR, de Bono JS, et al. Abiraterone in metastatic prostate cancer without previous chemotherapy. *N Engl J Med.* 2013;368(2):138-148.

5. Schrader AJ, Boegemann M, Ohlmann CH, et al. Enzalutamide in castration-resistant prostate cancer patients progressing after docetaxel and abiraterone. *Eur Urol.* 2014;65(1):30-36.

6. Alme AK, Karir BS, Faltas BM, Drake CG. Blocking immune checkpoints in prostate, kidney, and urothelial cancer: An overview. *Urol Oncol.* 2016;34(4):171-181.

7. Bill-Axelson A, Holmberg L, Garmo H, et al. Radical prostatectomy or watchful waiting in early prostate cancer. *N Engl J Med.* 2014;370(10):932-942.

8. Warlick C, Trock BJ, Landis P, Epstein JI, Carter HB. Delayed versus immediate surgical intervention and prostate cancer outcome. *J Natl Cancer Inst.* 2006;98(5):355-357.

9. Haas GP, Delongchamps N, Brawley OW, Wang CY, de la Roza G. The worldwide epidemiology of prostate cancer: perspectives from autopsy studies. *Can J Urol.* 2008;15(1):3866-3871.

10. Nguyen PL, Gu X, Lipsitz SR, et al. Cost implications of the rapid adoption of newer technologies for treating prostate cancer. *J Clin Oncol.* 2011;29(12):1517-1524.

11. Resnick MJ, Koyama T, Fan KH, et al. Long-term functional outcomes after treatment for localized prostate cancer. *N Engl J Med.* 2013;368(5):436-445.

12. Brawley OW. Prostate cancer epidemiology in the United States. *World J Urol.* 2012;30(2):195-200.

13. Al Olama AA, Kote-Jarai Z, Berndt SI, et al. A meta-analysis of 87,040 individuals identifies 23 new susceptibility loci for prostate cancer. *Nat Genet.* 2014;46(10):1103-1109.

14. Surcel CI, van Oort IM, Sooriakumaran P, et al. Prognostic effect of neuroendocrine differentiation in prostate cancer: A critical review. *Urol Oncol.* 2015;33(6):265.e261-267.

15. Santoni M, Conti A, Burattini L et al. Neuroendocrine differentiation in prostate cancer: novel insights and future therapeutic perspectives. *Biochim Biophys Acta.* 2014;1864(2)

16. Aggarwal R, Zhang T, Small EJ, Armstrong AJ. Neuroendocrine prostate cancer: subtypes, biology, and clinical outcomes. *J Natl Compr Canc Netw.* 2014;12(5):719-726.

17. Network CGAR. The Molecular Taxonomy of Primary Prostate Cancer. *Cell.* 2015;163(4):1011-1025.

18. Watson PA, Arora VK, Sawyers CL. Emerging mechanisms of resistance to androgen receptor inhibitors in prostate cancer. *Nat Rev Cancer.* 2015;15(12):701-711.

19. Rodon J, Dienstmann R, Serra V, Tabernero J. Development of PI3K inhibitors: lessons learned from early clinical trials. *Nat Rev Clin Oncol.* 2013;10(3):143-153.

20. Lamb LE, Zarif JC, Miranti CK. The androgen receptor induces integrin alpha6beta1 to promote prostate tumor cell survival via NF-kappaB and Bcl-xL Independently of PI3K signaling. *Cancer Res.* 2011;71(7):2739-2749.

21. Mateo J, Carreira S, Sandhu S, et al. DNA-Repair Defects and Olaparib in Metastatic Prostate Cancer. *N Engl J Med.* 2015;373(18):1697-1708.

22. da Silva HB, Amaral EP, Nolasco EL, et al. Dissecting major signaling pathways throughout the development of prostate cancer. *Prostate Cancer.* 2013;920612(10):29.

23. Gurel B, Iwata T, Koh CM, Yegnasubramanian S, Nelson WG, De Marzo AM. Molecular alterations in prostate cancer as diagnostic, prognostic, and therapeutic targets. *Adv Anat Pathol.* 2008;15(6):319-331.

24. Koh CM, Bieberich CJ, Dang CV, Nelson WG, Yegnasubramanian S, De Marzo AM. MYC and Prostate Cancer. *Genes Cancer.* 2010;1(6):617-628.

25. Ellwood-Yen K, Graeber TG, Wongvipat J, et al. Myc-driven murine prostate cancer shares molecular features with human prostate tumors. *Cancer Cell.* 2003;4(3):223-238.

26. Liu W, Xie CC, Zhu Y, et al. Homozygous deletions and recurrent amplifications implicate new genes involved in prostate cancer. *Neoplasia.* 2008;10(8):897-907.

27. Lapointe J, Li C, Giacomini CP, et al. Genomic profiling reveals alternative genetic pathways of prostate tumorigenesis. *Cancer Res.* 2007;67(18):8504-8510.

28. Nupponen NN, Kakkola L, Koivisto P, Visakorpi T. Genetic alterations in hormone-refractory recurrent prostate carcinomas. *The American journal of pathology.* 1998;153(1):141-148.

29. Gurel B, Iwata T, Koh CM, et al. Nuclear MYC protein overexpression is an early alteration in human prostate carcinogenesis. *Modern Pathology.* 2008;21(9):1156-1167.

30. Edwards J, Krishna NS, Witton CJ, Bartlett JM. Gene amplifications associated with the development of hormone-resistant prostate cancer. *Clin Cancer Res.* 2003;9(14):5271-5281.

31. Gray IC, Stewart LM, Phillips SM, et al. Mutation and expression analysis of the putative prostate tumour-suppressor gene PTEN. *Br J Cancer.* 1998;78(10):1296-1300.

32. Song MS, Salmena L, Pandolfi PP. The functions and regulation of the PTEN tumour suppressor. *Nat Rev Mol Cell Biol.* 2012;13(5):283-296.

33. Barbieri CE, Baca SC, Lawrence MS, et al. Exome sequencing identifies recurrent SPOP, FOXA1 and MED12 mutations in prostate cancer. *Nat Genet.* 2012;44(6):685-689.

34. Lotan TL, Gurel B, Sutcliffe S, et al. PTEN protein loss by immunostaining: analytic validation and prognostic indicator for a high risk surgical cohort of prostate cancer patients. *Clin Cancer Res.* 2011;17(20):6563-6573.

35. Verhagen PC, van Duijn PW, Hermans KG, et al. The PTEN gene in locally progressive prostate cancer is preferentially inactivated by bi-allelic gene deletion. *J Pathol.* 2006;208(5):699-707.

36. Yoshimoto M, Ding K, Sweet JM, et al. PTEN losses exhibit heterogeneity in multifocal prostatic adenocarcinoma and are associated with higher Gleason grade. *Modern Pathol.* 2013;26(3):435-447.

37. Kwabi-Addo B, Giri D, Schmidt K, et al. Haploinsufficiency of the Pten tumor suppressor gene promotes prostate cancer progression. *Proc Natl Acad Sci U S A.* 2001;98(20):11563-11568.

38. Trotman LC, Niki M, Dotan ZA, et al. Pten dose dictates cancer progression in the prostate. *PLoS Biol.* 2003;1(3):27.

39. Ma X, Ziel-van der Made AC, Autar B, et al. Targeted biallelic inactivation of Pten in the mouse prostate leads to prostate cancer accompanied by increased epithelial cell proliferation but not by reduced apoptosis. *Cancer Res.* 2005;65(13):5730-5739.

40. Wang S, Gao J, Lei Q, et al. Prostate-specific deletion of the murine Pten tumor suppressor gene leads to metastatic prostate cancer. *Cancer Cell.* 2003;4(3):209-221.

41. Clark JP, Cooper CS. ETS gene fusions in prostate cancer. *Nat Rev Urol.* 2009;6(8):429-439.

42. Tomlins SA, Bjartell A, Chinnaiyan AM, et al. ETS gene fusions in prostate cancer: from discovery to daily clinical practice. *Eur Urol.* 2009;56(2):275-286.

43. Demichelis F, Fall K, Perner S, et al. TMPRSS2:ERG gene fusion associated with lethal prostate cancer in a watchful waiting cohort. *Oncogene.* 2007;26(31):4596-4599.

44. Tomlins SA, Rhodes DR, Perner S, et al. Recurrent fusion of TMPRSS2 and ETS transcription factor genes in prostate cancer. *Science.* 2005;310(5748):644-648.

45. Furusato B, Gao CL, Ravindranath L, et al. Mapping of TMPRSS2-ERG fusions in the context of multi-focal prostate cancer. *Mod Pathol.* 2008;21(2):67-75.

46. Perner S, Mosquera JM, Demichelis F, et al. TMPRSS2-ERG fusion prostate cancer: an early molecular event associated with invasion. *Amer J Surg Pathol.* 2007;31(6):882-888.

47. Tomlins SA, Laxman B, Varambally S, et al. Role of the TMPRSS2-ERG gene fusion in prostate cancer. *Neoplasia.* 2008;10(2):177-188.

48. Yu J, Mani RS, Cao Q, et al. An integrated network of androgen receptor, polycomb, and TMPRSS2-ERG gene fusions in prostate cancer progression. *Cancer Cell.* 2010;17(5):443-454.

49. Sun C, Dobi A, Mohamed A, et al. TMPRSS2-ERG fusion, a common genomic alteration in prostate cancer activates C-MYC and abrogates prostate epithelial differentiation. *Oncogene.* 2008;27(40):5348-5353.

50. Wang J, Cai Y, Yu W, Ren C, Spencer DM, Ittmann M. Pleiotropic biological activities of alternatively spliced TMPRSS2/ERG fusion gene transcripts. *Cancer Res.* 2008;68(20):8516-8524.

51. Kumar-Sinha C, Tomlins SA, Chinnaiyan AM. Recurrent gene fusions in prostate cancer. *Nat Rev Cancer.* 2008;8(7):497-511.

52. Palanisamy N, Ateeq B, Kalyana-Sundaram S, et al. Rearrangements of the RAF kinase pathway in prostate cancer, gastric cancer and melanoma. *Nat Med.* 2010;16(7):793-798.

53. Cunha GR, Ricke W, Thomson A, et al. Hormonal, cellular, and molecular regulation of normal and neoplastic prostatic development. *J Steroid Biochem Mol Biol.* 2004;92(4):221-236.

54. Wu CT, Altuwaijri S, Ricke WA, et al. Increased prostate cell proliferation and loss of cell differentiation in mice lacking prostate epithelial androgen receptor. *Proc Natl Acad Sci U S A.* 2007;104(31):12679-12684.

55. Berger R, Febbo PG, Majumder PK, et al. Androgen-induced differentiation and tumorigenicity of human prostate epithelial cells. *Cancer Res.* 2004;64(24):8867-8875.

56. Whitacre DC, Chauhan S, Davis T, Gordon D, Cress AE, Miesfeld RL. Androgen induction of in vitro prostate cell differentiation. *Cell Growth Differ.* 2002;13(1):1-11.

57. Yoshimoto M, Cunha IW, Coudry RA, et al. FISH analysis of 107 prostate cancers shows that PTEN genomic deletion is associated with poor clinical outcome. *Br J Cancer.* 2007;97(5):678-685.

58. Yoshimoto M, Cutz JC, Nuin PA, et al. Interphase FISH analysis of PTEN in histologic sections shows genomic deletions in 68% of primary prostate cancer and 23% of high-grade prostatic intra-epithelial neoplasias. *Cancer Genet Cytogenet.* 2006;169(2):128-137.

59. Shaikhibrahim Z, Wernert N. ETS transcription factors and prostate cancer: the role of the family prototype ETS-1 (review). *Int J Oncol.* 2012;40(6):1748-1754.

60. Chen Y, Chi P, Rockowitz S, et al. ETS factors reprogram the androgen receptor cistrome and prime prostate tumorigenesis in response to PTEN loss. *Nat Med.* 2013;30(10).

61. Carver BS, Tran J, Gopalan A, et al. Aberrant ERG expression cooperates with loss of PTEN to promote cancer progression in the prostate. *Nat Genet.* 2009;41(5):619-624.

62. King JC, Xu J, Wongvipat J, et al. Cooperativity of TMPRSS2-ERG with PI3-kinase pathway activation in prostate oncogenesis. *Nat Genet.* 2009;41(5):524-526.

63. Klezovitch O, Risk M, Coleman I, et al. A causal role for ERG in neoplastic transformation of prostate epithelium. *Proc Natl Acad Sci U S A.* 2008;105(6):2105-2110.

64. Cunha GR. Mesenchymal-epithelial interactions: past, present, and future. *Differentiation.* 2008;76(6):578-586.

65. Cress AE, Rabinovitz I, Zhu W, Nagle RB. The a6b1 and a6b4 integrins in human prostate cancer progression. *Cancer Metastas Rev.* 1995;14(3):219-228.

66. Schalken JA, van Leenders G. Cellular and molecular biology of the prostate: stem cell biology. *Urology.* 2003;62(5 Suppl 1):11-20.

67. Verhagen AP, Ramaekers FC, Aalders TW, Schaafsma HE, Debruyne FM, Schalken JA. Colocalization of basal and luminal cell-type cytokeratins in human prostate cancer. *Cancer Res.* 1992;52(22):6182-6187.

68. Wang ZA, Mitrofanova A, Bergren SK, et al. Lineage analysis of basal epithelial cells reveals their unexpected plasticity and supports a cell-of-origin model for prostate cancer heterogeneity. *Nature Cell Biol.* 2013;15(3):274-283.

69. de Muga S, Hernandez S, Agell L, et al. Molecular alterations of EGFR and PTEN in prostate cancer: association with high-grade and advanced-stage carcinomas. *Modern Pathology* 2010;23(5):703-712.

70. Peraldo-Neia C, Migliardi G, Mello-Grand M, et al. Epidermal Growth Factor Receptor (EGFR) mutation analysis, gene expression profiling and EGFR protein expression in primary prostate cancer. *BMC Cancer.* 2011;11:31.

71. Lamb LE, Knudsen BS, Miranti CK. E-cadherin-mediated survival of androgen-receptor-expressing secretory prostate epithelial cells derived from a stratified in vitro differentiation model. *J Cell Sci.* 2010;123(Pt 2):266-276.

72. van Leenders G, van Balken B, Aalders T, Hulsbergen-van de Kaa C, Ruiter D, Schalken J. Intermediate cells in normal and malignant prostate epithelium express c-MET: implications for prostate cancer invasion. *Prostate.* 2002;51(2):98-107.

73. Carvalho JR, Filipe L, Costa VL, et al. Detailed analysis of expression and promoter methylation status of apoptosis-related genes in prostate cancer. *Apoptosis.* 2010;15(8):956-965.

74. McDonnell TJ, Troncoso P, Brisbay SM, et al. Expression of the protooncogene bcl-2 in the prostate and its association with emergence of androgen-independent prostate cancer. *Cancer Res.* 1992;52(24):6940-6944.

75. English HF, Santen RJ, Isaacs JT. Response of glandular versus basal rat ventral prostatic epithelial cells to androgen withdrawal and replacement. *Prostate.* 1987;11(3):229-242.

76. Isaacs JT, Coffey DS. Etiology and disease process of benign prostatic hyperplasia. *Prostate Suppl.* 1989;2:33-50.

77. De Marzo AM, Meeker AK, Epstein JI, Coffey DS. Prostate stem cell compartments: expression of the cell cycle inhibitor p27Kip1 in normal, hyperplastic, and neoplastic cells. *Am J Pathol.* 1998;153(3):911-919.

78. Tokar EJ, Ancrile BB, Cunha GR, Webber MM. Stem/progenitor and intermediate cell types and the origin of human prostate cancer. *Differentiation.* 2005;73(9-10):463-473.

79. Ousset M, Van Keymeulen A, Bouvencourt G, et al. Multipotent and unipotent progenitors contribute to prostate postnatal development. *Nature cell biology.* 2012;14(11):1131-1138.

80. Wang X, Kruithof-de Julio M, Economides KD, et al. A luminal epithelial stem cell that is a cell of origin for prostate cancer. *Nature.* 2009;461(7263):495-500.

81. Leong KG, Wang BE, Johnson L, Gao WQ. Generation of a prostate from a single adult stem cell. *Nature.* 2008;456(7223):804-808.

82. Garraway IP, Sun W, Tran CP, et al. Human prostate sphere-forming cells represent a subset of basal epithelial cells capable of glandular regeneration in vivo. *Prostate.* 2010;70(5):491-501.

83. Lawson DA, Xin L, Lukacs RU, Cheng D, Witte ON. Isolation and functional characterization of murine prostate stem cells. *Proc Natl Acad Sci U S A.* 2007;104(1):181-186.

84. Xin L, Ide H, Kim Y, Dubey P, Witte ON. In vivo regeneration of murine prostate from dissociated cell populations of postnatal epithelia and urogenital sinus mesenchyme. *Proc Natl Acad Sci U S A.* 2003;1:11896-11903.

85. Xin L, Lawson DA, Witte ON. The Sca-1 cell surface marker enriches for a prostate-regenerating cell subpopulation that can initiate prostate tumorigenesis. *Proc Natl Acad Sci U S A.* 2005;102(19):6942-6947.

86. Xue Y, Smedts F, Debruyne FM, de la Rosette JJ, Schalken JA. Identification of intermediate cell types by keratin expression in the developing human prostate. *Prostate.* 1998;34(4):292-301.

87. Goldstein AS, Huang J, Guo C, Garraway IP, Witte ON. Identification of a cell of origin for human prostate cancer. *Science.* 2010;329(5991):568-571.

88. Lawson DA, Zong Y, Memarzadeh S, Xin L, Huang J, Witte ON. Basal epithelial stem cells are efficient targets for prostate cancer initiation. *Proc Natl Acad Sci U S A.* 2010;107(6):2610-2615.

89. Wang S, Garcia AJ, Wu M, Lawson DA, Witte ON, Wu H. Pten deletion leads to the expansion of a prostatic stem/progenitor cell subpopulation and tumor initiation. *Proc Natl Acad Sci U S A.* 2006;103(5):1480-1485.

90. Choi N, Zhang B, Zhang L, Ittmann M, Xin L. Adult murine prostate basal and luminal cells are self-sustained lineages that can both serve as targets for prostate cancer initiation. *Cancer Cell.* 2012;21(2):253-265.

91. Pienta KJ, Abate-Shen C, Agus DB, et al. The current state of preclinical prostate cancer animal models. *Prostate.* 2008;68(6):629-639.

92. Valkenburg KC, Williams BO. Mouse models of prostate cancer. *Prostate Cancer.* 2011;895238(10):23.

93. Abate-Shen C, Shen MM. Mouse models of prostate carcinogenesis. *Trends Genet.* 2002;18(5):S1-5.

94. McNeal JE. The zonal anatomy of the prostate. *Prostate.* 1981;2(1):35-49.

95. Hayward SW, Haughney PC, Rosen MA, et al. Interactions between adult human prostatic epithelium and rat urogenital sinus mesenchyme in a tissue recombination model. *Differentiation.* 1998;63(3):131-140.

96. Goldstein AS, Drake JM, Burnes DL, et al. Purification and direct transformation of epithelial progenitor cells from primary human prostate. *Nat Protoc.* 2011;6(5):656-667.

97. Heer R, Collins AT, Robson CN, Shenton BK, Leung HY. KGF suppresses a2b1 integrin function and promotes differentiation of the transient amplifying population in human prostatic epithelium. *J Cell Sci.* 2006;119(Pt 7):1416-1424.

98. Peehl DM, Wong ST, Stamey TA. Vitamin A regulates proliferation and differentiation of human prostatic epithelial cells. *Prostate.* 1993;23(1):69-78.

99. van Leenders GJ, Schalken JA. Epithelial cell differentiation in the human prostate epithelium: implications for the pathogenesis and therapy of prostate cancer. *Crit Rev Oncol Hematol.* 2003;27(46):S3-10.

100. Gandarillas A. The mysterious human epidermal cell cycle, or an oncogene-induced differentiation checkpoint. *Cell Cycle.* 2012;11(24):4507-4516.

101. Watt FM, Frye M, Benitah SA. MYC in mammalian epidermis: how can an oncogene stimulate differentiation? *Nat Rev Cancer.* 2008;8(3):234-242.

102. Berger PL, Frank SB, Schulz VV, et al. Transient induction of ING4 by Myc drives prostate epithelial cell differentiation and its disruption drives prostate tumorigenesis. *Cancer research.* 2014;74(12):3357-3368.

103. Cascon A, Robledo M. MAX and MYC: a heritable breakup. *Cancer Res.* 2012;72(13):3119-3124.

104. Rahl PB, Lin CY, Seila AC, et al. c-Myc regulates transcriptional pause release. *Cell.* 2010;141(3):432-445.

105. Varlakhanova NV, Knoepfler PS. Acting locally and globally: Myc's ever-expanding roles on chromatin. *Cancer Res.* 2009;69(19):7487-7490.

106. Luscher B, Vervoorts J. Regulation of gene transcription by the oncoprotein MYC. *Gene.* 2012;494(2):145-160.

107. Peukert K, Staller P, Schneider A, Carmichael G, Hanel F, Eilers M. An alternative pathway for gene regulation by Myc. *Embo J.* 1997;16(18):5672-5686.

108. Chang TC, Yu D, Lee YS, et al. Widespread microRNA repression by Myc contributes to tumorigenesis. *Nat Genet.* 2008;40(1):43-50.

109. Ma L, Young J, Prabhala H, et al. miR-9, a MYC/MYCN-activated microRNA, regulates E-cadherin and cancer metastasis. *Nat Cell Biol.* 2010;12(3):247-256.

110. Thomas LR, Tansey WP. Proteolytic control of the oncoprotein transcription factor Myc. *Adv Cancer Res.* 2011;110:77-106.

111. Vervoorts J, Luscher-Firzlaff J, Luscher B. The ins and outs of MYC regulation by posttranslational mechanisms. *J Biol Chem.* 2006;281(46):34725-34729.

112. Cawley S, Bekiranov S, Ng HH, et al. Unbiased mapping of transcription factor binding sites along human chromosomes 21 and 22 points to widespread regulation of noncoding RNAs. *Cell.* 2004;116(4):499-509.

113. Li Z, Van Calcar S, Qu C, Cavenee WK, Zhang MQ, Ren B. A global transcriptional regulatory role for c-Myc in Burkitt's lymphoma cells. *Proc Natl Acad Sci U S A.* 2003;100(14):8164-8169.

114. Buttyan R, Sawczuk IS, Benson MC, Siegal JD, Olsson CA. Enhanced expression of the c-myc protooncogene in high-grade human prostate cancers. *Prostate.* 1987;11(4):327-337.

115. Fleming WH, Hamel A, MacDonald R, et al. Expression of the c-myc protooncogene in human prostatic carcinoma and benign prostatic hyperplasia. *Cancer Res.* 1986;46(3):1535-1538.

116. Al Olama AA, Kote-Jarai Z, Giles GG, et al. Multiple loci on 8q24 associated with prostate cancer susceptibility. *Nat Genet.* 2009;41(10):1058-1060.

117. Porkka KP, Tammela TL, Vessella RL, Visakorpi T. RAD21 and KIAA0196 at 8q24 are amplified and overexpressed in prostate cancer. *Genes Chromosomes Cancer.* 2004;39(1):1-10.

118. Tsuchiya N, Kondo Y, Takahashi A, et al. Mapping and gene expression profile of the minimally overrepresented 8q24 region in prostate cancer. *Am J Pathol.* 2002;160(5):1799-1806.

119. Bernard D, Pourtier-Manzanedo A, Gil J, Beach DH. Myc confers androgen-independent prostate cancer cell growth. *The Journal of clinical investigation.* 2003;112(11):1724-1731.

120. Gao L, Schwartzman J, Gibbs A, et al. Androgen receptor promotes ligand-independent prostate cancer progression through c-Myc upregulation. *PLoS One.* 2013;8(5).

121. Grad JM, Dai JL, Wu S, Burnstein KL. Multiple androgen response elements and a Myc consensus site in the androgen receptor (AR) coding region are involved in androgen-mediated up-regulation of AR messenger RNA. *Mol Endocrinol.* 1999;13(11):1896-1911.

122. Nadiminty N, Tummala R, Lou W, et al. MicroRNA let-7c suppresses androgen receptor expression and activity via regulation of Myc expression in prostate cancer cells. *J Biol Chem.* 2012;287(2):1527-1537.

123. Yu X, Wang Y, Jiang M, et al. Activation of beta-Catenin in mouse prostate causes HGPIN and continuous prostate growth after castration. *Prostate.* 2009;69(3):249-262.

124. Kang GH, Lee S, Lee HJ, Hwang KS. Aberrant CpG island hypermethylation of multiple genes in prostate cancer and prostatic intraepithelial neoplasia. *J Pathol.* 2004;202(2):233-240.

125. Yegnasubramanian S, Kowalski J, Gonzalgo ML, et al. Hypermethylation of CpG islands in primary and metastatic human prostate cancer. *Cancer Res.* 2004;64(6):1975-1986.

126. Zhu H, Zhou X, Redfield S, Lewin J, Miele L. Elevated Jagged-1 and Notch-1 expression in high grade and metastatic prostate cancers. *Am J Transl Res.* 2013;5(3):368-378.

127. Bin Hafeez B, Adhami VM, Asim M, et al. Targeted knockdown of Notch1 inhibits invasion of human prostate cancer cells concomitant with inhibition of matrix metalloproteinase-9 and urokinase plasminogen activator. *Clin Cancer Res.* 2009;15(2):452-459.

128. Zhang X, Lee C, Ng PY, Rubin M, Shabsigh A, Buttyan R. Prostatic neoplasia in transgenic mice with prostate-directed overexpression of the c-myc oncoprotein. *Prostate.* 2000;43(4):278-285.

129. Schreiber-Agus N, Meng Y, Hoang T, et al. Role of Mxi1 in ageing organ systems and the regulation of normal and neoplastic growth. *Nature.* 1998;393(6684):483-487.

130. Eilers M, Eisenman RN. Myc's broad reach. *Genes Dev.* 2008;22(20):2755-2766.

131. Takahashi K, Yamanaka S. Induction of pluripotent stem cells from mouse embryonic and adult fibroblast cultures by defined factors. *Cell.* 2006;126(4):663-676.

132. Hanna J, Cheng AW, Saha K, et al. Human embryonic stem cells with biological and epigenetic characteristics similar to those of mouse ESCs. *Proc Natl Acad Sci U S A.* 2010;107(20):9222-9227.

133. Nakagawa M, Koyanagi M, Tanabe K, et al. Generation of induced pluripotent stem cells without Myc from mouse and human fibroblasts. *Nat Biotechnol.* 2008;26(1):101-106.

134. Cartwright P, McLean C, Sheppard A, Rivett D, Jones K, Dalton S. LIF/STAT3 controls ES cell self-renewal and pluripotency by a Myc-dependent mechanism. *Development.* 2005;132(5):885-896.

135. Varlakhanova NV, Cotterman RF, deVries WN, et al. Myc maintains embryonic stem cell pluripotency and self-renewal. *Differentiation.* 2010;80(1):9-19.

136. Xu D, Popov N, Hou M, et al. Switch from Myc/Max to Mad1/Max binding and decrease in histone acetylation at the telomerase reverse transcriptase promoter during differentiation of HL60 cells. *Proc Natl Acad Sci U S A.* 2001;98(7):3826-3831.

137. Bouchard C, Dittrich O, Kiermaier A, et al. Regulation of cyclin D2 gene expression by the Myc/Max/Mad network: Myc-dependent TRRAP recruitment and histone acetylation at the cyclin D2 promoter. *Genes Dev.* 2001;15(16):2042-2047.

138. Sumi T, Tsuneyoshi N, Nakatsuji N, Suemori H. Apoptosis and differentiation of human embryonic stem cells induced by sustained activation of c-Myc. *Oncogene.* 2007;26(38):5564-5576.

139. Bull JJ, Muller-Rover S, Patel SV, Chronnell CM, McKay IA, Philpott MP. Contrasting localization of c-Myc with other Myc superfamily transcription factors in the human hair follicle and during the hair growth cycle. *J Invest Dermatol.* 2001;116(4):617-622.

140. Gandarillas A, Watt FM. Changes in expression of members of the fos and jun families and myc network during terminal differentiation of human keratinocytes. *Oncogene.* 1995;11(7):1403-1407.

141. Gandarillas A, Watt FM. c-Myc promotes differentiation of human epidermal stem cells. *Genes Dev.* 1997;11(21):2869-2882.

142. Gebhardt A, Frye M, Herold S, et al. Myc regulates keratinocyte adhesion and differentiation via complex formation with Miz1. *J Cell Biol.* 2006;172(1):139-149.

143. Hashiro M, Matsumoto K, Okumura H, Hashimoto K, Yoshikawa K. Growth inhibition of human keratinocytes by antisense c-myc oligomer is not coupled to induction of differentiation. *Biochem Biophys Res Commun.* 1991;174(1):287-292.

144. Frye M, Gardner C, Li ER, Arnold I, Watt FM. Evidence that Myc activation depletes the epidermal stem cell compartment by modulating adhesive interactions with the local microenvironment. *Development.* 2003;130(12):2793-2808.

145. Watt FM. Role of integrins in regulating epidermal adhesion, growth and differentiation. *Embo J.* 2002;21(15):3919-3926.

146. McMahon SB, Wood MA, Cole MD. The essential cofactor TRRAP recruits the histone acetyltransferase hGCN5 to c-Myc. *Mol Cell Biol.* 2000;20(2):556-562.

147. Pellakuru LG, Iwata T, Gurel B, et al. Global levels of H3K27me3 track with differentiation in vivo and are deregulated by MYC in prostate cancer. *Am J Pathol.* 2012;181(2):560-569.

148. Efroni S, Duttagupta R, Cheng J, et al. Global transcription in pluripotent embryonic stem cells. *Cell Stem Cell.* 2008;2(5):437-447.

149. Koh CM, Iwata T, Zheng Q, Bethel C, Yegnasubramanian S, De Marzo AM. Myc enforces overexpression of EZH2 in early prostatic neoplasia via transcriptional and post-transcriptional mechanisms. *Oncotarget.* 2011;2(9):669-683.

150. Xu K, Wu ZJ, Groner AC, et al. EZH2 oncogenic activity in castration-resistant prostate cancer cells is Polycomb-independent. *Science.* 2012;338(6113):1465-1469.

151. Dong JT. Prevalent mutations in prostate cancer. *J Cell Biochem.* 2006;97(3):433-447.

152. Cuadrado A, Nebreda AR. Mechanisms and functions of p38 MAPK signalling. *The Biochemical journal.* 2010;429(3):403-417.

153. Wagner EF, Nebreda AR. Signal integration by JNK and p38 MAPK pathways in cancer development. *Nat Rev Cancer.* 2009;9(8):537-549.

154. Belleudi F, Purpura V, Torrisi MR. The receptor tyrosine kinase FGFR2b/KGFR controls early differentiation of human keratinocytes. *PLoS One.* 2011;6(9):21.

155. Turner N, Grose R. Fibroblast growth factor signalling: from development to cancer. *Nat Rev Cancer.* 2010;10(2):116-129.

156. Keyse SM. Dual-specificity MAP kinase phosphatases (MKPs) and cancer. *Cancer Metastas Rev.* 2008;27(2):253-261.

157. Uzgare AR, Kaplan PJ, Greenberg NM. Differential expression and/or activation of P38MAPK, erk1/2, and jnk during the initiation and progression of prostate cancer. *Prostate.* 2003;55(2):128-139.

158. Rajashekhar G, Kamocka M, Marin A, et al. Pro-inflammatory angiogenesis is mediated by p38 MAP kinase. *J Cell Physiol.* 2011;226(3):800-808.

159. Royuela M, Arenas MI, Bethencourt FR, Sanchez-Chapado M, Fraile B, Paniagua R. Regulation of proliferation/apoptosis equilibrium by mitogen-activated protein kinases in normal, hyperplastic, and carcinomatous human prostate. *Hum Pathol.* 2002;33(3):299-306.

160. Lotan TL, Lyon M, Huo D, et al. Up-regulation of MKK4, MKK6 and MKK7 during prostate cancer progression: an important role for SAPK signalling in prostatic neoplasia. *J Pathol.* 2007;212(4):386-394.

161. Ricote M, Garcia-Tunon I, Bethencourt F, et al. The p38 transduction pathway in prostatic neoplasia. *J Pathol.* 2006;208(3):401-407.

162. Ricote M, Garcia-Tunon I, Fraile B, et al. P38 MAPK protects against TNF-alpha-provoked apoptosis in LNCaP prostatic cancer cells. *Apoptosis.* 2006;11(11):1969-1975.

163. Loda M, Capodieci P, Mishra R, et al. Expression of mitogen-activated protein kinase phosphatase-1 in the early phases of human epithelial carcinogenesis. *The American journal of pathology.* 1996;149(5):1553-1564.

164. Rauhala HE, Porkka KP, Tolonen TT, Martikainen PM, Tammela TL, Visakorpi T. Dual-specificity phosphatase 1 and serum/glucocorticoid-regulated kinase are downregulated in prostate cancer. *International journal of cancer. Journal international du cancer.* 2005;117(5):738-745.

165. Magi-Galluzzi C, Mishra R, Fiorentino M, et al. Mitogen-activated protein kinase phosphatase 1 is overexpressed in prostate cancers and is inversely related to apoptosis. *Lab Invest.* 1997;76(1):37-51.

166. Magi-Galluzzi C, Montironi R, Cangi MG, Wishnow K, Loda M. Mitogen-activated protein kinases and apoptosis in PIN. *Virchows Arch.* 1998;432(5):407-413.

167. Ross AE, Marchionni L, Vuica-Ross M, et al. Gene expression pathways of high grade localized prostate cancer. *Prostate.* 2011;25(10):21373.

168. Manetsch M, Che W, Seidel P, Chen Y, Ammit AJ. MKP-1: a negative feedback effector that represses MAPK-mediated pro-inflammatory signaling pathways and cytokine secretion in human airway smooth muscle cells. *Cell Signal.* 2012;24(4):907-913.

169. Ueda T, Bruchovsky N, Sadar MD. Activation of the androgen receptor N-terminal domain by interleukin-6 via MAPK and STAT3 signal transduction pathways. *J Biol Chem.* 2002;277(9):7076-7085.

170. Zauberman A, Zipori D, Krupsky M, Ben-Levy R. Stress activated protein kinase p38 is involved in IL-6 induced transcriptional activation of STAT3. *Oncogene.* 1999;18(26):3886-3893.

171. Culig Z, Puhr M. Interleukin-6: a multifunctional targetable cytokine in human prostate cancer. *Mol Cell Endocrinol.* 2012;360(1-2):52-58.

172. Lin DL, Whitney MC, Yao Z, Keller ET. Interleukin-6 induces androgen responsiveness in prostate cancer cells through up-regulation of androgen receptor expression. *Clin Cancer Res.* 2001;7(6):1773-1781.

173. Gan L, Wang J, Xu H, Yang X. Resistance to docetaxel-induced apoptosis in prostate cancer cells by p38/p53/p21 signaling. *Prostate.* 2011;71(11):1158-1166.

174. Liu C, Zhu Y, Lou W, et al. Functional p53 determines docetaxel sensitivity in prostate cancer cells. *Prostate.* 2013;73(4):418-427.

175. Frey MR, Golovin A, Polk DB. Epidermal growth factor-stimulated intestinal epithelial cell migration requires Src family kinase-dependent p38 MAPK signaling. *J Biol Chem.* 2004;279(43):44513-44521.

176. Lewis DA, Spandau DF. UVB-induced activation of NF-kB is regulated by the IGF-1R and dependent on p38 MAPK. *J Invest Dermatol.* 2008;128(4):1022-1029.

177. McCawley LJ, Li S, Wattenberg EV, Hudson LG. Sustained activation of the mitogen-activated protein kinase pathway. A mechanism underlying receptor tyrosine kinase specificity for matrix metalloproteinase-9 induction and cell migration. *J Biol Chem.* 1999;274(7):4347-4353.

178. Kwabi-Addo B, Ozen M, Ittmann M. The role of fibroblast growth factors and their receptors in prostate cancer. *Endocr Relat Cancer.* 2004;11(4):709-724.

179. Memarzadeh S, Xin L, Mulholland DJ, et al. Enhanced paracrine FGF10 expression promotes formation of multifocal prostate adenocarcinoma and an increase in epithelial androgen receptor. *Cancer Cell.* 2007;12(6):572-585.

180. Acevedo VD, Gangula RD, Freeman KW, et al. Inducible FGFR-1 activation leads to irreversible prostate adenocarcinoma and an epithelial-to-mesenchymal transition. *Cancer Cell.* 2007;12(6):559-571.

181. Kwabi-Addo B, Ropiquet F, Giri D, Ittmann M. Alternative splicing of fibroblast growth factor receptors in human prostate cancer. *Prostate.* 2001;46(2):163-172.

182. Houde M, Laprise P, Jean D, Blais M, Asselin C, Rivard N. Intestinal epithelial cell differentiation involves activation of p38 mitogen-activated protein kinase that regulates the homeobox transcription factor CDX2. *J Biol Chem.* 2001;276(24):21885-21894.

183. Sharma GD, He J, Bazan HE. p38 and ERK1/2 coordinate cellular migration and proliferation in epithelial wound healing: evidence of cross-talk activation between MAP kinase cascades. *J Biol Chem.* 2003;278(24):21989-21997.

184. Ventura JJ, Tenbaum S, Perdiguero E, et al. p38a MAP kinase is essential in lung stem and progenitor cell proliferation and differentiation. *Nat Genet.* 2007;39(6):750-758.

185. Wang X, Goh CH, Li B. p38 mitogen-activated protein kinase regulates osteoblast differentiation through osterix. *Endocrinology.* 2007;148(4):1629-1637.

186. Dashti SR, Efimova T, Eckert RL. MEK6 regulates human involucrin gene expression via a p38a - and p38d -dependent mechanism. *J Biol Chem.* 2001;276(29):27214-27220.

187. Allen M, Svensson L, Roach M, Hambor J, McNeish J, Gabel CA. Deficiency of the stress kinase p38a results in embryonic lethality: characterization of the kinase dependence of stress responses of enzyme-deficient embryonic stem cells. *J Exp Med.* 2000;191(5):859-870.

188. Sabio G, Arthur JS, Kuma Y, et al. p38gamma regulates the localisation of SAP97 in the cytoskeleton by modulating its interaction with GKAP. *Embo J.* 2005;24(6):1134-1145.

189. Schindler EM, Hindes A, Gribben EL, et al. p38delta Mitogen-activated protein kinase is essential for skin tumor development in mice. *Cancer Res.* 2009;69(11):4648-4655.

190. Efimova T, Broome AM, Eckert RL. A regulatory role for p38d MAPK in keratinocyte differentiation. Evidence for p38d-ERK1/2 complex formation. *J Biol Chem.* 2003;278(36):34277-34285.

191. Keren A, Tamir Y, Bengal E. The p38 MAPK signaling pathway: a major regulator of skeletal muscle development. *Mol Cell Endocrinol.* 2006;252(1-2):224-230.

192. Engel FB, Schebesta M, Duong MT, et al. p38 MAP kinase inhibition enables proliferation of adult mammalian cardiomyocytes. *Genes Dev.* 2005;19(10):1175-1187.

193. Hui L, Bakiri L, Mairhorfer A, et al. p38alpha suppresses normal and cancer cell proliferation by antagonizing the JNK-c-Jun pathway. *Nat Genet.* 2007;39(6):741-749.

194. Puri PL, Wu Z, Zhang P, et al. Induction of terminal differentiation by constitutive activation of p38 MAP kinase in human rhabdomyosarcoma cells. *Genes Dev.* 2000;14(5):574-584.

195. Hall JP, Davis RJ. Inhibition of the p38 pathway upregulates macrophage JNK and ERK activities, and the ERK, JNK, and p38 MAP kinase pathways are reprogrammed during differentiation of the murine myeloid M1 cell line. *J Cell Biochem.* 2002;86(1):1-11.

196. Danilenko DM. Preclinical and early clinical development of keratinocyte growth factor, an epithelial-specific tissue growth factor. *Toxicol Pathol.* 1999;27(1):64-71.

197. Mehta PB, Robson CN, Neal DE, Leung HY. Keratinocyte growth factor activates p38 MAPK to induce stress fibre formation in human prostate DU145 cells. *Oncogene.* 2001;20(38):5359-5365.

198. Miki T, Bottaro DP, Fleming TP, et al. Determination of ligand-binding specificity by alternative splicing: two distinct growth factor receptors encoded by a single gene. *Proc Natl Acad Sci U S A.* 1992;89(1):246-250.

199. Donjacour AA, Thomson AA, Cunha GR. FGF-10 plays an essential role in the growth of the fetal prostate. *Dev Biol.* 2003;261(1):39-54.

200. Lin Y, Liu G, Zhang Y, et al. Fibroblast growth factor receptor 2 tyrosine kinase is required for prostatic morphogenesis and the acquisition of strict androgen dependency for adult tissue homeostasis. *Development.* 2007;134(4):723-734.

201. Leong KG, Gao WQ. The Notch pathway in prostate development and cancer. *Differentiation.* 2008;76(6):699-716.

202. Kopan R, Ilagan MX. The canonical Notch signaling pathway: unfolding the activation mechanism. *Cell.* 2009;137(2):216-233.

203. Wang MM. Notch signaling and Notch signaling modifiers. *Int J Biochem Cell Biol.* 2011;43(11):1550-1562.

204. Fischer A, Gessler M. Delta-Notch--and then? Protein interactions and proposed modes of repression by Hes and Hey bHLH factors. *Nucleic Acids Res.* 2007;35(14):4583-4596.

205. Weng AP, Millholland JM, Yashiro-Ohtani Y, et al. c-Myc is an important direct target of Notch1 in T-cell acute lymphoblastic leukemia/lymphoma. *Genes & development.* 2006;20(15):2096-2109.

206. Shimizu K, Chiba S, Saito T, Kumano K, Hamada Y, Hirai H. Functional diversity among Notch1, Notch2, and Notch3 receptors. *Biochem Biophys Res Commun.* 2002;291(4):775-779.

207. Yuan Z, Friedmann DR, VanderWielen BD, Collins KJ, Kovall RA. Characterization of CSL (CBF-1, Su(H), Lag-1) mutants reveals differences in signaling mediated by Notch1 and Notch2. *J Biol Chem.* 2012;287(42):34904-34916.

208. Barolo S, Walker RG, Polyanovsky AD, Freschi G, Keil T, Posakony JW. A notch-independent activity of suppressor of hairless is required for normal mechanoreceptor physiology. *Cell.* 2000;103(6):957-969.

209. Martinez Arias A, Zecchini V, Brennan K. CSL-independent Notch signalling: a checkpoint in cell fate decisions during development? *Curr Opin Genet Dev.* 2002;12(5):524-533.

210. Johnson JE, Macdonald RJ. Notch-independent functions of CSL. *Curr Top Dev Biol.* 2011;97:55-74.

211. Minter LM, Osborne BA. Canonical and non-canonical Notch signaling in CD4(+) T cells. *Curr Top Microbiol Immunol.* 2012;360:99-114.

212. Fortini ME. Notch signaling: the core pathway and its posttranslational regulation. *Dev Cell.* 2009;16(5):633-647.

213. Roy M, Pear WS, Aster JC. The multifaceted role of Notch in cancer. *Curr Opin Genet Dev.* 2007;17(1):52-59.

214. Shih Ie M, Wang TL. Notch signaling, gamma-secretase inhibitors, and cancer therapy. *Cancer Res.* 2007;67(5):1879-1882.

215. Tzoneva G, Ferrando AA. Recent advances on NOTCH signaling in T-ALL. *Curr Top Microbiol Immunol.* 2012;360:163-182.

216. Van Vlierberghe P, Ferrando A. The molecular basis of T cell acute lymphoblastic leukemia. *J Clin Invest.* 2012;122(10):3398-3406.

217. Weng AP, Ferrando AA, Lee W, et al. Activating mutations of NOTCH1 in human T cell acute lymphoblastic leukemia. *Science.* 2004;306(5694):269-271.

218. Wang NJ, Sanborn Z, Arnett KL, et al. Loss-of-function mutations in Notch receptors in cutaneous and lung squamous cell carcinoma. *Proc Natl Acad Sci U S A.* 2011;108(43):17761-17766.

219. Demehri S, Turkoz A, Kopan R. Epidermal Notch1 loss promotes skin tumorigenesis by impacting the stromal microenvironment. *Cancer Cell.* 2009;16(1):55-66.

220. Ranganathan P, Weaver KL, Capobianco AJ. Notch signalling in solid tumours: a little bit of everything but not all the time. *Nat Rev Cancer.* 2011;11(5):338-351.

221. South AP, Cho RJ, Aster JC. The double-edged sword of Notch signaling in cancer. *Semin Cell Dev Biol.* 2012;23(4):458-464.

222. Belandia B, Powell SM, Garcia-Pedrero JM, Walker MM, Bevan CL, Parker MG. Hey1, a mediator of notch signaling, is an androgen receptor corepressor. *Mol Cell Biol.* 2005;25(4):1425-1436.

223. Lavery DN, Villaronga MA, Walker MM, Patel A, Belandia B, Bevan CL. Repression of androgen receptor activity by HEYL, a third member of the Hairy/Enhancer-of-split-related family of Notch effectors. *J Biol Chem.* 2011;286(20):17796-17808.

224. Wang XD, Leow CC, Zha J, et al. Notch signaling is required for normal prostatic epithelial cell proliferation and differentiation. *Dev Biol.* 2006;290(1):66-80.

225. Whelan JT, Kellogg A, Shewchuk BM, Hewan-Lowe K, Bertrand FE. Notch-1 signaling is lost in prostate adenocarcinoma and promotes PTEN gene expression. *J Cell Biochem.* 2009;107(5):992-1001.

226. Santagata S, Demichelis F, Riva A, et al. JAGGED1 expression is associated with prostate cancer metastasis and recurrence. *Cancer Res.* 2004;64(19):6854-6857.

227. Shou J, Ross S, Koeppen H, de Sauvage FJ, Gao WQ. Dynamics of notch expression during murine prostate development and tumorigenesis. *Cancer Res.* 2001;61(19):7291-7297.

228. Yong T, Sun A, Henry MD, Meyers S, Davis JN. Down regulation of CSL activity inhibits cell proliferation in prostate and breast cancer cells. *J Cell Biochem.* 2011;112(9):2340-2351.

229. Wang XD, Shou J, Wong P, French DM, Gao WQ. Notch1-expressing cells are indispensable for prostatic branching morphogenesis during development and re-growth following castration and androgen replacement. *J Biol Chem.* 2004;279(23):24733-24744.

230. Ye QF, Zhang YC, Peng XQ, Long Z, Ming YZ, He LY. Silencing Notch-1 induces apoptosis and increases the chemosensitivity of prostate cancer cells to docetaxel through Bcl-2 and Bax. *Oncol Lett.* 2012;3(4):879-884.

231. Danza G, Di Serio C, Ambrosio MR, et al. Notch3 is activated by chronic hypoxia and contributes to the progression of human prostate cancer. *Int J Cancer.* 2013;1(10):28293.

232. Long Q, Johnson BA, Osunkoya AO, et al. Protein-coding and microRNA biomarkers of recurrence of prostate cancer following radical prostatectomy. *Am J Pathol.* 2011;179(1):46-54.

233. Danza G, Di Serio C, Rosati F, et al. Notch signaling modulates hypoxia-induced neuroendocrine differentiation of human prostate cancer cells. *Mol Cancer Res.* 2012;10(2):230-238.

234. Orr B, Grace OC, Vanpoucke G, Ashley GR, Thomson AA. A role for notch signaling in stromal survival and differentiation during prostate development. *Endocrinology.* 2009;150(1):463-472.

235. Wu X, Xu K, Zhang L, et al. Differentiation of the ductal epithelium and smooth muscle in the prostate gland are regulated by the Notch/PTEN-dependent mechanism. *Dev Biol.* 2011;356(2):337-349.

236. Carroll DK, Carroll JS, Leong CO, et al. p63 regulates an adhesion programme and cell survival in epithelial cells. *Nat Cell Biol.* 2006;8(6):551-561.

237. Nguyen BC, Lefort K, Mandinova A, et al. Cross-regulation between Notch and p63 in keratinocyte commitment to differentiation. *Genes Dev.* 2006;20(8):1028-1042.

238. Romano RA, Smalley K, Magraw C, et al. DeltaNp63 knockout mice reveal its indispensable role as a master regulator of epithelial development and differentiation. *Development.* 2012;139(4):772-782.

239. Krebs LT, Xue Y, Norton CR, et al. Characterization of Notch3-deficient mice: normal embryonic development and absence of genetic interactions with a Notch1 mutation. *Genesis.* 2003;37(3):139-143.

240. Beatus P, Lundkvist J, Oberg C, Lendahl U. The notch 3 intracellular domain represses notch 1-mediated activation through Hairy/Enhancer of split (HES) promoters. *Development.* 1999;126(17):3925-3935.

241. Dang TP, Eichenberger S, Gonzalez A, Olson S, Carbone DP. Constitutive activation of Notch3 inhibits terminal epithelial differentiation in lungs of transgenic mice. *Oncogene.* 2003;22(13):1988-1997.

242. Ohashi S, Natsuizaka M, Yashiro-Ohtani Y, et al. NOTCH1 and NOTCH3 coordinate esophageal squamous differentiation through a CSL-dependent transcriptional network. *Gastroenterology.* 2010;139(6):2113-2123.

243. Watt FM, Estrach S, Ambler CA. Epidermal Notch signalling: differentiation, cancer and adhesion. *Curr Opin Cell Biol.* 2008;20(2):171-179.

244. Okuyama R, Tagami H, Aiba S. Notch signaling: its role in epidermal homeostasis and in the pathogenesis of skin diseases. *J Dermatol Sci.* 2008;49(3):187-194.

245. Brown MD, Gilmore PE, Hart CA, et al. Characterization of benign and malignant prostate epithelial Hoechst 33342 side populations. *Prostate.* 2007;67(13):1384-1396.

246. Valdez JM, Zhang L, Su Q, et al. Notch and TGFβ form a reciprocal positive regulatory loop that suppresses murine prostate basal stem/progenitor cell activity. *Cell Stem Cell.* 2012;11(5):676-688.

247. Pedrosa AR, Graça JL, Carvalho S, Peleteiro MC, Duarte A, Trindade A. Notch signaling dynamics in the adult healthy prostate and in prostatic tumor development. *Prostate.* 2016;76(1):80-96.

248. Palomero T, Lim WK, Odom DT, et al. NOTCH1 directly regulates c-MYC and activates a feed-forward-loop transcriptional network promoting leukemic cell growth. *Proc Natl Acad Sci U S A.* 2006;103(48):18261-18266.

249. Davidson BL, McCray PB, Jr. Current prospects for RNA interference-based therapies. *Nature reviews. Genetics.* 2011;12(5):329-340.

250. Hannon GJ. RNA interference. *Nature.* 2002;418(6894):244-251.

251. Fellmann C, Lowe SW. Stable RNA interference rules for silencing. *Nature cell biology.* 2014;16(1):10-18.

252. Singer O, Verma IM. Applications of lentiviral vectors for shRNA delivery and transgenesis. *Current gene therapy.* 2008;8(6):483-488.

253. Moffat J, Grueneberg DA, Yang X, et al. A lentiviral RNAi library for human and mouse genes applied to an arrayed viral high-content screen. *Cell.* 2006;124(6):1283-1298.

254. Wiederschain D, Wee S, Chen L, et al. Single-vector inducible lentiviral RNAi system for oncology target validation. *Cell cycle.* 2009;8(3):498-504.

255. Lis JT, Schleif R. Size fractionation of double-stranded DNA by precipitation with polyethylene glycol. *Nucleic acids research.* 1975;2(3):383-389.

256. Cariello NF, Keohavong P, Sanderson BJ, Thilly WG. DNA damage produced by ethidium bromide staining and exposure to ultraviolet light. *Nucleic acids research.* 1988;16(9):4157.

257. Grundemann D, Schomig E. Protection of DNA during preparative agarose gel electrophoresis against damage induced by ultraviolet light. *BioTechniques.* 1996;21(5):898-903.

258. McIntyre GJ, Fanning GC. Design and cloning strategies for constructing shRNA expression vectors. *BMC biotechnology.* 2006;6:1.

259. Gu S, Jin L, Zhang Y, et al. The loop position of shRNAs and pre-miRNAs is critical for the accuracy of dicer processing in vivo. *Cell.* 2012;151(4):900-911.

260. Wee S, Wiederschain D, Maira SM, et al. PTEN-deficient cancers depend on PIK3CB. *Proceedings of the National Academy of Sciences of the United States of America.* 2008;105(35):13057-13062.

261. Guo Y, Liu J, Li YH, et al. Effect of vector-expressed shRNAs on hTERT expression. *World journal of gastroenterology : WJG.* 2005;11(19):2912-2915.

262. Devroe E, Silver PA. Retrovirus-delivered siRNA. *BMC biotechnology.* 2002;2:15.

263. Reuter JS, Mathews DH. RNAstructure: software for RNA secondary structure prediction and analysis. *BMC bioinformatics.* 2010;11:129.

264. Ehrt S, Schnappinger D. Isolation of plasmids from E. coli by alkaline lysis. *Methods Mol Biol.* 2003;235:75-78.

265. Davis HE, Morgan JR, Yarmush ML. Polybrene increases retrovirus gene transfer efficiency by enhancing receptor-independent virus adsorption on target cell membranes. *Biophys Chem.* 2002;97(2-3):159-172.

266. Feng Y, Zhang X, Graves P, Zeng Y. A comprehensive analysis of precursor microRNA cleavage by human Dicer. *RNA.* 2012;18(11):2083-2092.

267. Li L, Lin X, Khvorova A, Fesik SW, Shen Y. Defining the optimal parameters for hairpin-based knockdown constructs. *Rna.* 2007;13(10):1765-1774.

268. Moullan N, Mouchiroud L, Wang X, et al. Tetracyclines Disturb Mitochondrial Function across Eukaryotic Models: A Call for Caution in Biomedical Research. *Cell reports.* 2015.

269. Mullick A, Xu Y, Warren R, et al. The cumate gene-switch: a system for regulated expression in mammalian cells. *BMC biotechnology.* 2006;6:43.

270. Chen Q, Gao S, He W, et al. Xist repression shows time-dependent effects on the reprogramming of female somatic cells to induced pluripotent stem cells. *Stem cells.* 2014;32(10):2642-2656.

271. Ma HT, On KF, Tsang YH, Poon RY. An inducible system for expression and validation of the specificity of short hairpin RNA in mammalian cells. *Nucleic acids research.* 2007;35(4):e22.

272. Zhang F, Wen Y, Guo X. CRISPR/Cas9 for genome editing: progress, implications and challenges. *Human molecular genetics.* 2014;23(R1):R40-46.

273. Frank SB, Miranti CK. Disruption of prostate epithelial differentiation pathways and prostate cancer development. *Frontiers in oncology.* 2013;3:273.

274. Uzgare AR, Xu Y, Isaacs JT. In vitro culturing and characteristics of transit amplifying epithelial cells from human prostate tissue. *Journal of cellular biochemistry.* 2004;91(1):196-205.

275. Kwon OJ, Zhang L, Xin L. Stem Cell Antigen-1 Identifies a Distinct Androgen-Independent Murine Prostatic Luminal Cell Lineage with Bipotent Potential. *Stem cells.* 2016;34(1):191-202.

276. Wang ZA, Toivanen R, Bergren SK, Chambon P, Shen MM. Luminal cells are favored as the cell of origin for prostate cancer. *Cell reports.* 2014;8(5):1339-1346.

277. Taylor RA, Toivanen R, Frydenberg M, et al. Human epithelial basal cells are cells of origin of prostate cancer, independent of CD133 status. *Stem cells.* 2012;30(6):1087-1096.

278. Lu TL, Huang YF, You LR, et al. Conditionally ablated Pten in prostate basal cells promotes basal-to-luminal differentiation and causes invasive prostate cancer in mice. *The American journal of pathology.* 2013;182(3):975-991.

279. Agarwal S, Hynes PG, Tillman HS, et al. Identification of Different Classes of Luminal Progenitor Cells within Prostate Tumors. *Cell reports.* 2015;13(10):2147-2158.

280. Kwon OJ, Zhang L, Ittmann MM, Xin L. Prostatic inflammation enhances basal-to-luminal differentiation and accelerates initiation of prostate cancer with a basal cell origin. *Proceedings of the National Academy of Sciences of the United States of America.* 2014;111(5):E592-600.

281. Heer R, Collins AT, Robson CN, Shenton BK, Leung HY. KGF suppresses alpha2beta1 integrin function and promotes differentiation of the transient amplifying population in human prostatic epithelium. *Journal of cell science.* 2006;119(Pt 7):1416-1424.

282. Belleudi F, Purpura V, Torrisi MR. The receptor tyrosine kinase FGFR2b/KGFR controls early differentiation of human keratinocytes. *PloS one.* 2011;6(9):e24194.

283. Conacci-Sorrell M, McFerrin L, Eisenman RN. An overview of MYC and its interactome. *Cold Spring Harbor perspectives in medicine.* 2014;4(1):a014357.

284. McKeown MR, Bradner JE. Therapeutic strategies to inhibit MYC. *Cold Spring Harbor perspectives in medicine.* 2014;4(10).

285. Deng G, Ma L, Meng Q, et al. Notch signaling in the prostate: critical roles during development and in the hallmarks of prostate cancer biology. *Journal of cancer research and clinical oncology.* 2015.

286. Kwon OJ, Valdez JM, Zhang L, et al. Increased Notch signalling inhibits anoikis and stimulates proliferation of prostate luminal epithelial cells. *Nature communications.* 2014;5:4416.

287. Valdez JM, Zhang L, Su Q, et al. Notch and TGFbeta form a reciprocal positive regulatory loop that suppresses murine prostate basal stem/progenitor cell activity. *Cell stem cell.* 2012;11(5):676-688.

288. Mazzone M, Selfors LM, Albeck J, et al. Dose-dependent induction of distinct phenotypic responses to Notch pathway activation in mammary epithelial cells. *Proc Natl Acad Sci U S A.* 2010;107(11):5012-5017.

289. Rangarajan A, Talora C, Okuyama R, et al. Notch signaling is a direct determinant of keratinocyte growth arrest and entry into differentiation. *The EMBO journal.* 2001;20(13):3427-3436.

290. Hodkinson PS, Elliott PA, Lad Y, et al. Mammalian NOTCH-1 activates beta1 integrins via the small GTPase R-Ras. *The Journal of biological chemistry.* 2007;282(39):28991-29001.

291. Carvalho FL, Simons BW, Eberhart CG, Berman DM. Notch signaling in prostate cancer: a moving target. *The Prostate.* 2014;74(9):933-945.

292. Alonso G, Ambrosino C, Jones M, Nebreda AR. Differential activation of p38 mitogen-activated protein kinase isoforms depending on signal strength. *The Journal of biological chemistry.* 2000;275(51):40641-40648.

293. Huang MJ, Cheng YC, Liu CR, Lin S, Liu HE. A small-molecule c-Myc inhibitor, 10058-F4, induces cell-cycle arrest, apoptosis, and myeloid differentiation of human acute myeloid leukemia. *Experimental hematology.* 2006;34(11):1480-1489.

294. Wang J, Ma X, Jones HM, et al. Evaluation of the antitumor effects of c-Myc-Max heterodimerization inhibitor 100258-F4 in ovarian cancer cells. *Journal of translational medicine.* 2014;12:226.

295. Guo J, Parise RA, Joseph E, et al. Efficacy, pharmacokinetics, tisssue distribution, and metabolism of the Myc-Max disruptor, 10058-F4 [Z,E]-5-[4-ethylbenzylidine]-2-thioxothiazolidin-4-one, in mice. *Cancer chemotherapy and pharmacology.* 2009;63(4):615-625.

296. Kent WJ, Sugnet CW, Furey TS, et al. The human genome browser at UCSC. *Genome research.* 2002;12(6):996-1006.

297. Andrade-Lima LC, Veloso A, Paulsen MT, Menck CF, Ljungman M. DNA repair and recovery of RNA synthesis following exposure to ultraviolet light are delayed in long genes. *Nucleic acids research.* 2015;43(5):2744-2756.

298. Lefkofsky HB, Veloso A, Ljungman M. Transcriptional and post-transcriptional regulation of nucleotide excision repair genes in human cells. *Mutation research.* 2015;776:9-15.

299. Gagan J, Dey BK, Layer R, Yan Z, Dutta A. Notch3 and Mef2c proteins are mutually antagonistic via Mkp1 protein and miR-1/206 microRNAs in differentiating myoblasts. *The Journal of biological chemistry.* 2012;287(48):40360-40370.

300. Consortium EP. An integrated encyclopedia of DNA elements in the human genome. *Nature.* 2012;489(7414):57-74.

301. Harrold S, Genovese C, Kobrin B, Morrison SL, Milcarek C. A comparison of apparent mRNA half-life using kinetic labeling techniques vs decay following administration of transcriptional inhibitors. *Analytical biochemistry.* 1991;198(1):19-29.

302. Herrick DJ, Ross J. The half-life of c-myc mRNA in growing and serum-stimulated cells: influence of the coding and 3' untranslated regions and role of ribosome translocation. *Molecular and cellular biology.* 1994;14(3):2119-2128.

303. Edick MJ, Tesfay L, Lamb LE, Knudsen BS, Miranti CK. Inhibition of integrin-mediated crosstalk with epidermal growth factor receptor/Erk or Src signaling pathways in autophagic prostate epithelial cells induces caspase-independent death. *Molecular biology of the cell.* 2007;18(7):2481-2490.

304. Root DE, Hacohen N, Hahn WC, Lander ES, Sabatini DM. Genome-scale loss-of-function screening with a lentiviral RNAi library. *Nature methods.* 2006;3(9):715-719.

305. Campeau E, Ruhl VE, Rodier F, et al. A versatile viral system for expression and depletion of proteins in mammalian cells. *PloS one.* 2009;4(8):e6529.

306. Hogarty MD, Norris MD, Davis K, et al. ODC1 is a critical determinant of MYCN oncogenesis and a therapeutic target in neuroblastoma. *Cancer research.* 2008;68(23):9735-9745.

307. Gruber AR, Fallmann J, Kratochvill F, Kovarik P, Hofacker IL. AREsite: a database for the comprehensive investigation of AU-rich elements. *Nucleic acids research.* 2011;39(Database issue):D66-69.

308. Paulsen MT, Veloso A, Prasad J, et al. Use of Bru-Seq and BruChase-Seq for genome-wide assessment of the synthesis and stability of RNA. *Methods.* 2014;67(1):45-54.

309. Pedrosa AR, Graca JL, Carvalho S, Peleteiro MC, Duarte A, Trindade A. Notch signaling dynamics in the adult healthy prostate and in prostatic tumor development. *The Prostate.* 2016;76(1):80-96.

310. Baeten JT, Lilly B. Differential Regulation of NOTCH2 and NOTCH3 Contribute to Their Unique Functions in Vascular Smooth Muscle Cells. *The Journal of biological chemistry.* 2015;290(26):16226-16237.

311. Bhat V, Sun Y, Weger S, Raouf A. Notch-induced expression of FZD7 requires noncanonical NOTCH3 signalling in human breast epithelial cells. *Stem cells and development.* 2016.

312. Gomi K, Arbelaez V, Crystal RG, Walters MS. Activation of NOTCH1 or NOTCH3 signaling skews human airway basal cell differentiation toward a secretory pathway. *PloS one.* 2015;10(2):e0116507.

313. Mori M, Mahoney JE, Stupnikov MR, et al. Notch3-Jagged signaling controls the pool of undifferentiated airway progenitors. *Development.* 2015;142(2):258-267.

314. Ortica S, Tarantino N, Aulner N, Israel A, Gupta-Rossi N. The 4 Notch receptors play distinct and antagonistic roles in the proliferation and hepatocytic differentiation of liver progenitors. *FASEB journal : official publication of the Federation of American Societies for Experimental Biology.* 2014;28(2):603-614.

315. Park JS, Kim YS, Yoo MA. The role of p38b MAPK in age-related modulation of intestinal stem cell proliferation and differentiation in Drosophila. *Aging.* 2009;1(7):637-651.

316. Brown D, Hikim AP, Kovacheva EL, Sinha-Hikim I. Mouse model of testosterone-induced muscle fiber hypertrophy: involvement of p38 mitogen-activated protein kinase-mediated Notch signaling. *J Endocrinol.* 2009;201(1):129-139.

317. Gonsalves FC, Weisblat DA. MAPK regulation of maternal and zygotic Notch transcript stability in early development. *Proceedings of the National Academy of Sciences of the United States of America.* 2007;104(2):531-536.

318. Kiec-Wilk B, Grzybowska-Galuszka J, Polus A, Pryjma J, Knapp A, Kristiansen K. The MAPK-dependent regulation of the Jagged/Notch gene expression by VEGF, bFGF or PPAR gamma mediated angiogenesis in HUVEC. *Journal of physiology and pharmacology : an official journal of the Polish Physiological Society.* 2010;61(2):217-225.

319. Marderosian M, Sharma A, Funk AP, et al. Tristetraprolin regulates Cyclin D1 and c-Myc mRNA stability in response to rapamycin in an Akt-dependent manner via p38 MAPK signaling. *Oncogene.* 2006;25(47):6277-6290.

320. Kim TK, Hemberg M, Gray JM, et al. Widespread transcription at neuronal activity-regulated enhancers. *Nature.* 2010;465(7295):182-187.

321. Lam MT, Li W, Rosenfeld MG, Glass CK. Enhancer RNAs and regulated transcriptional programs. *Trends in biochemical sciences.* 2014;39(4):170-182.

322. Mathelier A, Fornes O, Arenillas DJ, et al. JASPAR 2016: a major expansion and update of the open-access database of transcription factor binding profiles. *Nucleic acids research.* 2016;44(D1):D110-115.

323. Cisneros E, Latasa MJ, Garcia-Flores M, Frade JM. Instability of Notch1 and Delta1 mRNAs and reduced Notch activity in vertebrate neuroepithelial cells undergoing S-phase. *Molecular and cellular neurosciences.* 2008;37(4):820-831.

324. Liu XD, Zhang LY, Zhu TC, Zhang RF, Wang SL, Bao Y. Overexpression of miR-34c inhibits high glucose-induced apoptosis in podocytes by targeting Notch signaling pathways. *International journal of clinical and experimental pathology.* 2015;8(5):4525-4534.

325. Furukawa S, Kawasaki Y, Miyamoto M, Hiyoshi M, Kitayama J, Akiyama T. The miR-1-NOTCH3-Asef pathway is important for colorectal tumor cell migration. *PloS one.* 2013;8(11):e80609.

326. Bertrand FE, McCubrey JA, Angus CW, Nutter JM, Sigounas G. NOTCH and PTEN in prostate cancer. *Advances in biological regulation.* 2014;56:51-65.

327. Cress AE, Rabinovitz I, Zhu W, Nagle RB. The alpha 6 beta 1 and alpha 6 beta 4 integrins in human prostate cancer progression. *Cancer metastasis reviews.* 1995;14(3):219-228.

328. Yoshida Y, Hayashi Y, Suda M, et al. Notch signaling regulates the lifespan of vascular endothelial cells via a p16-dependent pathway. *PloS one.* 2014;9(6):e100359.

329. Andersson ER, Lendahl U. Therapeutic modulation of Notch signalling--are we there yet? *Nat Rev Drug Discov.* 2014;13(5):357-378.

330. Andrawes MB, Xu X, Liu H, et al. Intrinsic selectivity of Notch 1 for Delta-like 4 over Delta-like 1. *J Biol Chem.* 2013;288(35):25477-25489.

331. Ladi E, Nichols JT, Ge W, et al. The divergent DSL ligand Dll3 does not activate Notch signaling but cell autonomously attenuates signaling induced by other DSL ligands. *J Cell Biol.* 2005;170(6):983-992.

332. Geffers I, Serth K, Chapman G, et al. Divergent functions and distinct localization of the Notch ligands DLL1 and DLL3 in vivo. *J Cell Biol.* 2007;178(3):465-476.

333. Kangsamaksin T, Murtomaki A, Kofler NM, et al. NOTCH decoys that selectively block DLL/NOTCH or JAG/NOTCH disrupt angiogenesis by unique mechanisms to inhibit tumor growth. *Cancer Discov.* 2015;5(2):182-197.

334. Limbourg FP, Takeshita K, Radtke F, Bronson RT, Chin MT, Liao JK. Essential role of endothelial Notch1 in angiogenesis. *Circulation.* 2005;111(14):1826-1832.

335. Krebs LT, Xue Y, Norton CR, et al. Notch signaling is essential for vascular morphogenesis in mice. *Genes Dev.* 2000;14(11):1343-1352.

336. Domenga V, Fardoux P, Lacombe P, et al. Notch3 is required for arterial identity and maturation of vascular smooth muscle cells. *Genes Dev.* 2004;18(22):2730-2735.

337. Shi J, Fallahi M, Luo JL, Petrie HT. Nonoverlapping functions for Notch1 and Notch3 during murine steady-state thymic lymphopoiesis. *Blood.* 2011;118(9):2511-2519.

338. Joutel A. Pathogenesis of CADASIL: transgenic and knock-out mice to probe function and dysfunction of the mutated gene, Notch3, in the cerebrovasculature. *Bioessays.* 2011;33(1):73-80.

339. Hu W, Liu T, Ivan C, et al. Notch3 pathway alterations in ovarian cancer. *Cancer Res.* 2014;74(12):3282-3293.

340. Ortica S, Tarantino N, Aulner N, Israël A, Gupta-Rossi N. The 4 Notch receptors play distinct and antagonistic roles in the proliferation and hepatocytic differentiation of liver progenitors. *FASEB J.* 2014;28(2):603-614.

341. Kent S, Hutchinson J, Balboni A, Decastro A, Cherukuri P, Direnzo J. ΔNp63α promotes cellular quiescence via induction and activation of Notch3. *Cell Cycle.* 2011;10(18):3111-3118.

342. Chen CF, Dou XW, Liang YK, et al. Notch3 overexpression causes arrest of cell cycle progression by inducing Cdh1 expression in human breast cancer cells. *Cell Cycle.* 2016;15(3):432-440.

343. Pradeep CR, Köstler WJ, Lauriola M, et al. Modeling ductal carcinoma in situ: a HER2-Notch3 collaboration enables luminal filling. *Oncogene.* 2012;31(7):907-917.

344. Cui H, Kong Y, Xu M, Zhang H. Notch3 functions as a tumor suppressor by controlling cellular senescence. *Cancer Res.* 2013;73(11):3451-3459.

345. Sansone P, Ceccarelli C, Berishaj M, et al. Self-renewal of CD133(hi) cells by IL6/Notch3 signalling regulates endocrine resistance in metastatic breast cancer. *Nat Commun.* 2016;7:10442.

346. Zhang S, Chung WC, Wu G, Egan SE, Xu K. Tumor-suppressive activity of Lunatic Fringe in prostate through differential modulation of Notch receptor activation. *Neoplasia.* 2014;16(2):158-167.

347. Xu X, Choi SH, Hu T, et al. Insights into Autoregulation of Notch3 from Structural and Functional Studies of Its Negative Regulatory Region. *Structure.* 2015;23(7):1227-1235.

348. Yu X, Alder JK, Chun JH, et al. HES1 inhibits cycling of hematopoietic progenitor cells via DNA binding. *Stem Cells.* 2006;24(4):876-888.

349. Dang L, Yoon K, Wang M, Gaiano N. Notch3 signaling promotes radial glial/progenitor character in the mammalian telencephalon. *Dev Neurosci.* 2006;28(1-2):58-69.

350. Guentchev M, McKay RD. Notch controls proliferation and differentiation of stem cells in a dose-dependent manner. *Eur J Neurosci.* 2006;23(9):2289-2296.

351. Agha-Mohammadi S, O'Malley M, Etemad A, Wang Z, Xiao X, Lotze MT. Second-generation tetracycline-regulatable promoter: repositioned tet operator elements optimize transactivator synergy while shorter minimal promoter offers tight basal leakiness. *J Gene Med.* 2004;6(7):817-828.

352. Le Bras S, Loyer N, Le Borgne R. The multiple facets of ubiquitination in the regulation of notch signaling pathway. *Traffic.* 2011;12(2):149-161.

353. Carvalho FL, Marchionni L, Gupta A, et al. HES6 promotes prostate cancer aggressiveness independently of Notch signalling. *J Cell Mol Med.* 2015;19(7):1624-1636.

354. Waegemans E, Van de Walle I, De Medts J, et al. Notch3 activation is sufficient but not required for inducing human T-lineage specification. *J Immunol.* 2014;193(12):5997-6004.

355. Borggrefe T, Liefke R. Fine-tuning of the intracellular canonical Notch signaling pathway. *Cell Cycle.* 2012;11(2):264-276.

356. Zavadil J, Cermak L, Soto-Nieves N, Böttinger EP. Integration of TGF-beta/Smad and Jagged1/Notch signalling in epithelial-to-mesenchymal transition. *EMBO J.* 2004;23(5):1155-1165.

357. Chen J, Imanaka N, Griffin JD. Hypoxia potentiates Notch signaling in breast cancer leading to decreased E-cadherin expression and increased cell migration and invasion. *Br J Cancer.* 2010;102(2):351-360.

358. Guruharsha KG, Kankel MW, Artavanis-Tsakonas S. The Notch signalling system: recent insights into the complexity of a conserved pathway. *Nat Rev Genet.* 2012;13(9):654-666.

359. Estrach S, Cordes R, Hozumi K, Gossler A, Watt FM. Role of the Notch ligand Delta1 in embryonic and adult mouse epidermis. *J Invest Dermatol.* 2008;128(4):825-832.

360. Nickoloff BJ, Qin JZ, Chaturvedi V, Denning MF, Bonish B, Miele L. Jagged-1 mediated activation of notch signaling induces complete maturation of human keratinocytes through NF-kappaB and PPARgamma. *Cell Death Differ.* 2002;9(8):842-855.

361. Matsumoto T, Turesson I, Book M, Gerwins P, Claesson-Welsh L. p38 MAP kinase negatively regulates endothelial cell survival, proliferation, and differentiation in FGF-2-stimulated angiogenesis. *J Cell Biol.* 2002;156(1):149-160.

362. Golde TE, Koo EH, Felsenstein KM, Osborne BA, Miele L. γ-Secretase inhibitors and modulators. *Biochim Biophys Acta.* 2013;1828(12):2898-2907.

363. Wu Y, Cain-Hom C, Choy L, et al. Therapeutic antibody targeting of individual Notch receptors. *Nature.* 2010;464(7291):1052-1057.

364. Falk R, Falk A, Dyson MR, et al. Generation of anti-Notch antibodies and their application in blocking Notch signalling in neural stem cells. *Methods.* 2012;58(1):69-78.

365. Whiteman P, de Madrid BH, Taylor P, et al. Molecular basis for Jagged-1/Serrate ligand recognition by the Notch receptor. *J Biol Chem.* 2013;288(10):7305-7312.

366. Liu SK, Bham SA, Fokas E, et al. Delta-like ligand 4-notch blockade and tumor radiation response. *J Natl Cancer Inst.* 2011;103(23):1778-1798.

367. Fukuda D, Aikawa E, Swirski FK, et al. Notch ligand delta-like 4 blockade attenuates atherosclerosis and metabolic disorders. *Proc Natl Acad Sci U S A.* 2012;109(27):E1868-1877.

368. Lapointe J, Li C, Higgins JP, et al. Gene expression profiling identifies clinically relevant subtypes of prostate cancer. *Proc Natl Acad Sci U S A.* 2004;101(3):811-816.

369. Ding XY, Ding J, Wu K, et al. Cross-talk between endothelial cells and tumor via delta-like ligand 4/Notch/PTEN signaling inhibits lung cancer growth. *Oncogene.* 2012;31(23):2899-2906.

370. Niessen K, Fu Y, Chang L, Hoodless PA, McFadden D, Karsan A. Slug is a direct Notch target required for initiation of cardiac cushion cellularization. *J Cell Biol.* 2008;182(2):315-325.

371. Adepoju O, Wong A, Kitajewski A, et al. Expression of HES and HEY genes in infantile hemangiomas. *Vasc Cell.* 2011;3:19.